Catalytic Conversion of Glycerol to Value-Added Liquid Chemicals

A Thesis Submitted to the College of Graduate Studies and Research

in partial fulfilment of the requirements for the degree of

Master of Science

in the Department of Chemical Engineering

University of Saskatchewan

Saskatoon, Saskatchewan

By

Kapil Dev Pathak

COPYRIGHT

ABSTRACT

Glycerol is one of the by-products of transesterification of fatty acids for the production of bio-diesel. Value-added products such as hydrogen, wood stabilizers and liquid chemicals from catalytic treatment of glycerol can improve the economics of the bio-diesel production process. Catalytic conversion of glycerol can be used for production of value-added liquid chemicals. In this work, a systematic study has been conducted to evaluate the effects of operating conditions on glycerol conversion to liquid chemical products in the presence of acid catalysts.

Central composite design for response surface method was used to design the experimental plan. Experiments were performed in a fixed-bed reactor using HZSM-5, HY, silica-alumina and γ-alumina catalysts. The temperature, carrier gas flow rate and weight hourly space velocity (WHSV) were maintained in the range of 350-500 ^{o}C, 20-50 mL/min and 5.40-21.60 h^{-1}, respectively.

The main liquid chemicals detected in liquid product were acetaldehyde, acrolein, formaldehyde and hydroxyacetone. Under all experimental conditions complete glycerol conversion was obtained over silica-alumina and γ-alumina. A maximum liquid product yield of approximately 83 g/100g feed was obtained with these two catalysts when the operating conditions were maintained at 380 ^{o}C, 26 mL/min and 8.68 h^{-1}. Maximum glycerol conversions of 100 wt% and 78.8 wt% were obtained in the presence of HY and HZSM-5 at temperature, carrier gas flow rate and WHSV of 470 ^{o}C, 26 mL/min and 8.68 h^{-1}. HY and HZSM-5 produced maximum liquid product of 80.9 and 59.0 g/100 g feed at temperature of 425 and 470 ^{o}C, respectively.

Silica-alumina produced the maximum acetaldehyde (~24.5 g/100 g feed) whereas γ-alumina produced the maximum acrolein (~25 g/100 g feed). Also, silica-alumina

produced highest formaldehyde yield of 9g/100 g feed whereas HY produced highest acetol yield of 14.7 g/100 g feed. The effect of pore size of these catalysts was studied on optimum glycerol conversion and liquid product yield. Optimum conversion increased from 80 to 100 wt% and optimum liquid product increased from 59 to 83.3 g/100 g feed when the pore size of catalyst was increased from 0.54 in case of HZSM-5 to 0.74 nm in case of HY, after which the effect of pore size was minimal.

ACKNOWLEDGMENT

DEDICATION

This work is dedicated to

My Parents

TABLE OF CONTENTS

LIST OF TABLES

LIST OF FIGURES

ABBREVIATIONS

ANOVA	Analysis of Variance
C	Carrier Gas Flow Rate, mL/min
C_R	Char and Residue Yield, g/100 g feed
C_T	Char and Residue Collected, g
F	Glycerol Fed, g
G	Gas Product Yield, g/100 g feed
G_T	Gas Collected, g
L	Liquid Product Yield, g/100 g feed
L_T	Total Liquid Product Including Unconverted Glycerol, g
RSM	Response Surface Methodology
T	Temperature, ^{o}C
TPD	Temperature Programmed Desorption
W	Weight Hourly Space Velocity, h^{-1}
X	Glycerol Conversion, wt%
XRD	X-ray Diffraction
SEM	Scanning Electron Microscope
FTIR	Fourier Transformed Infrared Spectroscopy

1   INTRODUCTION

Limited resources of conventional fuels such as petrodiesel have led to the search for alternative fuels. Recently, there has been a growing concern about the increasing air pollution caused by the combustion of petrodiesel. In addition, depleting resources of conventional fuels has caused an increase in its price. Biodiesel is an alternative fuel produced from renewable sources such as vegetable oil. It has a proven performance for air pollution reduction. However, the price of biodiesel is presently more as compared to petrodiesel (Haas, 2005).

Biodiesel is produced through transesterification reaction in which fatty acids present in vegetable or animal oil are reacted with alcohols. Glycerol is produced as a by-product in this reaction (Dalai et al., 2000). Higher cost of biodiesel is primarily due to the raw material cost (Zhang et al., 2003). The economics of biodiesel production may be improved if value-added products such as hydrogen, synthesis gas or liquid chemicals may be produced from by-product glycerol. Also, increased production of biodiesel could lead to glut of glycerol in the market. This may cause the price of glycerol to fall by as much as 50 percent (Claude, 1998).

The production of value-added chemicals from glycerol may lead to a decrease in biodiesel prices. Furthermore, it will improve glycerol market. Production of value added chemicals from glycerol is a cracking reaction. Possible methods for utilization of glycerol are pyrolysis, steam gasification and catalytic cracking. Pyrolysis is heating of glycerol to a high temperature in the absence of air. The high temperature makes

pyrolysis an energy intensive method of transforming glycerol. Stream gasification is the co-feeding glycerol with steam. This again needs energy for steam generation. Catalytic cracking has a unique advantage in that the reaction occurs at low temperatures. Thus, catalytic cracking is a less energy intensive process.

Thiruchitrambalam et al. (2004) reported that glycerol can be completely converted into H_2 rich syn-gas using pyrolysis at 800 ^{o}C in a fixed bed reactor. Cortright et al. (2002) reported the production of H_2 from aqueous phase carbohydrate reforming of glycerol over Pt/Al_2O_3 catalysts. H_2 yield of 64.8 mol% from glycerol was reported in this work. Buhler et al. (2002) reported the production of allyl alcohol, acetaldehyde, acrolein, methanol CO, CO_2 H_2 from the treatment of glycerol under supercritical conditions. A low glycerol conversion (0.4-31 wt%) was reported in this work. An extensive review of literature has been done (see Chapter 2) for value-added products from glycerol and on the available cracking catalysts such as zeolites, silica-alumina and γ-alumina.

It appears from literature that there has been no study on the production of liquid chemicals from catalytic conversion of glycerol at low temperature and atmospheric pressure. Thus there is a knowledge gap that needs to be filled. This has led to the following research objectives for the present work.

1.1   Research objectives

The main objective of this work was to study the potential of production of value-added liquid chemicals such as acetaldehyde, acrolein, formaldehyde and acetol from glycerol via cracking reaction using HZSM-5, HY, silica-alumina and γ-alumina. These catalysts were chosen because of their wide range of pore size, total acidity and BET surface area. Furthermore, HZSM-5, HY and γ-alumina are crystalline whereas silica-

alumina is non crystalline material. The overall objective was achieved in the various phases of research program as described below:

1.1.1 Phase I: Catalyst characterization

The objective of this phase was to study the physiochemical properties of HZSM-5, HY, silica-alumina and γ-alumina. To achieve this objective, catalysts were characterized using different techniques such as temperature programmed desorption of NH_3, X-ray diffraction, BET surface area analysis, SEM and FTIR.

1.1.2 Phase II: Catalyst performance evaluation

The objective of this research phase was to study the effects of operating parameters such as temperature, carrier gas flow rate and WHSV on glycerol conversion, liquid, gas and char yield using HZSM-5, HY, silica-alumina and γ-alumina catalysts. The operating conditions were optimized to maximize the glycerol conversion, liquid product yield and yields of liquid chemicals such as acetaldehyde, acrolein, formaldehyde and acetol for each of the above mentioned catalysts.

1.1.3 Phase III: Effect of physiochemical properties on catalysts' activity

In this phase, the effects of catalysts' physiochemical properties on optimum glycerol conversion, liquid product yield and yields of acetaldehyde, acrolein, formaldehyde and acetol were evaluated.

Chapter 2 presents a comprehensive literature review on glycerol uses and different acid catalysts used for cracking of glycerol. Experimental design and details of product identification and catalyst characterization are discussed in Chapter 3. Chapter 4 presents the discussion on the experimental results. The conclusions and recommendations from this work are given in Chapter 5.

2   LITERATURE REVIEW

The main aim of this work is to study the potential of production of value-added liquid chemicals from glycerol. Therefore, a review of the literature has been done to find out the reported processing methods of glycerol to value-added products. A detailed review of literature based on sources of glycerol, products obtained from glycerol and structure and catalytic properties of various acid catalysts is presented in this section.

2.1   Glycerol production and consumption

Glycerol is produced in soap industry from direct saponification. Olechemical industry is a major source of glycerol production where it is obtained from fat splitting of glycerides and bio-fuels such as biodiesel. Claude (1998) has indicated various uses of glycerol in cosmetic, soap, pharmaceutical, food and tobacco industry as shown in Figure 2.1. The soap and cosmetic industry constituted 28 % whereas polyglycerols, esters, food and drinks and resale constituted up to 47 % of glycerol utilization. Glycerol is a topic of research recently and the researchers are keen to find out its alternate applications for fuels and chemicals (Garcia et al., 1995; Neher et al., 1995; Buhler et al., 2000; Cortright et al., 2002).

2.2   Glycerol as by-product of biodiesel

Glycerol is a by-product during transesterification of fatty acids to produce biodiesel (Dalai et al., 2000). Biodiesel is a mixture of fatty acid esters. Typical reaction to produce biodiesel is given by the following equation:
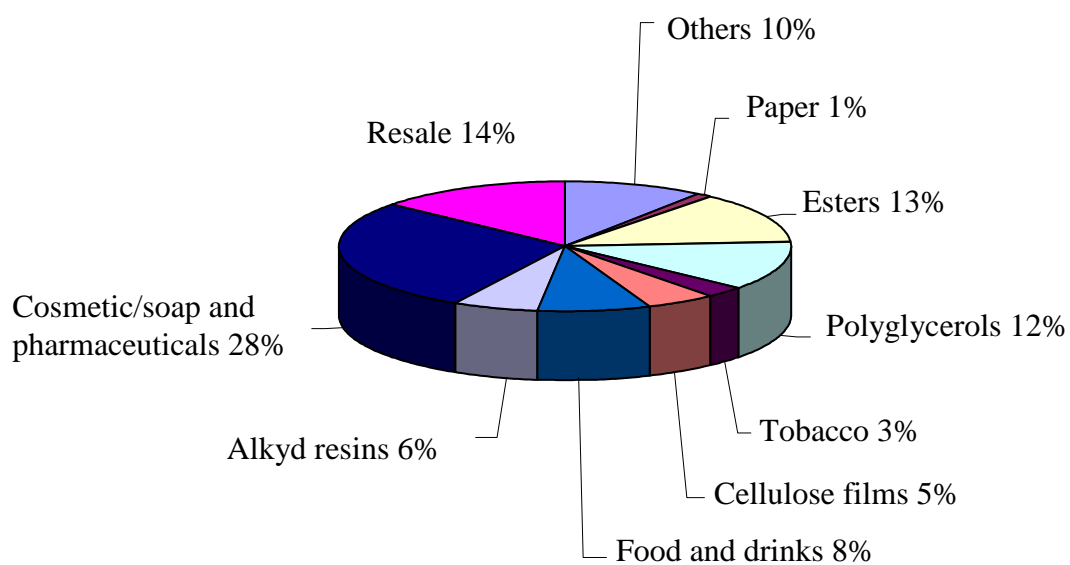
Figure 2.1: Distribution of glycerol uses as of 1995 (Claude, 1998)

Others 10%

Paper 1%

Resale 14%

Esters 13%

Cosmetic/soap and
pharmaceuticals 28%

Polyglycerols 12%

Tobacco 3%

Alkyd resins 6%

Cellulose films 5%

Food and drinks 8%

$$Triglycerides + Alcohol \rightarrow Fatty\ acid\ esters + Glycerol \tag{2.1}$$
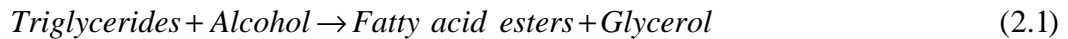
Typical feed stocks for biodiesel production are canola and soy oil (Prakash, 1998). Alcohols used are methanol, ethanol or a mixture of these. During the trans-esterification reaction about 10 wt% (of fatty acid) glycerol is produced. Production of glycerol is expected to increase with increase in production of biodiesel (Haas, 2005).

2.2.1 Biodiesel potential in Canada

Prakash (1998) reported that the production of canola and soy oils in 1996 in Canada was 1,153 million tons and 166,000 tons, respectively. It was assumed that if 10 wt% of canola and soy oil could be used for the production of biodiesel it would result in 277 million liters of biodiesel per year. Furthermore, 108 million liters of biodiesel could be obtained from tall oil (a by-product from the treatment of pine pulp). This would add up to a total biodiesel production to 385 million liters per year which in turn would lead to the production of 38.5 million liters of glycerol per year in the Canadian glycerol market.

The federal government of Canada has planned to produce 500 million liters of biodiesel per year by the year 2010 to meet the Kyoto protocol (Smith, 2004). With 10 wt% production of glycerol, this would lead to ~50 million liters of glycerol/year in the Canadian market. Xu et al. (1996) reported that increasing demand for biodiesel may create a glut of glycerol, which could become available as a feedstock at low or negative cost. However, for biodiesel to economically compete with petrodiesel its price must come down.

2.2.2 Making biodiesel a competitive fuel

A number of strategies have been proposed to improve the economics of biodiesel production and make it a viable fuel. Government subsidies could help to improve the economic competitiveness of biodiesel, however, it is desirable to minimize the dependence on such supports (Haas, 2005). Raw material cost leads to high price of biodiesel. The price of biodiesel is strongly influenced by the price of alcohol, one of the reactant in trans-esterification reaction (Bungay, 2004) and the purity of reactants (Barnwal, 2005). Use of less expensive feed stocks such as animal fat (Peterson et al., 1997; Ma et al., 1998) and restaurant grease has been proposed for biodiesel production. Recently, soapstock, a byproduct of refining of vegetable oils has been used as a feedstock for biodiesel (Haas, 2005). In addition to that, glycerol can be processed to value added products. Value can be added to glycerol by utilizing it in existing applications and at the same time finding novel ways to utilize glycerol such as fuels (H_2, syn-gas) and value-added liquid chemicals such as aldehydes and ketones. Utilization of glycerol to produce value-added secondary products would improve the economics of biodiesel. In the following sections a detailed study of the reported work on value-added products from glycerol is presented.

2.3 Value-added products from glycerol

Glycerol can be converted to value-added products by pyrolysis, steam gasification and catalytic treatment. The literature review on pyrolysis and steam gasification of glycerol with different process conditions such as temperature and steam to glycerol ratio is discussed in this section. Also, catalytic conversion of glycerol into

value-added chemicals using different catalyst such as nickel and platinum is discussed in this section.

2.3.1 Production of hydrogen and syn-gas from glycerol

The available literature on production of hydrogen and syn-gas from glycerol by pyrolyis and steam gasification is discussed in this section.

Chaudhari and Bakhshi (2002) reported the production of hydrogen and syn-gas from pyrolysis of glycerol in a fixed bed reactor. Pyrolyis was performed with and without a carrier gas (nitrogen). One set of experiments was performed at 400 and 500 ^{o}C and glycerol flow rate of 2.0 g/h without using any carrier gas. It was reported that the operation was quite difficult without using carrier gas because of char formation in the feed inlet.

Another set of pyrolysis experiments was performed in a fixed bed reactor with the nitrogen flow rate of 50 mL/min over a temperature range from 350 to 700 ^{o}C and glycerol flow rate from 2.2 to 4.0 g/h. It was reported that complete conversion of glycerol occurred at 700 ^{o}C. Furthermore, gas yield obtained was 50 wt% but no liquid product was observed. The residue was 6.3 wt% whereas the remaining mass percent was char.

Chaudhari and Bakhshi (2002) also performed steam gasification of glycerol with steam flow rate of 2.5, 5 and 10 g/h at 600 and 700 ^{o}C with glycerol flow rate of 4 g/h. It was reported that approximately 80 wt% of glycerol was converted when steam flow rate of 10 g/h at 700 ^{o}C was used. Furthermore, 92.3 mol% syn-gas with H_2/CO ratio of 2 was produced. Gaseous product was around 70 wt%. It was reported that syn-gas can be further converted to hydrogen by water-gas shift reaction which can be used

in fuel cell applications. Syn-gas can also be converted to green diesel using Fischer-Tropsch reaction (Chaudhari and Bakhshi, 2002).

Steam gasification of glycerol was performed by Stein and Antal (1983) and Chaudhari and Bakhshi (2002). Results of Chaudhari and Bakhshi (2002) showed that steam gasification of glycerol does not produce liquid product at 600 and 700 $^{\circ}$C in a fixed bed reactor. These results are in contrast with results of Stein and Antal (1983), who reported that steam gasification of glycerol produced liquid product consisting of acrolein and acetaldehyde at 600 to 675 $^{\circ}$C in a laminar flow reactor.

Xu et al. (1996) reported carbon catalyzed gasification of the organic feed stocks such as glycerol, glucose, whole biomass feed stocks (bagasse liquid extract and sewage sludge) and cellobiose using supercritical water. Catalysts used were spruce wood charcoal, macademia shell charcoal, coal activated carbon and coconut shell activated carbon. The range of parameters investigated for gasification was temperature from 500 to 600 $^{\circ}$C, WHSV 14.6 to 22.2 h $^{-1}$ and pressure 251 to 340 MPa. It was reported that glycerol was easily and completely gasified to 54.3 mol% hydrogen rich gas with low (2 mol%) yield of CO. The presence of catalyst had little effect on the gas composition.

Cortright et al. (2002) reported the production of hydrogen from sorbitol, glycerol and ethylene glycol at temperatures of 227 $^{\circ}$C and 225 $^{\circ}$C and under high pressure in a single-reactor aqueous-phase reforming process. Platinum supported on γ-alumina was used as catalyst. Hydrogen yield was reported to be higher using sorbitol, glycerol and ethylene glycol than that of glucose. The hydrogen yields from glycerol reforming were 64.8 and 57 mol% at 225 and 265 $^{\circ}$C, respectively. Liquid products consisted of ethanol, 1,2-propanediol, acetic acid, ethylene glycol, acetaldehyde, 2-propanol, propionic acid, acetone, propionaldehyde and lactic acid.

Huber et al. (2003) reported the production of H_2 from glycerol, sorbitol and ethylene glycol by aqueous phase reforming at temperature near 227 ^oC and pressures of 2.58 and 5.14 MPa in presence of Sn promoted Raney-Ni catalyst. The feed concentration was 1 to 5 wt% in water. It was reported that addition of tin decreased the rate of methane formation. Gas composition was 66 mol% of H_2 and 32 mol% CO_2, when glycerol was used as feed.

Czernik et al. (2000) reported catalytic steam reforming of bio-oil derived fraction and crude glycerol (a by-product from trans-esterification of vegetable oil with methanol) in a fluidized bed reactor to produce hydrogen. Commercial Ni catalyst was used. Superheated steam was used to fluidize the catalyst. The temperature of crude glycerol was maintained at 60-80 ^oC and it was reported that at lower viscosity in this temperature range it was easy to pump and atomize glycerol. Glycerol was fed at 78 g/h with a steam rate of 145 g/h and WHSV of 1600 h^{-1}. Concentration of major gas products was found to be constant but methane production increased from 500 parts per million (ppm) to 2200 ppm when the run time was increased from 0 to 250 min. Hydrogen yield was around 77 wt% and it was suggested that hydrogen yield can be increased if higher amount of steam is used. The conversion of carbon monoxide in the gas through water-gas shift to CO_2 and H_2 would increase the hydrogen yield to 95 wt%.

2.3.2 Production of liquid chemicals from glycerol

In this section the available literature on production of liquid chemicals from glycerol is presented.

Buhler et al. (2002) reported the production of value added chemical such as methanol, acetalydehyde, acrolein, allyl alcohol, acetone, ethanol, carbon dioxide,

carbon monoxide and hydrogen from glycerol under supercritical conditions. The temperature range investigated was 349 to 475 ^{o}C and pressure was maintained at 25, 35 and 45 MPa. The reaction was carried out in tubular reactor with reaction time in the range from 32 to 165 s. It was reported that the decomposition of glycerol primarily followed ionic mechanism at low temperature and high pressure and free radical mechanism at high temperature and low pressure. The amount of acetaldehyde and formaldehyde decreased with increase in temperature whereas amount of allyl alcohol and methanol increased with increase in temperature.

McMorn et al. (1999) reported oxidation of glycerol using hydrogen peroxide in liquid phase reaction at temperature of 20 and 70 ^{o}C. Products from this process included, formic acid esters of glycerol and mixture of acetals. In addition to that trace amounts of hydroxyacetone, glyceraldehyde and glyceric acid were also identified.

Garcia et al. (1995) reported the oxidation of aqueous solution of glycerol at 60 ^{o}C under atmospheric pressure and pH of 2, 7 and 11. The catalysts used in the study were Pd and Pt promoted with Bi on active charcoal. The glyceric acid yield of 30, 55 and 77 wt% was obtained at pH of 7, 9 and 11, respectively using Pd catalyst. 70 wt% yield of glyceric acid was obtained at 90-100 wt% conversion of glycerol under basic conditions. It was reported that the selectivity towards oxidation of secondary alcohol group was improved by promoting Pt with metals such as Bi and resulted in dihydroxyacetone yield of 30 wt% at 60 wt% conversion. Fordham et al. (1995) reported further oxidation of glyceric acid to hydroxypyruvic and tartronic acids at 50 ^{o}C and atmospheric pressure. Pt promoted with Bi, supported on activated carbon, was used as catalyst. It was reported that oxidation of primary and secondary alcohol group resulted in formation of tartonic and hydroxypyruvic acid, respectively. The maximum yield of

83 wt% at 90 wt% conversion of glyceric acid was obtained for tartonic acid at pH of 9-11.

Neher et al. (1995) reported that acrolein can be produced from dehydration of glycerol in the liquid (temperature from 180 to 340 $^\circ$C and pressure of 70 bar) as well as gas phase (temperature from 250 to 340 $^\circ$C). HZSM-5 was used as catalyst for feed of glycerol-water mixture (glycerol content 10 to 40 wt%) was Acrolein yield of 65% was reported at 15 to 25 wt% glycerol conversion.

2.4   Chemistry of glycerol cracking

Thermal cracking of the oxygenated compounds such as glycerol has complex chemistry (Wang et al., 1996). A large numbers of primary and secondary products were generated through many different pathways. It was also reported that the partial thermal cracking of oxygenated hydrocarbons would produce hydrogen, carbon monoxide, carbon dioxide, methane and coke by primary decomposition reactions.

Antal et al. (1985) reported that the decomposition of glycerol in supercritical water follows two major pathways. At lower temperature, heterolytic acid catalyzed carbonium ion mechanism resulted in formation of acrolein by elimination of water from glycerol. At higher temperatures (above 600 $^\circ$C) however, homolytic cleavage of C-C bond resulted in the formation of acetaldehyde. Experiments were performed using NaHSO$_4$ as catalyst at 500 $^\circ$C.

Buhler et al. (2002) reported that the free radical reaction pathway dominated at lower pressure and high temperature. Formation of gaseous product was favoured at higher temperatures and it was as a result of free radical reaction pathway. The proposed reaction pathways by Buhler et al. (2002) for the formation of acetalydehyde and acrolein are shown in Figure 2.2.

12
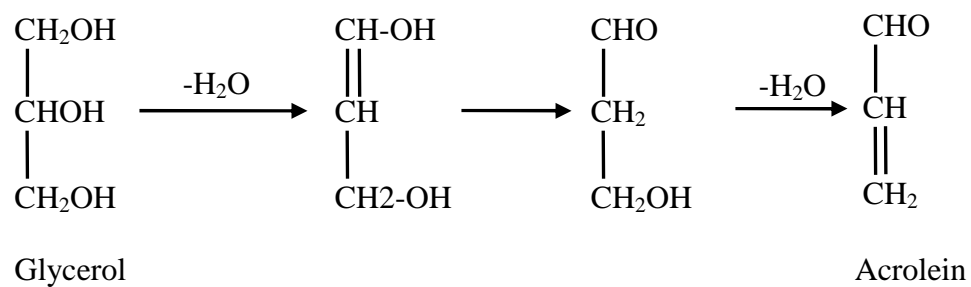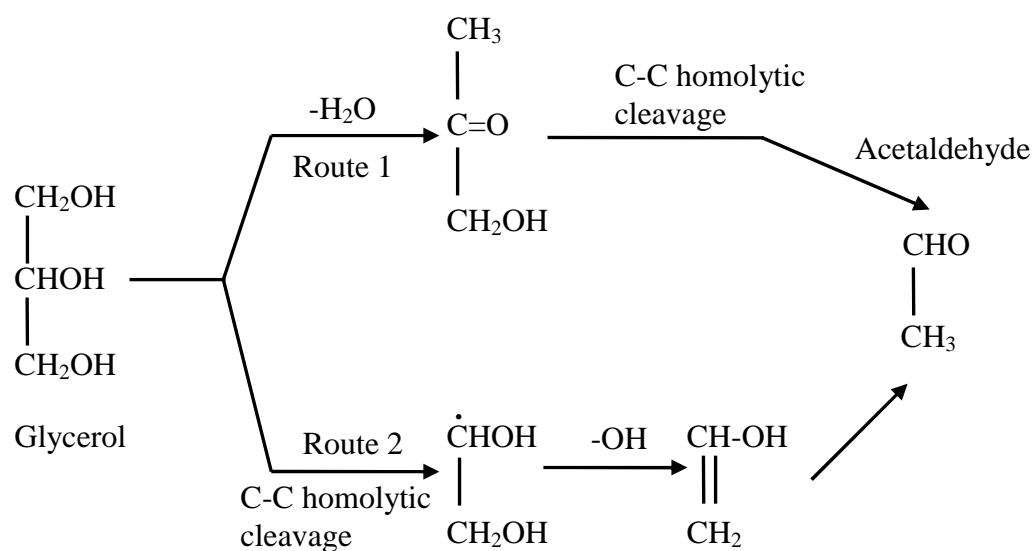
Figure 2.2: Proposed reaction pathways for acetaldehyde and acrolein yield during supercritical treatment of glycerol (Buhler et al., 2002)

2.5   Selection of catalyst for catalytic conversion of glycerol

The role of acidic catalysts for deoxygenation, cracking and enhanced hydrocarbon formation is well reported in literature (Gates, 1979). The production of value-added chemicals from glycerol is a cracking reaction where bigger glycerol molecule is broken down into smaller molecules. Cracking reactions catalyzed by acid surfaces proceed by carbonium ion intermediates. Some of the more common cracking catalysts are HZSM-5, HY, silica-alumina and γ-alumina. In this section the structure and catalytic properties of these catalysts are described.

2.5.1   Structure and catalytic properties of HZSM-5

Zeolites are porous crystalline aluminosilicates composed of AlO_4 and SiO_4 tetrahedra which form three dimensional networks linked through oxygen atoms. The composition of zeolites can be represented by empirical formula expressed as

$$M^{n+}_{x/n}(AlO_2^-)_x(SiO_2)_y.mH_2O$$
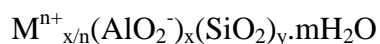
where, M is a cation with charge n+, m is the number of water molecules of crystallization, x+y is the number of tetrahedra in the unit cell. The basic tetrahedral units combine to form square and hexagonal plane faces, which combine further to form sodalite cages and hexagonal cubes (Bhatia, 1989).

The basic unit of ZSM-5 zeolite is composed of 5 silica-alumina tetrahedra linked into a pentagon. These pentagons are linked together by the sharing of oxygen atoms. The basic units join together to form secondary building units (SBU) in the form of chain and sheet building unit. The sheet structure is repeated in the third dimension to form linear channels of slightly elliptical cross-section (0.56x0.54 nm). Further channels occur in the other two dimensions, one sinusoidal with cross-section (0.55x0.51 nm) and the other a tortuous system created by the overlapping of the first two (Bhatia, 1989).

Particular composition of given ZSM-5 zeolite (eg. type of cation M, the value of y/x) determine most of the properties of ZSM-5. For example, ion exchange capacity, catalytic activity and water sorption vary with the Al content (Olson et al., 1981). Hydrophobic nature of ZSM-5 is dependent on Si/Al ratio, however the properties such as X-ray diffraction pattern, framework density, pore size and pore volume are independent of the composition (Chen, 1976).

The catalytic activity of ZSM-5 is attributed to strong acid sites and three dimensional intersecting channels (Bhatia, 1989). The acid sites in ZSM-5 lie on inter crystalline surface on the zeolite (Jacobs et al., 1981). The unique pore size and high surface area makes ZSM-5 useful as shape selective catalyst (Falamaki et al., 1997; Grieken et al., 2000). High silica to alumina ratio for ZSM-5 makes it stable under hydrothermal treatment (Kumar et al., 2002). The three dimensional structure remains intact at severe conditions of temperature. The catalyst pretreatment conditions have significant impact on acidity and acidic site distribution (Vedrine et al., 1982).

ZSM-5 is altered by ion-exchange with various cations to increase its activity and selectivity. Examples include exchange of Na^+ with H^+ to yield HZSM-5. HZSM-5 is also referred to as protonated form of ZSM-5. HZSM-5 has superior acidity as compared to other forms of ZSM-5 such as Na-ZSM-5, B-ZSM-5 or Mg-ZSM-5 (Furrer, 1988).

It has been reported that a wide variety of organic compounds could be transformed into hydrocarbons over zeolite catalyst typically over HZSM-5. HZSM-5 was reported to be an effective catalyst for completely converting feeds such as alcohols and methanol to 42-45 mol% C_6-C_{10} hydrocarbons at 371 ^{o}C and atmospheric pressure. Major deoxygenation route was reported to be dehydration (Derouane et al., 1978).

ZSM-5 with its intermediate pore size sorbs molecules as large as *o-* and *m*-xylene (~0.69 nm) while larger molecules such as 1,3,5-trimethylbenzene (~0.78 nm) are not able to penetrate the small pores. Also, larger molecules result in catalyst deactivation by forming coke and HZSM-5 catalyst resists coking by inhibiting larger molecules into the catalyst.

2.5.2   Structure and catalytic properties of Y- zeolite

Y-zeolite is a natural crystalline aluminosilicate zeolite with chemical composition $[Na_2Ca][Al_2Si_4O_{12}].H_2O$. Y-zeolites is formed when the secondary building units combine through hexagonal faces forming a hexagonal ring. Pore diameter (0.74 nm) of 12-membered ring Y-zeolite is large enough to allow access to bulky molecules such as $(C_4H_9)_3N$, isoparaffins, cyclohexane and aromatics (Campbell, 1983). Microporous acidic Y-zeolite was reported to be an effective catalyst for transformation of *m*-xylene through disproportionation reaction which was attributed to the presence of strong Bronsted acid sites and higher micro pore volume (Molina et al., 1994). HY was selected in addition to HZSM-5 to investigate the effect of pore size and structure on the product yields from catalytic conversion of glycerol.

The pore size and definite shape of zeolites imparts shape selective properties to them. The product selectivity occurs when the pore opening of the zeolite is such that it admits only certain molecules and large molecules are excluded. Also, product selectivity occurs if among all the product formed only those with proper dimension can diffuse out and appear as products. Larger molecules are retained inside the pores of catalyst and converted into smaller molecules or to carbonaceous deposits within the pores causing pore blockage.

2.5.3 Structure and catalytic properties of silica-alumina

The structure of silica-alumina is silica tetrahedral lattice in which some of the silicon atoms have been replaced by aluminum atoms. The silicon atoms in silica are bonded to four oxygen atoms whereas in alumina, aluminum atoms are bonded to only three oxygen atoms. This imbalance is resolved forcibly by silica by accommodating each aluminum atom in its four fold coordination using hydrogen atom derived from residual water content. The two possible structures of silica-alumina are shown in Figure 2.3.

Silica-alumina is amorphous solid and has both Bronsted and Lewis acidity (Katikaneni et al., 1995). Silica-alumina possesses cracking efficiencies for several reactions such as *m*-xylene isomerization, cumene cracking and heptane cracking (Sato et al., 2001).

2.5.4 Structure and catalytic properties of γ-alumina

γ-alumina is an important industrial material and finds vast applications in refining and petrochemsitry. γ-alumina was used as catalyst in the dehydration of alcohols and in Clauss process (Digne et al., 2004). The precise crystallographic structure of γ- alumina is still under debate. Detailed review of literature on the structure of γ- alumina was done by Wolverton et al. (2000) and Gutiérrez et al. (2001). Surface properties of γ-alumina make it useful as microporous catalyst (Pinto et al., 2004).

—Si — O — Si — O — Si —

O   OH   O

—Si — O — Al — O — Si —

O   O   O

Lewis acidity

—Si — O — Si — O — Si —

O   O   H⊕   O
              ⊖

—Si — O — Al — O — Si —

O   O   O
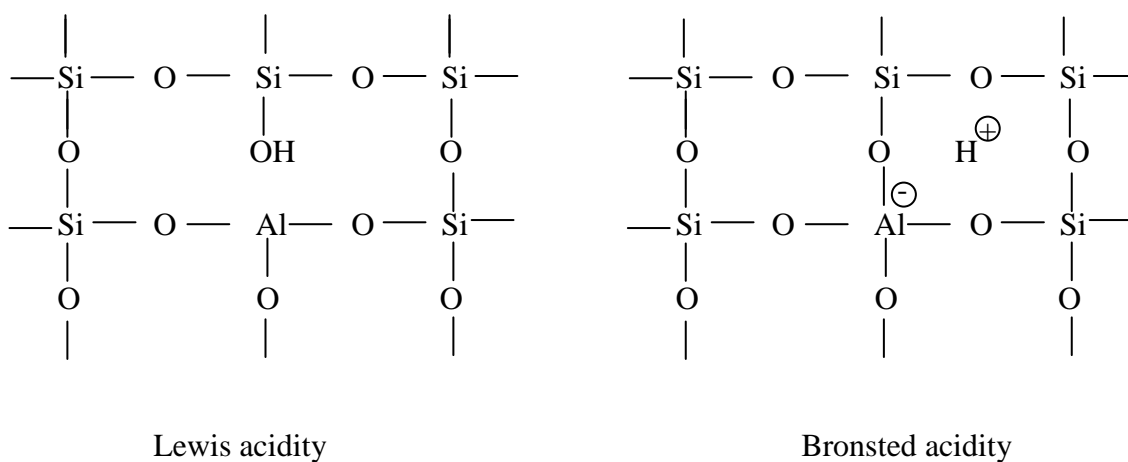
Bronsted acidity

Figure 2.3: Typical structure of silica-alumina and the origin of Lewis and Bronsted acidity (Campbell, 1983)

2.6   Catalyst Deactivation

Catalytic conversion often leads to a number of undesirable side reactions. As a result of these reactions a carbonaceous deposit referred to as coke is produced on the catalyst (Nam et al., 1987). Coke reduces the catalytic activity for desired reaction and thus substantially reduces rate of conversion and/or selectivity of the catalyst. Deactivation of ZSM-5 occurs primarily due to fouling which is gradual covering of catalyst surface with coke. The catalyst activity is reduced due to decrease in active surface area and increased diffusion resistance which is due of physical coverage of active sites or plugging (full or partial) of the pores of the catalyst (Furrer, 1988). Formations of polyalkylaromatics such as polyethylbenzene, which are the reported coke precursors, have been inhibited over ZSM-5 (Chandrawar et al., 1982).

3   EXPERIMENTAL

This chapter describes the design and construction of experimental setup for catalytic conversion of glycerol. Preparation of catalyst and experimental procedure are described in this section. Statistical design of experiments and the techniques used to analyze the liquid and gas products from the experiments are also described in detail in this section.

3.1   Catalysts for glycerol conversion

In this work, four catalysts namely HZSM-5, HY, silica-alumina and γ-alumina were used for the production of value added liquids from glycerol.

Y-zeolite was procured from Zeolyst International, Netherlands. Y-zeolite was treated with 1M solution of ammonium chloride at 80 ^{o}C, then dried at 110 ^{o}C and calcined at 550 ^{o}C for 4 hours to get the HY form.

Silica-alumina catalyst was procured from Aldrich St. Louis, MO, USA. Silica-alumina was calcined at 550 ^{o}C for 4 hours prior to use in the experiments.

γ-alumina was procured from Sud Chemicals, India. It was calcined at 550 ^{o}C for 4 hours before use in the reactions.

HZSM-5 was prepared by hydrothermal treatment of silica and alumina source in presence of an organic template in an autoclave (supplied by Parr Inc, IL, USA) according to method described in literature (Argauer and Landolt, 1972). The detailed synthesis procedure is reported elsewhere (Sang et al., 2004).

The chemicals used in the preparation were terta ethyl orthosilicate as silica source (Sigma-Aldrich St. Louis, MO, USA), sodium aluminate as aluminum source (Fisher Scientific Company, New Jersey, USA), tetra propyl ammonium bromide as organic template (Aldrich, St. Louise, MO, USA), NaOH to maintain pH and conc. H_2SO_4.

3.2 Catalyst characterization

Catalysts were characterized to measure the properties such as pore size, surface area, structure and acidity and thus understand the performance of the catalyst. The different techniques used included: temperature programmed desorption (TPD), powder X-ray diffraction (XRD), BET surface area analyis, scanning electron microscope and fourier transformed infrared (FTIR) spectroscopy. These techniques have been briefly described in the following sections.

3.2.1 Temperature programmed desorption (TPD)

Temperature programmed desoption was used to determine the number and strength of acid sites of the catalysts. The catalyst was saturated under a flow of ammonia after which the temperature of the sample was gradually increased and the amount of ammonia desorbed was recorded as a function of time. The temperature at which ammonia desorbs is associated with a particular type of acid site.

The TPD analysis was performed using CHEMBET 3000 (manufactured by Quantachrome Corporation, FL, USA). About 0.1 g of the catalyst sample was placed in U shaped quartz tube. The tube was then placed in an electrically heated furnace. The sample tube was heated from room temperature to 400 ^{o}C with heating rate of 10 ^{o}C per

min under the flow (20 mL/min) of NH_3 (1000 ppm NH_3 in N_2, supplied by Praxair, Mississauga, ON, Canada). The temperature was maintained at 400 ^{o}C for one hour after which the U tube was allowed to naturally cool down to 35 ^{o}C. Then the U tube was heated to 1050 ^{o}C at heating rate of 10 ^{o}C per min in argon gas (supplied by Praxair, Mississauga, ON, Canada) flow (20 mL/min). The TPD plot was logged using on-line data acquisition system.

3.2.2 Powder X-ray diffraction (XRD)

X-ray diffraction was used to identify the structure of the zeolite catalysts. It is also useful to determine if the material under investigation was crystalline or amorphous. Powdered sample of the calcined catalyst was bombarded with x-rays at various angles. Intensity of the reflected x-rays depends on the relative arrangement of atoms in the crystal. The angle of x-rays reflected from crystal depends on the dimensional characteristics of the lattice. Each material has a unique x-ray diffraction pattern. In case of ZSM-5 ion exchange with other cations yields essentially the same pattern with minor shift in relative intensity (Argauer and Landolt, 1972).

The XRD measurements were made with a Rigaku diffractometer (Rigaku Company, Tokyo, Japan) using Cu-K_α radiation filtered by a graphite monochromator at 40 KeV and 123 mA. The powdered samples were smeared on a glass slide with methanol and dried at room temperature. The X-ray diffractograms were recorded from 4° to 80° at a speed of 5° (2θ) per min.

3.2.3 BET surface area, pore size and pore volume

The BET surface area, pore size and pore volume measurements of the catalysts were done using a Micromeritics adsorption equipment (ASAP 2000, manufactured by Micromeritics Instruments Inc., Norcross, GA, USA) using N_2 gas (99.995% pure, supplied by Praxair, Mississauga, ON, Canada). BET analysis was performed on calcined catalyst. Each analysis required about 0.5 to 1.0 g of catalyst sample. Before the analysis catalyst sample was treated for 4 hours at 200 ^{o}C at a pressure of $5x10^{-4}$ torr to ensure that there was no adsorbed moisture on the catalyst surface. The adsoption and desorption isotherms used in the evaluation of BET surface area were obtained at the boiling temperature of nitrogen (-195 ^{o}C). These values are characteristic of a given catalyst sample and are reproducible.

3.2.4 Scanning electron microscopy (SEM)

Scanning electron microscope features of fresh and spent catalysts were studied by using a Phillips SEM 505 scanning electron microscope. The SEM instrument was operated at 300 KeV/SE and 50° inclination. Prior to analysis, all the samples were gold coated in a sputter coating unit (Edward Vacuum Components Ltd. Sussex, England). The micrographs were recorded using photographic techniques. The images were captured at magnification of 1:20,000.

3.2.5 Fourier transformed infrared spectroscopy (FTIR)

The IR measurements were made in the hydroxyl group and pyridine regions using Perkin Elmer Infrared spectrophotometer (Model spectrum GX). Pyridine vapors were adsorbed on the catalyst sample at 170 ^{o}C for 45 min, the sample was then allowed

to cool to room temperature and the spectra were recorded. All the spectra were obtained in the region 400-4000 cm^{-1} were differential absorption spectra with 2 cm^{-1} resolution. On the basis of the pyridine band between 1440 and 1640 cm^{-1}, the presence of Bronsted and Lewis acid sites was identified.

3.3   Experimental program

The scope of this experimental work was to study the potential of production of value-added liquid chemicals from the glycerol in a fixed bed micro reactor at atmospheric pressure. The effects of operating parameters such as temperature, carrier gas flow rate and weight hourly space velocity (WHSV) were investigated on glycerol conversion and liquid product yield. The operating parameters were optimized for maximum glycerol conversion and liquid product yield. The catalysts were characterized to understand the effect of fundamental properties such as pore size, surface area, crystallinity and acidity on the performance of catalysts in terms of glycerol conversion and total liquid product.

3.3.1   Statistical design of experiments

Design-Expert version 6.0.1, Stat-ease Inc., Minneapolis, USA was used for statistical design of experiments (DoE) and the same software was used for the analysis of experimental data. DoE is an organized approach that connects experiments in a rational manner giving more precise information in fewer experiments as compared to conventional design of experiments where one factor was varied at a time. One of the useful outcomes of DoE is response surface maps of experimental region.

Response surface method (RSM) is a collection of statistical and mathematical techniques useful for empirical modeling and analysis of problems (Noordin et al., 2004). RSM is especially useful when the response is influenced by several variables and the objective is to optimize the response. RSM also quantifies the relation among one or more measured response and the vital input factors (Thomas et al., 1997). Each factor is studied at a number of factor levels. In this research work, central composite inscribed (CCI) design was used to generate response surfaces.

The phases of the DoE approach are listed below:

1. Identification of the factors that may affect the outcome of the experiment or the response.

2. Choice of an appropriate experimental design for response surface modeling.

3. Determination of the experiments that need to be conducted.

4. Performing the experiments and collection of the data.

5. Data fitting and generation of plots that describe the trends of results and to draw conclusions.

Factorial design of experiments is more popular than other types of experimental design such as crossed and mixture. The design region is represented as a cube with possible combinations of factors (low and high) at the corners of this cube. Central composite design types are based on this cube with experimental points at corners, centers of faces and center of edges. The cubic designs are popular because they are symmetrical and straight forward to model which in turn facilitates easy interpretation of the results. Choice of the design is finally a tradeoff between the information required and the number of experiments to be conducted. The number of experimental runs is determined by the following equation:

$$N = 2^k + 2k + 6 \qquad\qquad (3.1)$$

Where, k is the number of factors in the design.

For three factor design k = 3, thus the number of experiments is 20 (Design Expert 6.0.1 manual). A template of design experiments is given in Table 3.1. In this design the effects of operating condition (factors) such as temperature, carrier gas flow rate and WHSV can be studied on the responses such as glycerol conversion and various liquid product, char and gas yields.

Once the experiments have been conducted the collected data are analyzed to quantify the relationship between one or more of the measured response and the input factors. Steps to analyze the collected data are summarized as follows:

1. Input of the response (eg. glycerol conversion in Table 3.1) to be analyzed into the design expert software

2. Choice of a transformation if desired.

3. Selection of the appropriate model to be used. The fit summary button displays the F-test, lack of fit test and other measures that could be helpful in selecting the appropriate model.

4. Performing the analysis of variance (ANOVA), post-ANOVA analysis of individual coefficients and case statistics for analysis of residuals and outlier detection.

5. Studying various diagnostic plots to statistically validate the model.

6. Generation of model graphs such as 3D plots and contours for interpretation of the results.

Table 3.1: Design of experiments obtained from Design Expert Software 6.0.1

EXP #	Temperature (^{o}C)	Carrier gas flow rate (mL/min)	WHSV (h^{-1})	Glycerol conversion (wt%)
1	380	26	8.68	
2	425	35	13.50	
3	425	35	13.50	
4	380	26	18.32	
5	500	35	13.50	
6	470	26	18.32	
7	470	44	18.32	
8	470	44	8.68	
9	350	35	13.50	
10	380	44	18.32	
11	425	35	13.50	
12	425	35	13.50	
13	470	26	8.68	
14	425	35	5.40	
15	380	44	8.68	
16	425	50	13.50	
17	425	35	13.50	
18	425	20	13.50	
19	425	35	13.50	
20	425	35	21.60	

3.3.1.1   Test of significance of the model

Least square technique is used to fit a model equation containing the input variables (factors) by minimizing the residual errors. Residual error is measured as the sum of squares of deviations between the actual and estimated responses. Test of significance of the model is performed using ANOVA by calculating the F-ratio. F-ratio, also called the variance ratio, is the ratio of variance due to effect of model and variance due to error term. F-ratio is also described as the ratio of regression mean square and mean square error. A good model must be significant. The test of significance is performed with the help of P-values. If the P-value is less than 0.05, the model is significant and vice-versa.

3.3.1.2   Test of significance of individual model coefficients

This test is performed by determination of probability value (P-value) for individual model coefficients. The insignificant model coefficients are deleted through backward elimination.

3.4   Experimental setup for catalytic conversion of glycerol

Catalytic conversion of glycerol was performed in a down flow fixed bed reactor at atmospheric pressure. A schematic diagram of the experimental setup is shown in Figure 3.1. The reactor consisted of an Inconel® 625 tube 530 mm in length with internal diameter of 9.5 mm, external diameter of 12.5 mm and fitted with Swagelok™ fittings at both ends. Feed was introduced through a 110 mm long feed line at feed inlet located at 55 mm from top flange of reactor. Near the feed inlet a T- joint was provided to have carrier gas flow into the reactor. Nitrogen was used as carrier gas (supplied by Praxair, Mississauga, ON, Canada). The flow of carrier gas was controlled
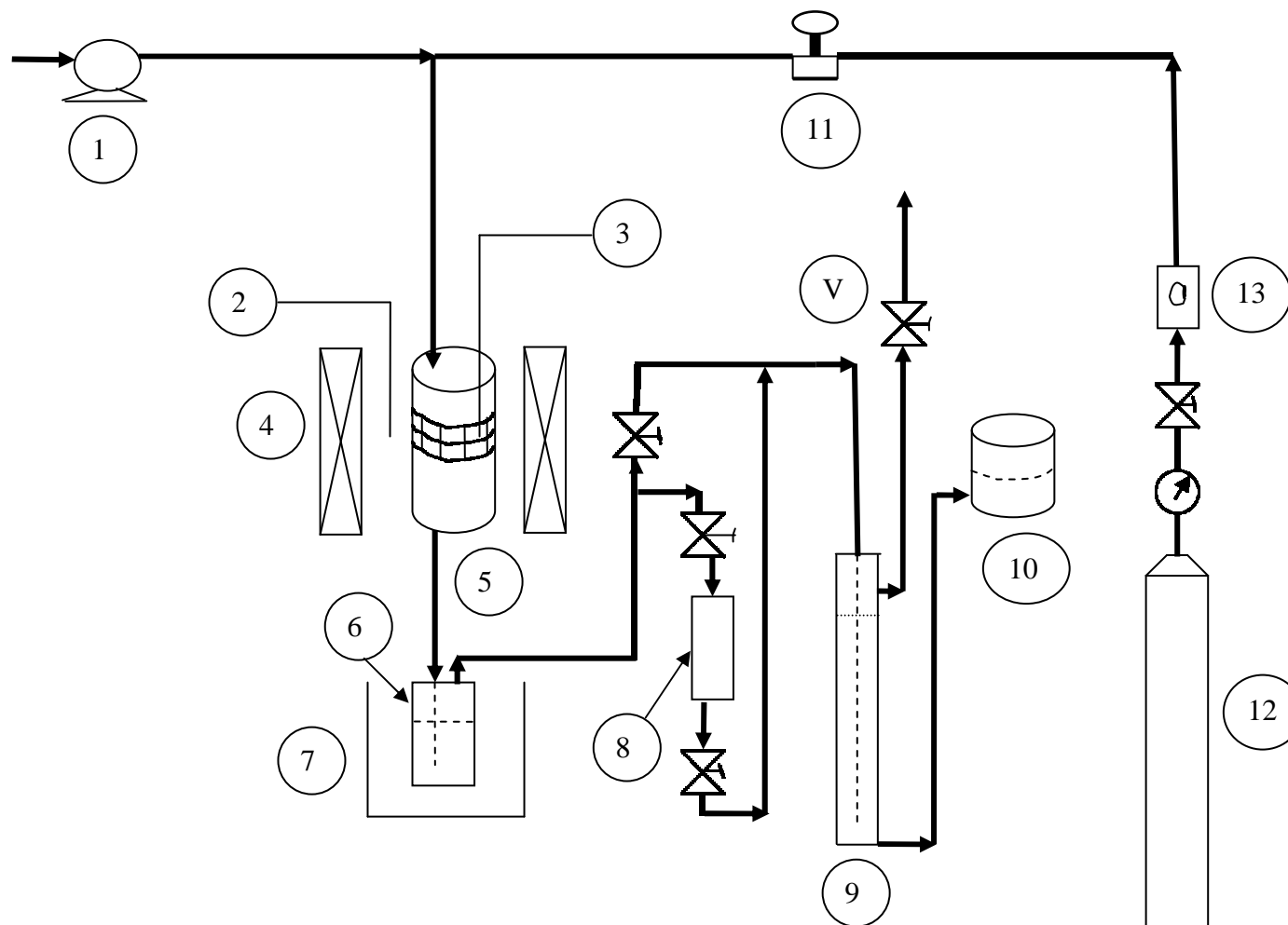
Figure 3.1: Schematic diagram for experimental set up for catalytic conversion of glycerol
1. Syringe pump 2. Temperature controller 3. Temperature indicator 4. Electric Furnace 5. Fixed bed reactor 6Liquid collector 7. Condenser 8. Sampler 9. Gas collector 10. Brine solution 11. Check valve 12. Nitrogen cylinder 13. Mass flow controller, V- valve

using a needle valve and the flow meter (supplied by Sierra Instruments Inc, California, USA) was used to record the carrier gas flow rate. Calibration of the flow meter was done using a bubble flow meter. The calibration curve for the flow meter is shown in Appendix H1. Catalyst was loaded into the reactor over a stainless steel mesh covered with quartz wool inserted at 280 mm from top flange of reactor. The catalyst was diluted using silicon carbide (80 mesh) particles (supplied by Exolon-Esk, Tonawanda, New York, USA). Dilution was done to maintain a constant bed height of 70 mm for all the experiments. The reactor was vertically mounted into an electrically heated annular furnace. The reactor was fitted with K-type thermocouple (accuracy $\pm$ 2-3 ^{o}C) in contact with outer wall of reactor. Reactor temperature was controlled by series SR22 microprocessor based tuning PID controller (supplied by Shimaden Co. Ltd., Tokyo, Japan). Another K-type thermocouple was buried into the catalyst bed using a stainless steel thermo-well.

Feed was pumped using a programmable syringe pump, Genie (supplied by Kent Scientific Corporation). The calibration curve for the pump is given in Appendix H1. The pump was capable of dispensing the feed at uniform rate, accurate up to three decimal places. The reactor was fitted with ice cooled condenser at the exit where most of the liquid products were collected and gas products were collected over saturated brine solution in a gas collector.

The setup was fitted with a gas sampler. It was used to continuously sample product gas when carrying out the deactivation studies of the catalysts. Initially, there was some problem with the syringe pump needle. The pump was fitted with 22 gage needle. It was found that there was high pressure drop in the needle of pump. This caused the pump to choke and it was not able to dispense any feed. Needles of bigger

opening were tried and finally 16 gage needle was found to be working satisfactorily to dispense desired flow rates of the feed.

3.5 A typical experimental run

The reactor was cleaned, dried and then loaded with the catalyst and sealed with Swagelok™ fitting at both ends. An anti-seal (supplied by Kleen Flo Tumbler, Montreal, Canada) was used to prevent sealing of joints at high temperature. After recording the reactor weight it was mounted into the annular furnace and the feed line and condenser were connected. Carrier gas (nitrogen) flow was established through the reactor at desired flow rate. Set point temperature was reached in 30 to 50 min while the flow of nitrogen was maintained through the reactor. Once the set point temperature reached injection of feed was started at a constant flow rate of 5.4 g/h. The run time of each experiment was 60 min. Run time of 60 min for experiments was chosen based on the time on stream study of the catalyst when the feed was pumped continuously for 90 min and it was found that there was no significant change in glycerol conversion as measured by the analysis of liquid product. After the 60 min run time carrier gas flow rate was maintained for 2 more min to flush the entire products from the reactor.

The liquid and gaseous products were passed through a Na-Cl - ice condenser where most of the liquid product was condensed and product gases were collected over a saturated brine solution. The amount of liquid and char produced was determined by the difference in weight of liquid collector and reactor before and after the reaction. The volume of produced gas was measured from the calibrated scale attached to the liquid collector. Samples calculations for mass balance are given in Appendix H3.

3.6 Analysis of products

The gas products from the experiments were analyzed using gas chromatographs HP 5880 and HP 5890. Liquid products were analyzed using Varian 3400 and Fison GC/MS 8000 series. The detailed discussion on methodology for these analyses is described below.

3.6.1 Gas product analysis

The gas products were analyzed using two gas chromatographs (GCs). H_2, CO and CO_2 were analyzed using an HP 5890 fitted with a thermal conductivity detector (TCD) having Carbosive S II column (3000 m, i.d. 3.18mm) with helium (supplied by Praxair, Mississauga, ON, Canada) as carrier gas. The program conditions were: initial temperature of 40 ^{o}C, initial temperature hold time of one min, heating rate of 12 ^{o}C/min, final temperature of 200 ^{o}C, final temperature hold time of one min and detector temperature of 250 ^{o}C.

Hydrocarbons such as CH_4, C_2+ were analyzed using HP 5880 GC. This GC was equipped with a flame ionization detector (FID) and Chromosorb 102 column (1.8 m, i.d. 3.18 mm). Helium was used as the carrier gas. Air and hydrogen (supplied by Praxair, Mississauga, ON, Canada) mixture was used to ignite the FID. HP 5880 was programmed using following conditions: initial temperature of 40 ^{o}C, initial temperature hold time of 3 min, column heating rate of 10 ^{o}C/min, final temperature of 200 ^{o}C, final hold time of 2 min and detector temperature of 250 ^{o}C. The GCs were calibrated using the standard gas mixtures (see Appendix H2).

3.6.2 Typical gas product analysis

A gas sample of 700 µL was injected into the TCD of HP 5890 GC using Gastight # 1001 syringe (supplied by Hamilton Co. Reno, Nevada). It took approximately 15 min to detect hydrogen, nitrogen, carbon monoxide and carbon dioxide. The GC oven was then allowed to cool to its initial temperature of 40 ^{o}C before another injection was made. Also, a gas sample of 700 µL was injected into the FID of HP 5880 GC. The analysis of gas sample in HP 5880 took approximately 21 min where hydrocarbons including methane were analyzed. The peak areas from the GCs were used to calculate number of moles of each component present in gas mixture at standard temperature and pressure (STP). The volume of the gas and composition of gas were calculated on nitrogen free basis (see Appendix H3).

3.6.3 Liquid product analysis

The compounds present in the liquid product obtained from catalytic conversion of glycerol were identified using GC-MS and quantified using Varian 3400 GC. The GC was equipped with the stabilwax (cross bonded, 30 m long, i.d. 0.25mm) capillary column. The GC-MS was programmed using: initial temperature of 40 ^{o}C, initial temperature hold time of 5 min, heating rate of 5 ^{o}C/min, final temperature of 200 ^{o}C, final temperature hold time of 15 min and the detector temperature of 220 ^{o}C. Split ratio in the injector was 1:20 at 220 ^{o}C. The residence time of the compounds identified by GC-MS matched closely when pure compounds were injected into Varian 3400 GC. The standard solutions of pure compounds were prepared and calibration curves were plotted for each of the liquid compounds (see Appendix H2).

3.6.4 Typical liquid product analysis

The liquid product from the experiments contained low boiling point chemicals such as acetaldehyde and acrolien. Some of the compounds including acrolein were unstable at room temperature, so the product liquid from experiments was always kept refrigerated. The product liquid sample was diluted with 2 parts of water and mixed thoroughly. A sample of 0.4 µL of this mixture was injected using Microliter # 95 syringe (supplied by Hamilton Co. Reno, Nevada) into the FID of Varian 3400 GC. The analysis of liquid product sample took approximately 52 min where compounds such as acetalydehyde, acrolien, acetone, acetol, allyl alcohol and formaldehyde etc. were identified. The peak areas were used to calculate the wt% of the components in the liquid product (see Appendix H3).

4 RESULTS AND DISCUSSION

4.1 Catalyst characterization

The catalysts used in the present research work were HZSM-5, HY, silica-alumina and γ-alumina. Physiochemical properties of these catalysts were studied using TPD, XRD, BET surface area, pore size, SEM and FTIR measurement techniques. Detailed results from catalyst characterization are described in the following section.

4.1.1 Temperature programmed desorption (TPD)

Temperature programmed desorption was carried out to study the acidic properties of different catalysts (Figure 4.1). Ammonia as basic molecule was adsorbed on acid centers of the catalysts. The increase in temperature for ammonia desorption corresponds to increase in the strength of acidity of catalysts. From the literature it is seen that there are three ranges for the desorption of ammonia, namely, 20-200, 200-350 and 350-550 ^{o}C, which correspond to weak, intermediate and strong acid centers, respectively (Lewandowski and Sarbak, 2000). If the desorption peak intensity is high then the number of acid sites is large and vice versa.

The TPD curve for HZSM-5 consists of two major peaks (see Figure 4.1). First peak at 250 ^{o}C corresponds to the intermediate acid sites whereas the peak beyond 400 ^{o}C corresponds to strong acid centers. Also, the intensity of the peak at 250 ^{o}C was more as compared to the one beyond 450 ^{o}C. This indicates that in HZSM-5 the number of intermediate acid sites is more as compared to strong acid centers, which are
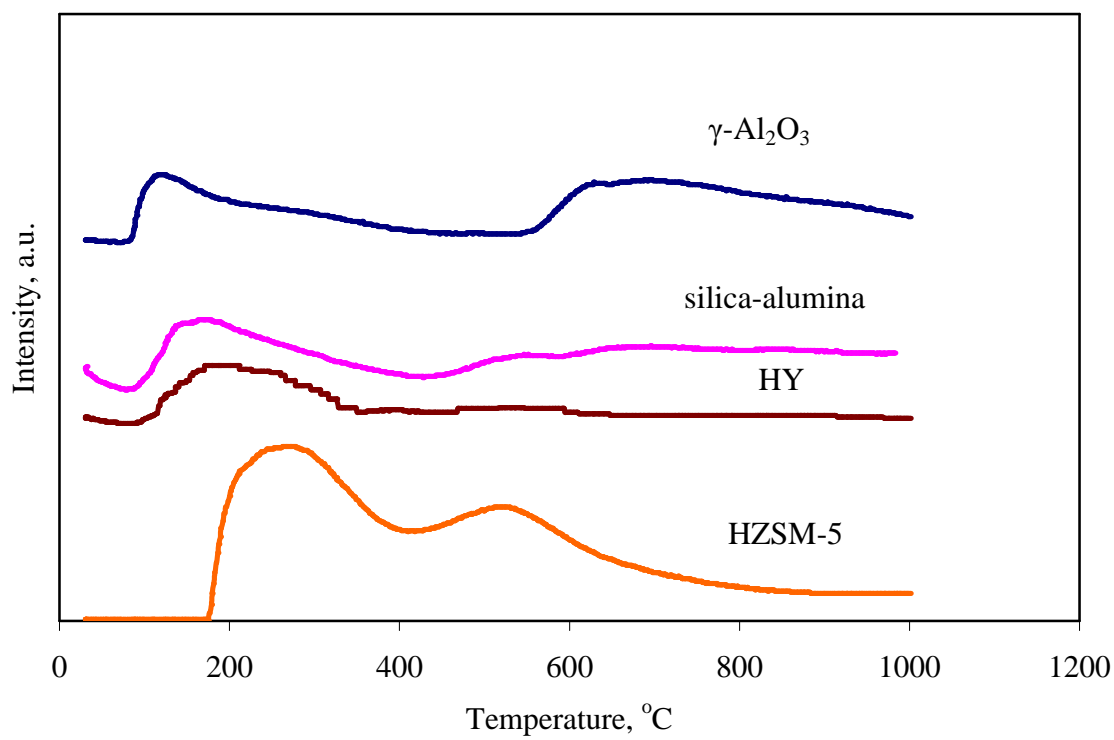
Figure 4.1: Temperature programmed desorption (TPD) profiles of different catalysts

similar to those reported in literature (Anderson et al., 1979; Katikaneni et al., 1998).

The TPD curve for HY has only one peak at temperature less than 200 $^{\circ}$C, which indicates the presence of weak-intermediate acid sites. TPD curve for silica-alumina consisted of a peak at temperature less than 200 $^{\circ}$C, however the intensity was more as compared to that for HY. This indicates that the number of weak acid sites present in silica-alumina was more as compared that of HY. This observation is similar to those reported in literature (Rajagopal et al., 1992; Rinaldi et al., 2004; Akpanudoh et al., 2005). The TPD profile for γ-alumina shows the presence of weak acid centers (peak at ~130 $^{\circ}$C) as well as strong acid centers (peak at ~620 $^{\circ}$C) in this catalyst.

4.1.2 X-Ray diffraction (XRD)

X-ray diffraction was carried out to identify the crystalline structure of different catalysts. The X-ray patterns for HZSM-5, HY, silica-alumina and γ-alumina are shown in Figure 4.2. Presence of crystalline structure was observed in the case of HZSM-5, HY and γ-alumina whereas no crystalline structure was observed for silica-alumina (Szostak, 1992; Zhong et al., 2001; Rinaldi et al., 2004).

4.1.3 BET surface area and pore size

The results of BET analysis for different catalysts are shown in Table 4.1. BET surface area analysis with HY was repeated and the results were reproducible. The BET surface areas for HZSM-5 and silica-alumina are comparable as observed from Table 4.1. The highest surface area (625 m^2/g) was observed for HY whereas γ-alumina showed the lowest surface area (235 m^2/g). The pore size of catalysts ranged from 0.54 to 11.2 nm. HZSM-5 has the smallest pore size (0.54 nm) and γ-alumina has biggest pore size (11.2 nm) among the catalysts chosen. HZSM-5 and HY were microporous
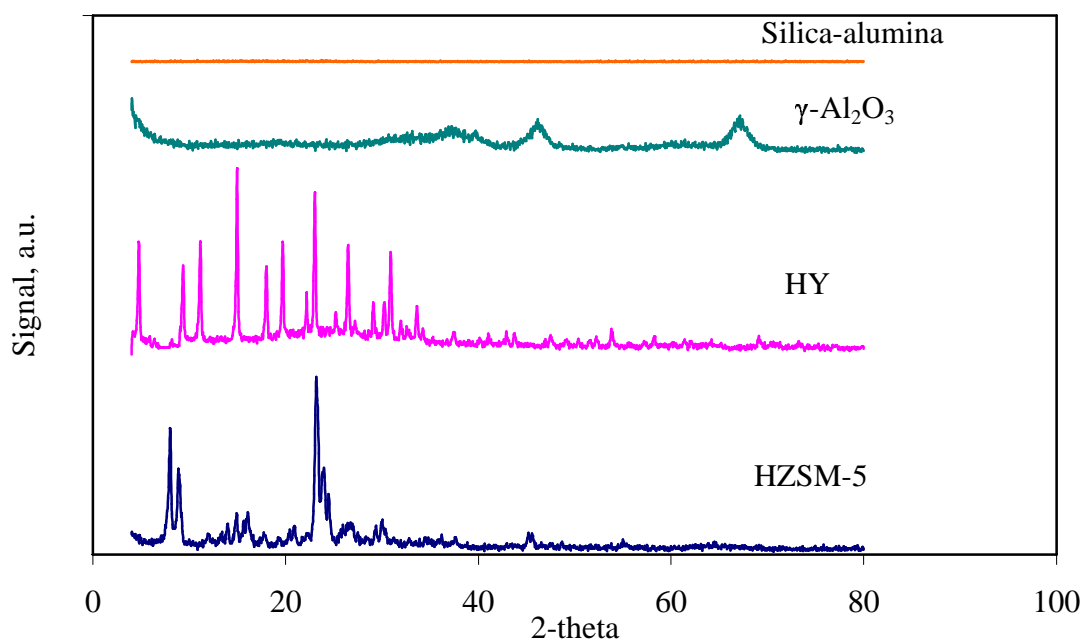
Figure 4.2: X-ray diffraction patterns for different catalysts
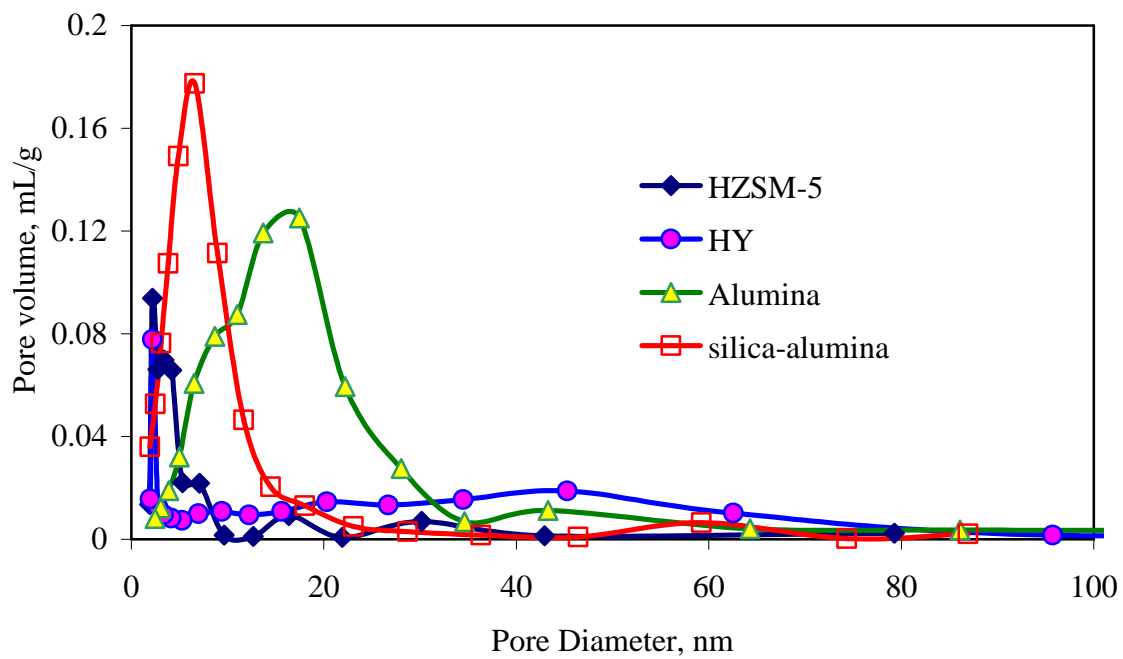
Figure 4.3: Pore size distribution for different catalysts

Table 4.1: BET surface area, pore size and pore volume of different catalysts

Catalyst	BET surface area (m^2/g)	Average Pore size (nm)	Pore volume (mL/g)
HZSM-5	319	0.54	0.16
HY	625 ± 11	0.74 ± 0.04	0.42 ± 0.03
Silica-alumina	321	3.15	0.77
γ-alumina	235	11.2	0.67

materials (pore size < 2 nm) whereas, silica-alumina and γ-alumina were mesoporous materials with pore size from 2-50 nm (Katikaneni et al., 1998; Bhatia, 1989; Satterfield, 1991). The surface area for HY matched with as reported by supplier (655 m^2/g). The surface area measurements for other catalysts also matched with those reported by the supplier. Figure 4.3 shows the pore size distribution for different catalysts. It was observed that HY, silica-alumina and γ-alumina have narrow pore size distribution as compared to HZSM-5.

4.1.4   Fourier transformed infrared spectroscopy (FTIR)

Pyridine adsorption was used to detect the presence of Bronsted and Lewis acid sites present in the catalysts (see Figure 4.4). HZSM-5 and HY have Bronsted (indicated by B in Figure 4.4) as well as Lewis acid sites (indicate by L) which are shown by the presence of peak at 1560 cm^{-1} and 1510 cm^{-1}, respectively. Similar observations were made by Adjaye et al. (1996) and Anand et al. (2003). γ-alumina has mainly Lewis acidity as indicated by the presence of peak at 1650 cm^{-1} whereas silica-alumina mainly has Bronsted acidity as shown by the presence of peak at 1560 cm^{-1}. These observations are in agreement with those reported in literature (Plyuto et al., 1999; Dabbagh et al., 2005).
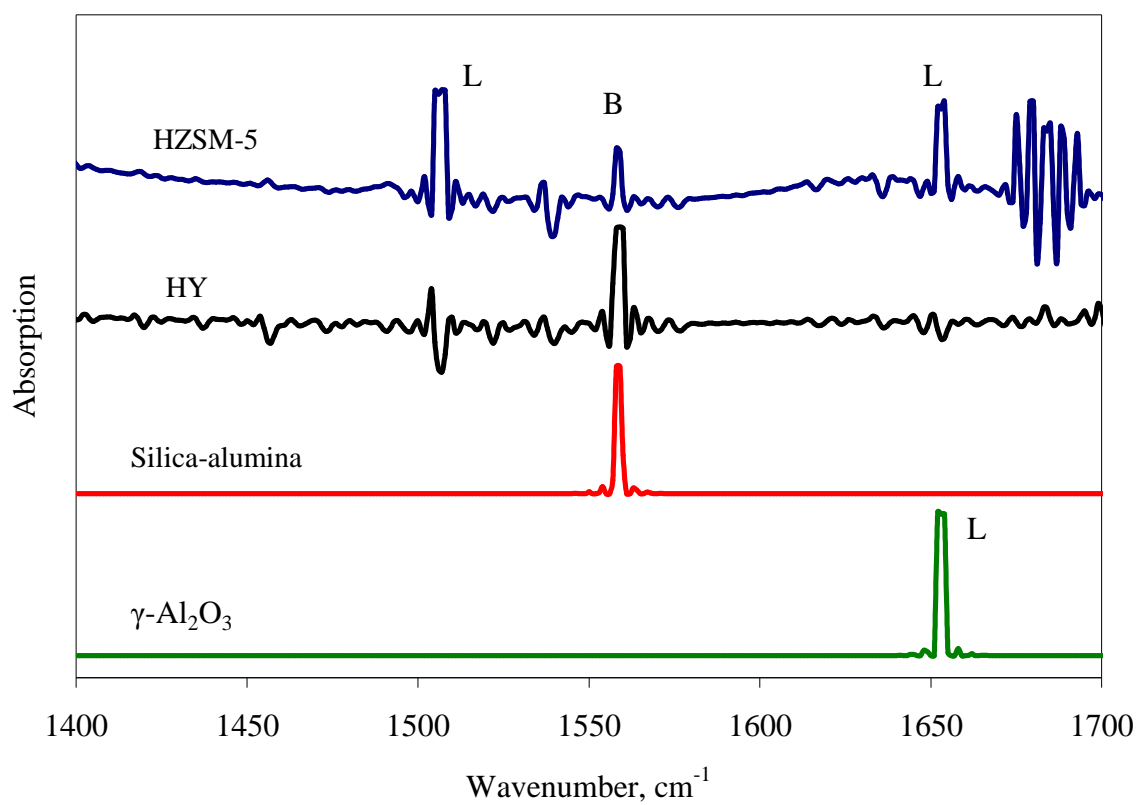
Figure 4.4: FTIR spectra of different catalysts in pyridine region

4.2 Catalyst performance studies on glycerol conversion, liquid, gas and char yield and acetaldehyde, acrolein, formaldehyde and acetol yields

In this work the performances of different catalysts such as HZSM-5, HY, silica-alumina and γ-alumina in terms of glycerol conversion, liquid, gas and char yield and acetaldehyde, acrolein, formaldehyde and acetol yield are described.

The preliminary experiments performed over HZSM-5 at 400 ^{o}C with 0.5 g of catalysts in a fixed bed reactor indicated that there is a potential to produce value added liquid chemicals from glycerol. Interestingly more that 90 wt% of the products were liquid with remarkably low yields of gas (4 to 6 wt%) and char. The glycerol conversion was only 46 wt%. The compounds identified in the liquid product were acetaldehyde, acrolein, acetone, acetol, acetic acid, propanoic acid, phenol, formaldehyde, isopropyl alcohol, allyl alcohol, glycerol formal and water. The gas product consisted of CO, CO_2, and hydrocarbons such as CH_4. Furthermore, Thiruchitrambalam et al. (2004) reported that H_2 rich syn-gas can be produced from pyrolysis of glycerol at 800 ^{o}C varying carrier gas flow rate from 30 to 70 mL/min.

Based on these preliminary experiments and the work reported in literature (Thiruchitrambalam et al., 2004; Cortright et al., 2002; Buhler et al., 2002) the temperature range of 350 to 500 ^{o}C, carrier gas flow rate of 20 to 50mL/min and WHSV of 5.40 to 21.60 h $^{-1}$ were chosen for investigation in this research work. WHSV is defined as the ratio of glycerol feed flow rate (maintained constant at 5.40 g/h) to catalysts wt. The WHSV range of 5.40 to 21.60 h $^{-1}$ corresponds to catalyst weight range from 1 to 0.25 g.

4.2.1 Statistical analysis of experimental data for glycerol conversion

Glycerol conversion was calculated from the following equation:

$$X = \left(1 - \frac{U}{F}\right) * 100 \qquad (4.1)$$

Where,   X =   Glycerol conversion, wt%

             U =   Unconverted glycerol in liquid product, g

             F =   Glycerol fed, g

The experimental results for glycerol conversion over different catalysts are given in Appendices A, B, C and D.

The time-on-stream study was conducted with all catalysts. No significant decrease in glycerol conversion was observed for a run time of 90 min (see Figure 4.5). Based on this study a run time of 60 minutes was chosen for each experiment. Material balance for all experiments using different catalysts was in the range from 90 to 96 percent. A few experiments were repeated for all catalysts under identical conditions. The results were reproducible within ± 4 %. Table 4.2 and 4.3 show the reproducibility of experimental results for liquid, gas and char yields and product yields of different liquid chemicals from glycerol conversion over HZSM-5.

Based on the variance analysis (see Appendix G; Table G1) linear model (empirical) was used to predict glycerol conversion over HZSM-5 with R^2 value of 0.96. The model coefficients to predict glycerol conversion (within the range of operating parameters) over this catalyst are given in Table 4.4. The coefficients of model terms would indicate if the corresponding factor has statistically significant effect on the glycerol conversion. For instance, in Table 4.4 the coefficients for interaction of temperature and carrier gas flow rate, temperature and WHSV and carrier gas flow rate
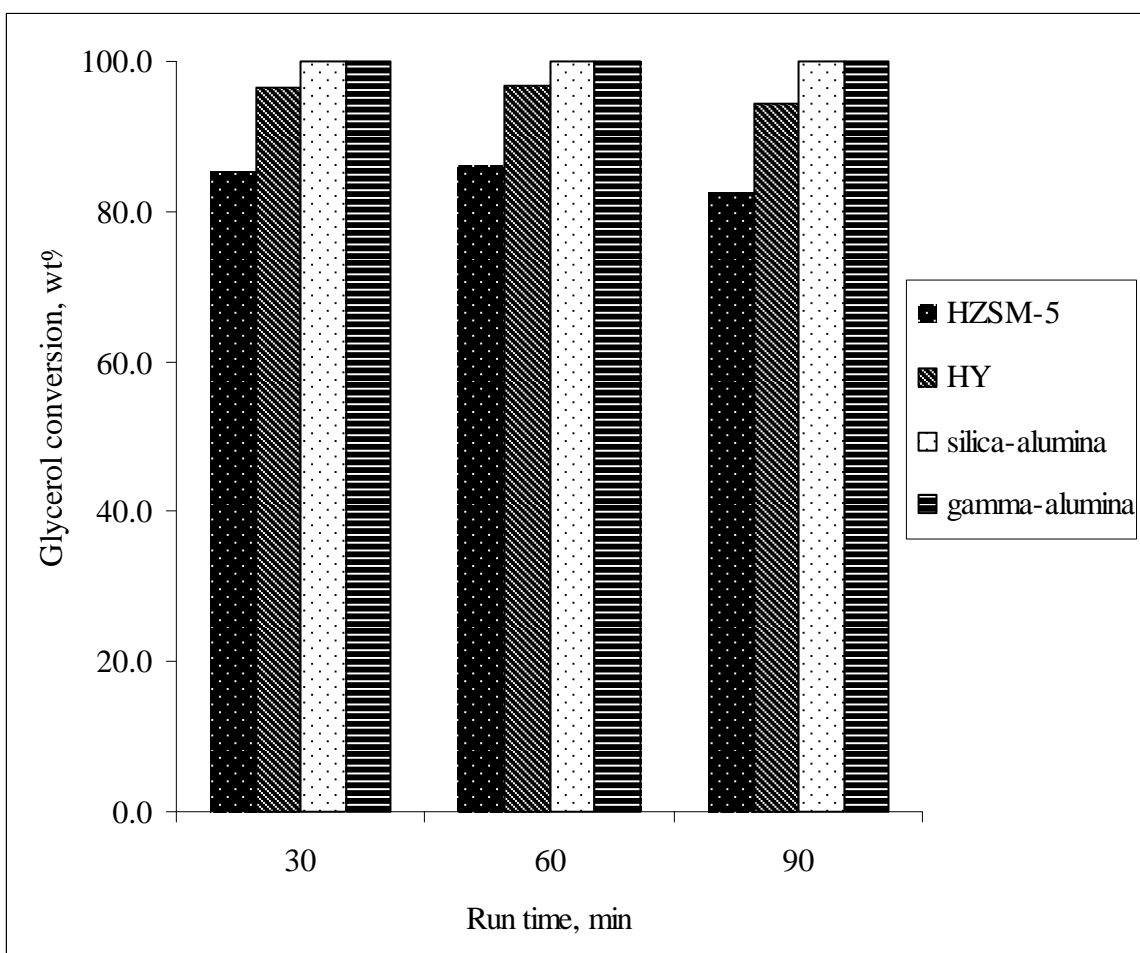
Figure 4.5: Time-on-stream study for different catalysts

Table 4.2: Reproducibility of experimental results for liquid, gas and char yield from glycerol conversion over HZSM-5

EXP #	Operating conditions			Glycerol fed (g)	Conversion (wt%)	Total liquid product (g)	Gas product (g)	Char and residue (g)	Total product (g)	Percentage of total Products (wt%)			Mass Balance (wt%)
	T (°C)	CGF (mL/min)	WHSV (h⁻¹)							Gas	Liquid	Char and residue	
2	425	35	13.50	4.99	52.6	4.34	0.04	0.13	4.51	0.82	96.30	2.88	91.7
3	425	35	13.50	5.10	46.3	4.37	0.03	0.22	4.62	0.84	94.50	4.66	94.8
11	425	35	13.50	5.15	44.0	4.57	0.04	0.22	4.57	0.86	93.30	4.53	94.2

Table 4.3: Reproducibility of experimental results for product yields of different liquid chemicals over HZSM-5

Compound wt %	Experiment number		
	2	3	11
Acetaldehyde	7.59	8.51	8.72
Acetone	0.47	0.53	0.21
Acrolein	5.04	5.89	7.00
Formaldehyde	7.47	8.51	7.72
IPA	0.26	0.49	0.25
Allyl Alcohol	8.32	6.77	6.42
Acetol	16.80	15.21	14.94
Acetic Acid	1.04	1.14	0.81
propionic Acid	2.84	2.45	2.21
Glycerol Formal	1.82	2.63	2.45
Phenol	0.23	0.29	0.15
Water	23.53	29.73	29.27
Unknowns	24.59	17.86	19.84
Total	100.00	100.00	100.00

Table 4.4: Significant model coefficients to predict glycerol conversion over HZSM-5 and HY

Factors	Glycerol conversion (wt%)	
	HZSM-5*	**HY
Intercept	-61.81	-406.32
T	0.33	2.07
C	-0.19	2.51
W	1.55	-4.46
T^2	0	-2.04E-03
C^2	0	0.01
W^2	0	-0.13
T*C	0	-8.27E-03
T*W	0	0.01
C*W	0	0.03

*Glycerol conversion over HZSM-5,

$$X = -61.81 + 0.33*T - 0.19*C + 1.55*W \qquad (4.2)$$

**Glycerol conversion over HY,

$$X = -406.32 + 2.07*T + 2.51*C - 4.46*W - 2.04E\text{-}03*T^2 + 0.01*C^2$$
$$- 0.13*W^2 - 8.27E\text{-}03*T*C + 0.01*T*W + 0.03*C*W \qquad (4.3)$$

Where,   X   =   glycerol conversion, wt%

T   =   temperature, ^{o}C

C   =   carrier gas flow rate, mL/min

W   =   weight hourly space velocity, h^{-1}
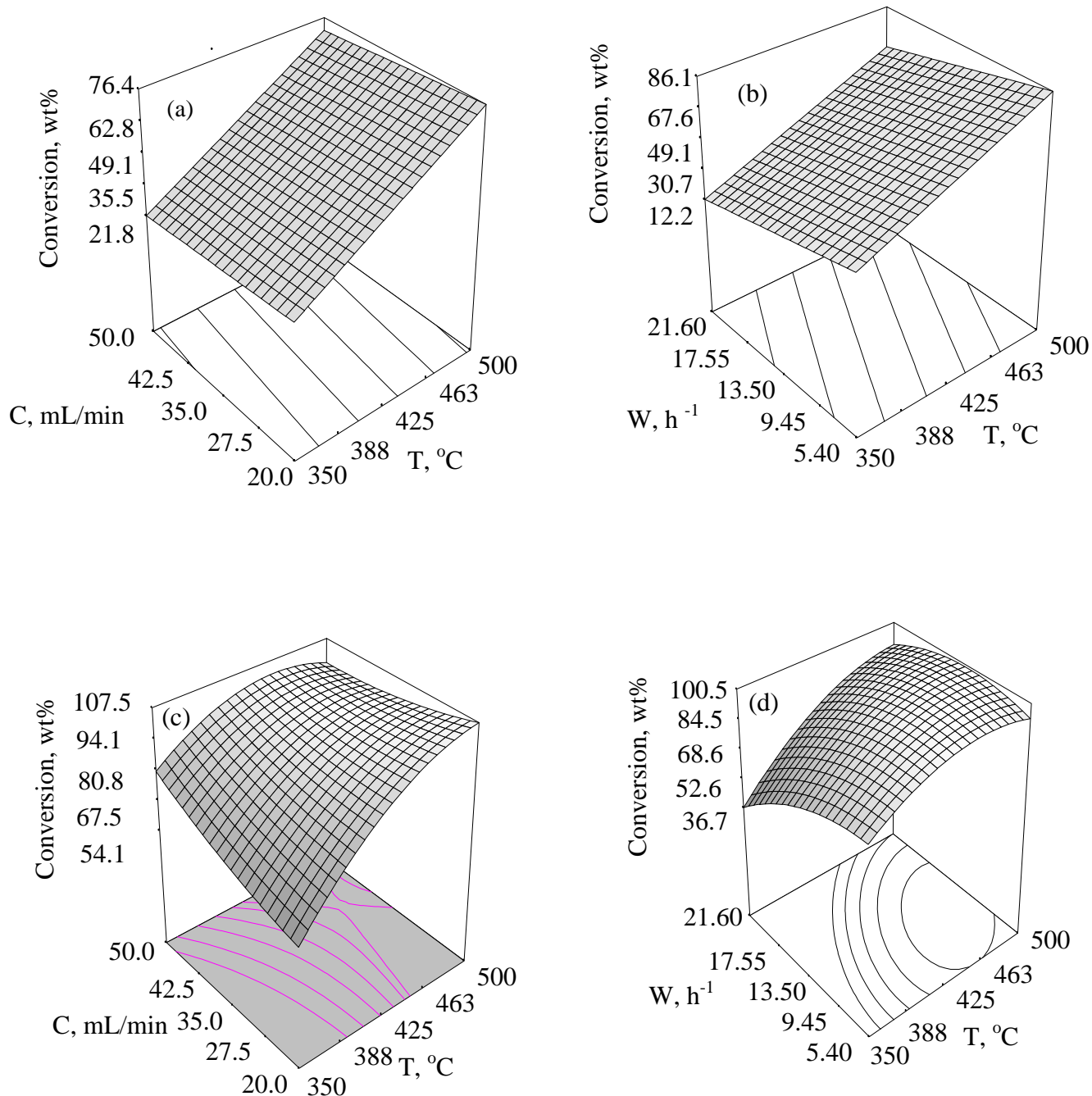
Figure 4.6: **Surface response for glycerol conversion: (a) effect of temperature and WHSV at carrier gas flow rate of 35 mL/min using HZSM-5; (b) effect of temperature and carrier gas flow rate at WHSV of 13.50 h^{-1} using HZSM-5; (c) effect of carrier gas flow rate and temperature at WHSV of 13.50 h^{-1} using HY; (d) effect of WHSV and temperature at carrier gas flow rate of 35 mL/min using HY**

are zero. This indicates that the interaction of temperature and carrier gas flow rate, temperature and WHSV and carrier gas flow rate are statistically insignificant for glycerol conversion. In the following discussion, table of significant coefficients will be given to predict the corresponding response. The empirical equations are generated as shown in equations 4.2 and 4.3.

The response surface to describe glycerol conversion over HZSM-5 is shown in Figure 4.6 (a) and (b). There was no significant change in glycerol conversion with change in the carrier gas flow rate within the range studied at a constant temperature as shown in Figure 4.6 (a). This was because HZSM-5 has intermediate and strong acid sites. Glycerol molecule would have strongly adsorbed on the acid surface to undergo cracking (Gates 1979). Thus, within the operating temperature range (350 to 500 $^{\circ}$C), carrier gas flow rate and hence residence time would not affect glycerol conversion in case of HZSM-5. On the other hand, it would appear that the operating temperature has significant effect on glycerol conversion. For example, glycerol conversion increased from 13.6 to 86.1 wt% when the temperature was increased from 350 to 500 $^{\circ}$C at WHSV of 5.40 h^{-1} when carrier gas flow rate was maintained constant at 35 mL/min as shown in Figure 4.6 (b). This could be due to diffusion limitations because of small pore size of HZSM-5. Therefore, glycerol conversion in this case was strongly dependent on temperature.

A quadratic model (see Appendix G; Table G1) was used to predict the glycerol conversion over HY. The model coefficients are shown in Table 4.4. In this case temperature, carrier gas flow rate and WHSV have significant effect on glycerol conversion. The surface response to describe glycerol conversion over HY is shown in Figure 4.6 (c) and (d). Glycerol conversion increased from 59 to 98 wt% when the

temperature was increased from 350 to 500 ^{o}C at carrier gas flow rate of 20 mL/min and WHSV of 13.50 h $^{-1}$. However, maximum conversion (100 wt%) was achieved at 470 ^{o}C and medium carrier gas flow rate of 26 mL/min. Glycerol conversion more than 100 wt% was predicted at 500 ^{o}C and carrier gas flow rate of 20 mL/min from the model to maintain the continuity of the response surface as shown in Figure 4.6 (c). Glycerol conversion increased from 36.7 to 100 wt% with the increase in temperature from 350 to 500 ^{o}C at WHSV of 5.40 h $^{-1}$ and carrier gas flow rate of 35 mL/min as shown in 4.6 (d). Higher glycerol conversion was achieved with HY as compared to HZSM-5 which could be due to somewhat larger pore size of the HY catalyst. Complete conversion of glycerol was attained from silica-alumina and γ-alumina which indicates that in addition to pore size, total acidity of the catalyst played important role on glycerol conversion.

Numerical optimization was performed to find out the optimum operating conditions for maximum glycerol conversion. Variable simplex was used as the optimization technique (Design Expert 6.0.1 manual). The optimum operating conditions for predicted and experimental maximum glycerol conversion are shown in Table 4.5. Low deviation between the predicted and experimental glycerol conversion confirmed that the model can predict the glycerol conversion accurately. It was observed that under similar operating conditions, higher glycerol conversion was obtained with HY than that with HZSM-5 as shown in Table 4.5. In the case of HY, complete conversion was attained in all experiments that were performed at temperatures greater than 470 ^{o}C. The minimum temperature giving the highest conversion was chosen for the optimization of operating conditions in case of HY.

Table 4.5: Predicted and experimental maximum glycerol conversion over HZSM-5 and HY at optimum conditions

Catalyst	Temperature (^{o}C)	Carrier gas flow rate (mL/min)	WHSV (h^{-1})	Glycerol conversion (wt%)	
				Predicted	Experimental
HZSM-5	470	26	8.68	77.2	78.8
HY	470	26	8.68	100	100

4.2.2 Statistical analysis of experimental data for liquid product yield

Liquid product yield (g/100 g feed) was calculated using the following equation:

$$L = \left\{ \frac{L_T - F(1-X)}{F} \right\} *100 \qquad (4.4)$$

Where, L =   Liquid product yield, g/100 g feed

L_T =   Total liquid (including unconverted glycerol), g

F =   Glycerol fed, g

X =   Fractional glycerol conversion

Liquid product yield under experimental conditions using different catalysts was in the range from 11 to 85 g/100g feed (see Appendix E1). Experimental results showed that the liquid product yield was higher over silica-alumina and γ-alumina than that over HZSM-5 and HY.

A possible reaction pathway for the catalytic conversion of glycerol is given in Figure 4.7. Free radical pathways dominate mainly at high temperature whereas ionic pathways dominate at low temperature (Buhler et al., 2002). It was proposed that liquid product (including acetaldehyde, acrolein, formaldehyde and acetol) was formed primarily through ionic pathways, which dominate over the free radical pathways at low temperature. Therefore liquid product yield should be favored at low temperature. However, in case of HZSM-5 and HY, in addition to reaction temperature, the pore size has significant effect on liquid product yield. Higher temperature was required to overcome the diffusion limitations imposed by smaller pore size of these catalysts. A trend of increasing glycerol conversion with increase in temperature was observed with these catalysts (see Figure 4.6). Liquid product yield is a function of glycerol conversion
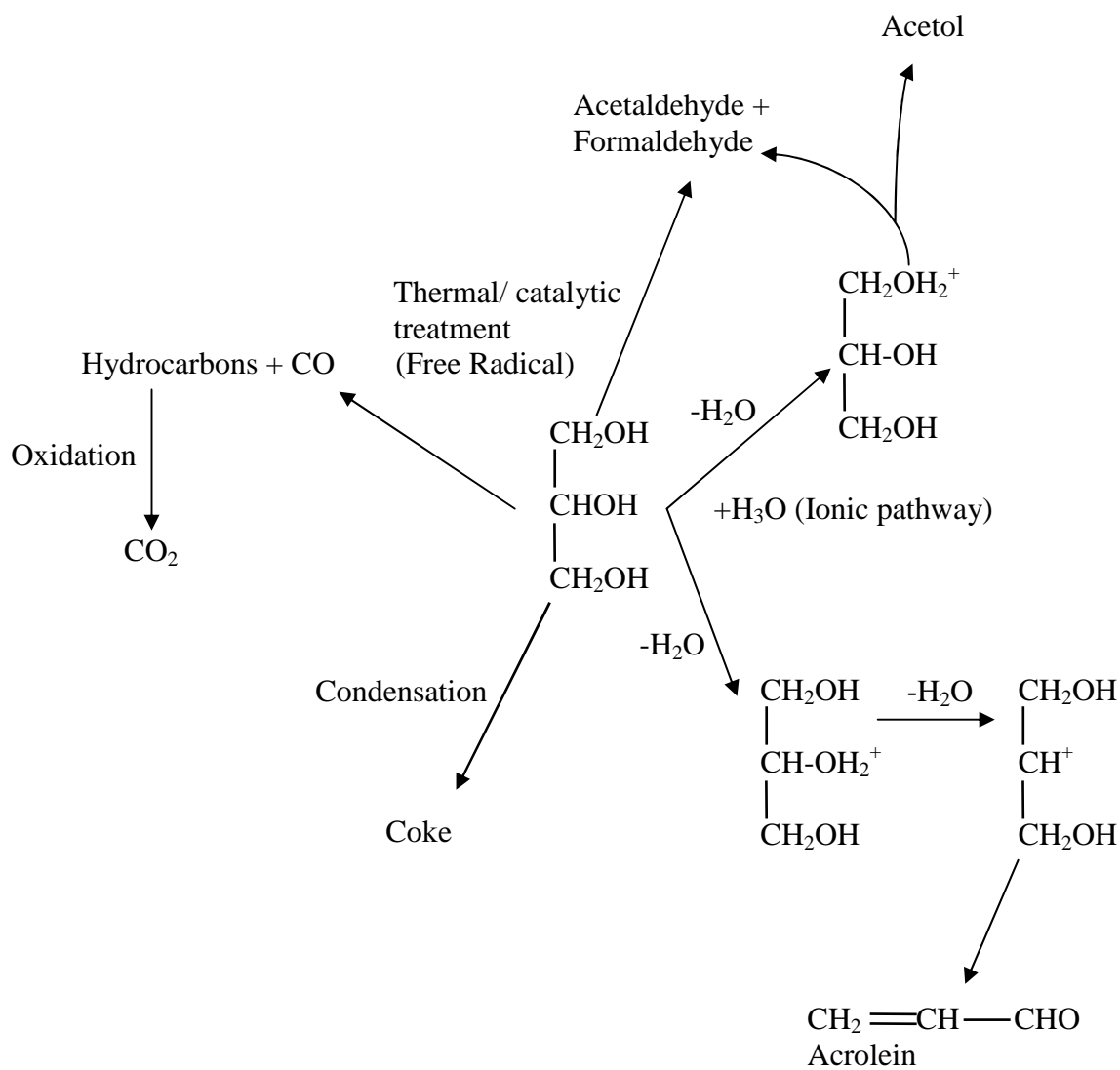
Figure 4.7: Proposed reaction pathways for catalytic conversion of glycerol

as shown Equation 4.4. Therefore, higher temperature seems to favor the liquid product yield with these catalysts with relatively large amount of micropores.

The model coefficients to predict liquid product yield using different catalysts is given in Table 4.6. The surface response for liquid product yield in case of HZSM-5 and HY is shown in Figure 4.8. In case of HZSM-5, temperature, carrier gas flow rate and WHSV were significant parameters to predict liquid product yield (see Appendix G; Table G2). Liquid product yield increased from 4.3 to 66.4 g/100 g feed with increase in temperature from 350 to 500 ^{o}C when carrier gas flow rate was maintained constant at 20 mL/min as shown in Figure 4.8 (a). At WHSV of 5.40 h $^{-1}$ liquid product yield increased from 1 to 69.6 g/100 g feed with increase in temperature from 350 to 500 ^{o}C as shown in Figure 4.8 (b).

Reduced quadratic model was used to predict (R^2 value of 0.95) liquid product yield using HY. In this case, temperature and WHSV were significant parameters to predict liquid product yield whereas the effect of carrier gas flow rate was insignificant (see Appendix G; Table G2). For example, as shown in Figure 4.8 (c) liquid product yield was around 46.8 g/100 g feed and did not change with variation in carrier gas flow rate from 20 to 50 mL/min at 350 ^{o}C. As shown in Table 4.6, large coefficient for temperature term accounts for the significant effect of temperature on liquid product yield. It was observed that at WHSV of 5.40 h $^{-1}$, the liquid product yield increased to 72 g/100 g feed at 463 ^{o}C and with further increase in temperature to 500 ^{o}C it decreased to 64.2 g/100 g feed as shown in Figure 4.8 (d). This decrease in liquid product yield at higher temperature was marked by increase in the gas product yield.

Table 4.6: Significant model coefficients to predict liquid product yield over different catalysts

Factors	Liquid product yield (g/100 g feed)			
	HZSM-5	HY	Silica-alumina	γ-alumina
Intercept	-81.25	-397.93	-256.85	105.49
T	0.34	2.15	-0.42	-0.01
C	-0.37	0	-2.64	-0.02
W	-1.08	-2.33	-5.26	-0.84
T^2	0	-2.52E-03	0	-2.19E-04
C^2	0	0	0	-8.59E-03
W^2	0	-20	0	-0.02
T*C	0	0	5.66E-03	2.67 E-03
T*W	0	0.02	0.01	3.32 E-03
C*W	0	0	0.03	-0.03
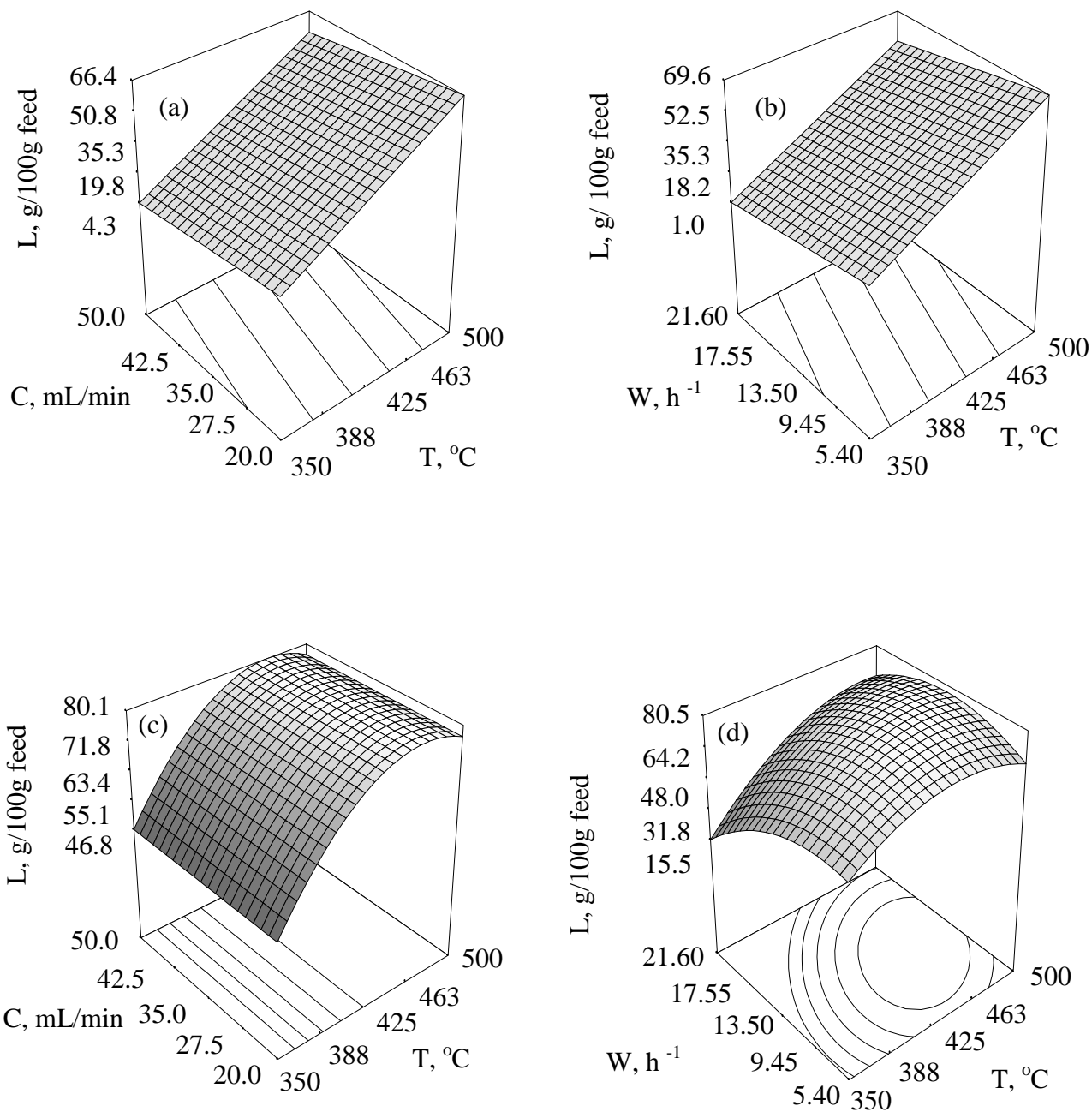
Figure 4.8: Response surface for liquid product yield (L): (a) effect of temperature and carrier gas flow rate at WHSV of 13.50 h⁻¹ using HZSM-5; (b) effect of temperature and WHSV at carrier gas flow rate of 35 mL/min using HZSM-5; (c) effect of temperature and carrier gas flow rate at WHSV of 13.50 h⁻¹ using HY; (d) effect of temperature and WHSV at carrier gas flow rate of 35 mL/min using HY

The response surface to predict (R^2 value of 0.88) liquid product yield using silica-alumina is shown in Figure 4.9 (a) and (b). It was interesting to observe that at lower temperature of 350 ^{o}C increase in carrier gas flow rate from 20 to 50 mL/min liquid product yield was almost 78 g/ 100 g feed, while at higher temperature of 500 ^{o}C there was a sharp increase in liquid product yield from 65 g/ 100 g feed at 20 mL/min to 82 g/100 g feed at 50 mL/min. With increase in carrier gas flow rate (decrease in residence time) higher liquid product yield is obtained because feed molecule would not get sufficient time to undergo cracking to produce gas products. Furthermore, at WHSV of 5.40 h $^{-1}$ with the increase in temperature from 350 to 500 ^{o}C liquid product yield decreased from 79.9 to 62.1 g/100 g feed when carrier gas flow rate was maintained constant at 35 mL/min. It could be due to the cracking of liquid products to gas products at higher temperature as evident from the possible reaction pathways (see Figure 4.7).

A quadratic model was significant to predict liquid product yield using γ-alumina with R^2 value of 0.84 (see Appendix G; Table G2). In this case temperature and WHSV were statistically significant parameters whereas carrier gas flow rate was insignificant. Liquid product yield decreased from 84 to 75.8 g/100 g feed when the temperature was increased from 350 to 500 ^{o}C and WHSV was maintained constant at 5.40 h $^{-1}$ as shown in Figure 4.9 (c). Also, the liquid product yield decreased from 80 to 73 g /100 g feed when temperature was increased from 350 to 500 ^{o}C at carrier gas flow rate of 50 mL/min and WHSV of 13.50 h $^{-1}$ as shown in Figure 4.9 (d).

In the case of silica-alumina and γ-alumina, the presence of large pore size offers negligible diffusional limitations to feed molecules. Therefore, liquid product yield with these catalysts was favored at low temperature as shown in Figure 4.9.
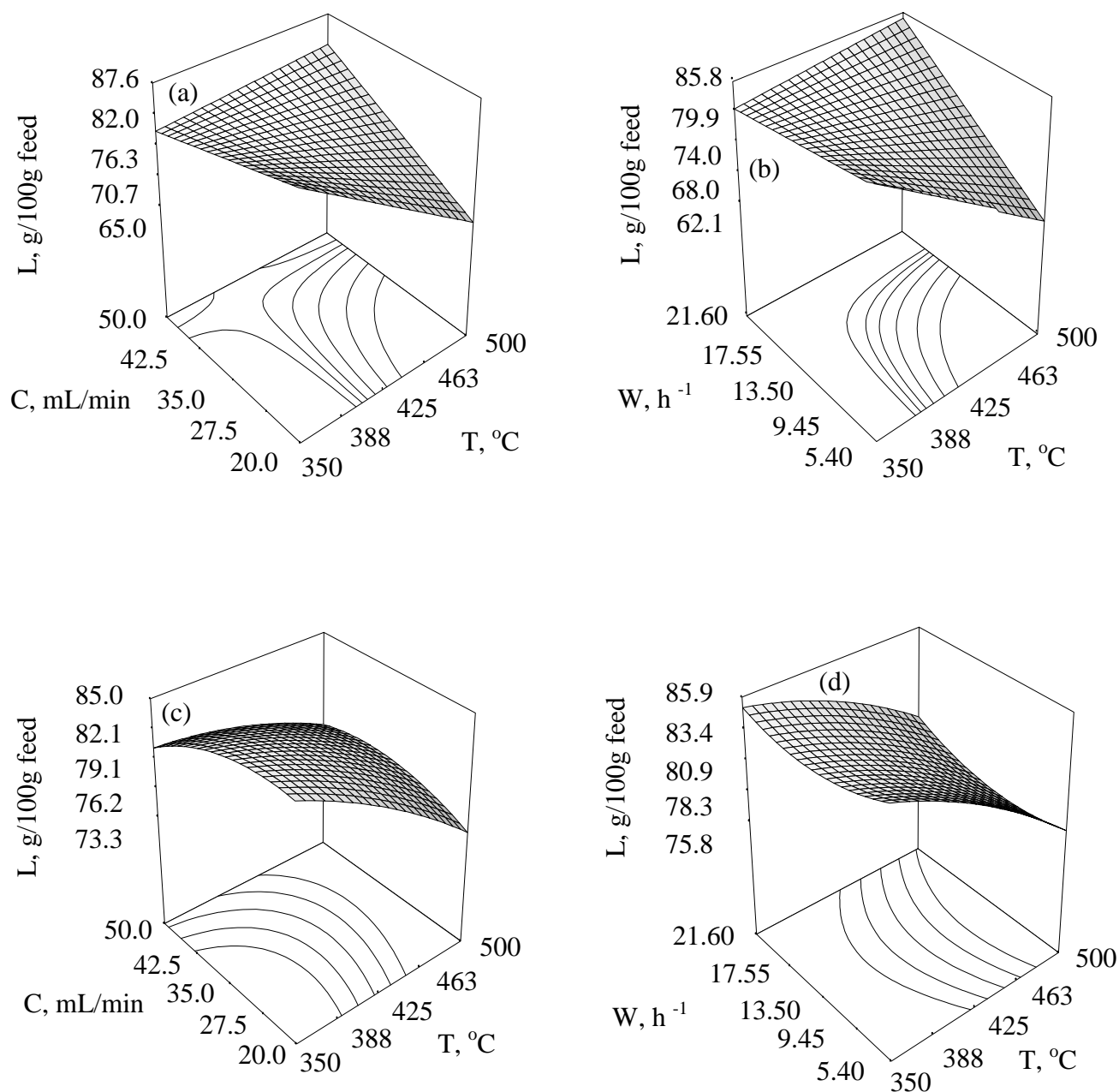
Figure 4.9: Response surface for liquid product yield (L): (a) effect of temperature and carrier gas flow rate at WHSV of 13.50 h $^{-1}$ using silica-alumina; (b) effect of temperature and WHSV at carrier gas flow rate of 35 mL/min using silica-alumina; (c) effect of temperature and carrier gas flow rate at WHSV of 13.50 h $^{-1}$ using γ-alumina; (d) effect of temperature and WHSV at carrier gas flow rate of 35 mL/min using γ-alumina

Numerical optimization was carried out to find the optimum conditions for maximum liquid product yield using different catalysts. The predicted and experimental liquid product yield at optimum operating conditions with different catalysts is shown in Table 4.7. It was interesting to observe that maximum liquid product yield was obtained at a lower temperature of 380 ^{o}C using silica-alumina and γ-alumina, whereas for HZSM-5 and HY higher temperature was required for liquid product yield. For example, liquid product yield of 80.9 g/100 g feed was obtained in case of HY at 425 ^{o}C, 50 mL/min and WHSV of 13.50 h^{-1} as compared to 64 g/ 100 g feed of liquid product yield at 470 ^{o}C, 26 mL/min and WHSV of 8.68 h^{-1} in case of HZSM-5.

In summary, silica-alumina and γ-alumina were the best catalysts to obtain maximum liquid product yield (~83 g/100 g feed) at temperature as low as 380 ^{o}C. HY was the second best catalyst with comparable liquid product yield (~81 g/100 g feed) at higher temperature of 425 ^{o}C. Furthermore, liquid product yield using silica-alumina and γ-alumina varied between a narrow range from 71 to 84 and 78 to ~86 g/100 g feed, respectively (see Appendix E1). The product yield of individual liquid components such as acetaldehyde, acrolein, formaldehyde and acetol is further optimized and discussed in the following section.

Table 4.7: Predicted and experimental maximum liquid product yield under optimum conditions over different catalysts

Catalyst	Temperature (^{o}C)	Carrier gas flow rate (mL/min)	WHSV (h^{-1})	Liquid product yield (g/ 100g feed)	
				Predicted	Experimental
HZSM-5	470	26	8.68	64.4	59.0
HY	425	50	13.50	82.8	80.9
Silica-alumina	380	26	8.68	83.4	83.5
γ-alumina	380	44	8.68	83.3	83.6

4.2.3 Statistical analysis of experimental data for product yield of liquid components

Identification of the liquid product composition was a major challenge. Special efforts were made in order to develop a methodology for identification of the liquid product constituents. In this work up to 90 wt% of the liquid products were identified. It was interesting to observe that four major chemicals constituted up to as much as 60 wt% of the liquid product. These chemicals were acetaldehyde (ethanal), acrolein (2-propenal), formaldehyde (methanal) and acetol (hydroxy acetone). Other chemicals present in the liquid product included acetone (di-methyl ketone), acetic acid (ethanoic acid), propionic acid, glycerol formal (mixture of 5-hydroxy-1,3-dioxane (60%) and 4-hydroxymethyl-1,3-dioxolane (40%)), isopropyl alcohol (2-propanol) and phenol (hydroxybenzene). It was observed that water was one of the products as well. The composition of liquid product obtained from glycerol conversion over HZSM-5, HY, silica-alumina and γ-alumina is given in Appendices A, B, C and D, respectively.

As acetaldehyde, acrolein, formaldehyde and acetol were the major chemicals present in the liquid product, it was of interest to study the effect of operating conditions on product yields of these chemicals over different catalysts.

The proposed reaction pathways for production of these chemicals are shown in Figure 4.7. It was proposed that at lower temperature, liquid products such as acetaldehyde, acrolein, formaldehyde and acetol were formed predominantly by ionic pathways. It was also proposed that acetaldehyde and formaldehyde were formed by free radical pathways as well. Gaseous product such as CO, CO_2, CH_4 and C_2+ hydrocarbons were formed through free radical pathways which dominate over the ionic pathways at higher temperature. Coke formation was the result of condensation and polymerization.

4.2.3.1 Acetaldehyde yield

Acetaldehyde was one of the valuable chemical present in the liquid product. Acetaldehyde yield under experimental conditions is given in Appendix F1. As much as 21 g/100 g feed of acetaldehyde was detected in liquid product. Model coefficients to predict acetaldehyde yield using different catalysts are given in Table 4.8. The effect of operating conditions on acetaldehyde yield with different catalysts is shown in Figure 4.10.

Buhler et al. (2002) proposed formation of acetaldehyde mainly through free radical pathways during supercritical treatment of glycerol. However, in this research work it is proposed that the formation of acetaldehyde takes place through free radical as well as ionic pathways. Therefore, the maximum acetaldehyde yield should occur at intermediate temperatures (425 to 470 ^{o}C). Furthermore, catalyst pore size and total acidity have important effect on acetaldehyde yield. HZSM-5 and HY have smaller pore sizes as compared to silica-alumina and γ-alumina. Therefore, in case of catalysts such as HZSM-5 and HY higher temperature was needed for maximum acetaldehyde yield. The higher temperature would increase the rate of mass transfer in the small pores. High temperature in case of these catalysts favored liquid product yield (see Figure 4.8) which lead to the higher acetaldehyde yield.

In the case of HZSM-5, HY and γ-alumina, temperature and WHSV were significant whereas in the case of silica-alumina temperature and carrier gas flow rate were significant parameters to predict acetaldehyde yield (see Appendix G; Table G3). An increasing trend of acetaldehyde yield with the increase in temperature in cases of HZSM-5 and HY are shown in 4.10 (a) and (b). This observation is in line with the proposed reaction pathways as explained earlier.

Table 4.8: Significant model coefficients to predict acetaldehdye yield over different catalysts

Factors	Acetaldehyde yield (g/100 g feed)			
	HZSM-5	HY	Silica-alumina	γ-alumina
Intercept	-20.40	-79.83	10.24	98.93
T	0.07	0.36	0.06	-0.49
C	-0.09	0	-1.07	0.36
W	0.24	-0.57	0	-0.20
T^2	0	-3.73E-04	0	6.30E-04
C^2	0	0	0.02	-4.95E-03
W^2	0	-0.06	0	0
T*C	0	0	0	0
T*W	0	4.72E-03	0	0
C*W	0	0	0	0
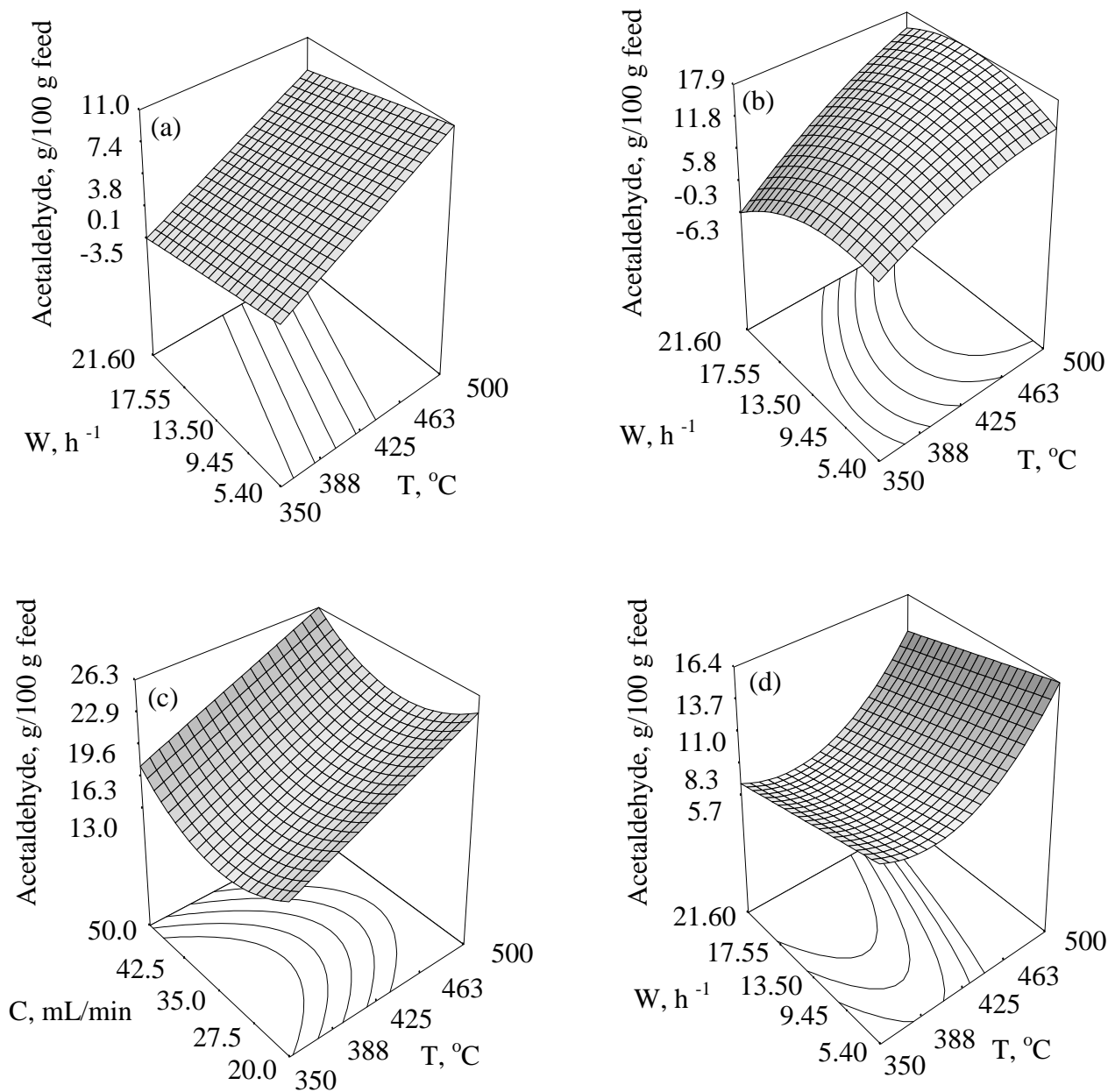
Figure 4.10: Response surface for acetaldehyde yield: (a) effect of temperature and WHSV at carrier gas flow rate at of 35 mL/min using HZSM-5; (b) effect of temperature and WHSV at carrier gas flow rate at of 35 mL/min using HY; (c) effect of temperature and carrier gas flow rate at WHSV of 13.50 h^{-1} using silica-alumina; (d) effect of temperature and carrier gas flow rate at WHSV of 13.50 h^{-1} using γ-alumina

In the case of HY, high temperature and medium WHSV seem to favor acetaldehyde yield. For example, acetaldehyde yield has increasing trend with increase in temperature. Maximum acetaldehyde yield (17.9 g/100 g feed) occurred at 500 ^{o}C and WHSV of 13.50 h $^{-1}$ as shown in Figure 4.10 (b). It was proposed that both acetaldehyde and formaldehyde formed through free radical as well as ionic pathways. In case of HY, it was observed that high temperature favored formation of acetaldehyde. This could be due to decrease in formaldehyde yield with increase in temperature of 425 ^{o}C (see Figure 4.12 (b)).

In the case of silica-alumina, acetaldehyde yield increased from 13 to 23.2 g/100 g feed with increase in temperature from 350 to 500 ^{o}C at carrier gas flow rate of 20 mL/min. It was observed that maximum acetaldehyde yield (24.5 g/100 g feed) occurred at temperature of 470 ^{o}C, carrier gas flow rate 44 mL/min and WHSV of 18.32 h $^{-1}$ as shown in Figure 4.10 (c). These observations support the proposed possible reaction pathways where acetaldehyde formation is favored at intermediate temperature. In case of silica-alumina (large pore size) there are less diffusion limitations as compared to HZSM-5 and HY and therefore acetaldehyde formation is favored at intermediate temperature.

In the case of γ-alumina, it was observed that there was no significant change in acetaldehyde yield with increase in temperature from 350 to 425 ^{o}C at all WHSVs and acetaldehyde yield was constant at about 6 g/100 g feed as shown in Figure 4.10 (d). With further increase in temperature to 500 ^{o}C there was sharp increase in acetaldehyde yield and it was 16.4 g/100 g feed at WHSV of 5.40 h $^{-1}$. Furthermore, with increase in WHSV from 5.40 to 21.60 h $^{-1}$ at 500 ^{o}C, acetaldehyde yield decreased from 16.4 to 13.7 g/100 g feed. Thus, it seemed that WHSV was a significant parameter only at higher

temperatures. It was observed that high temperature (500 ^{o}C) was needed for maximum acetaldehyde yield. This was because low temperature in this case seems to favor the formation of formaldehyde. For example, formaldehyde yield showed an increasing trend with increase in temperature up to 425 ^{o}C, however with further increase in temperature it showed a decreasing trend as shown in Figure 4.12 (d).

The predicted and experimental maximum acetaldehyde yield at optimum conditions with different catalysts is shown in Table 4.9. It was observed that silica-alumina produced maximum acetaldehyde (24 g/100 g feed) at 470 ^{o}C, carrier gas flow rate of 44 mL/min and WHSV of 18.32 h $^{-1}$. HY produced 17.8 g/100 g feed acetaldehyde at temperature of 500 ^{o}C, carrier gas flow rate of 35 mL/min and WHSV of 13.50 h $^{-1}$. At this temperature γ-alumina produced ~15 g/100 g feed of acetaldehyde. Maximum acetaldehyde obtained using HZSM-5 was ~ 11g/100 g feed at 470 ^{o}C, carrier gas flow rate of 26 mL/min and WHSV of 8.68 h $^{-1}$.

To summarize, silica-alumina was the best catalyst for maximum acetaldehyde yield at temperature of 470 ^{o}C, carrier gas flow rate of 35 mL/min and WHSV of 13.50 h $^{-1}$.

Table 4.9: Optimum operating conditions for maximum acetaldehyde yield over different catalysts

Catalyst	Temperature (^{o}C)	Carrier gas flow rate (mL/min)	WHSV (h^{-1})	Acetaldehyde yield (g/ 100g feed)	
				Predicted	Experimental
HZSM-5	470	26	8.68	8.9	11.2
HY	500	35	13.50	17.6	17.8
Silica-alumina	470	44	18.32	21.8	24.5
γ-alumina	500	35	13.50	14.8	15.1

4.2.3.2 Acrolein yield

Acrolein was another major chemical detected in the liquid product. It is used as a fungicide in agriculture industry. Under the experimental conditions acrolein present in the liquid product ranged from 1 to 25 g/100 g feed (see Appendix F2). The model coefficients and response surface to predict acrolein yield are given in Table 4.10 and Figure 4.11, respectively.

In this research work it is proposed that acrolein was formed through ionic pathways (see Figure 4.7). At lower temperature ionic pathways dominate over free radical pathways. Therefore, the formation of acrolein might be favored at low temperature. However, in the case of HZSM-5 and HY, due to small pore size as compared to silica-alumina and γ-alumina high temperature favors acrolein production. In case of silica-alumina and γ-alumina, large pore sizes offer negligible diffusion limitations and hence acrolein yield over these catalysts is favored at low temperatures as proposed by reaction pathways. The observed trends for acrolein yield using different catalysts are discussed in this section.

A linear model was statistically significant to predict acrolein yield in case of HZSM-5. It was observed that temperature, carrier gas flow rate and WHSV have significant effect on acrolein yield (see Appendix G; Table G4). Acrolein yield increased gradually with increase in temperature and it was 8.8 g/100 g feed at 500 ^{o}C and WHSV of 5.4 h^{-1} as shown in Figure 4.11 (a). It was observed that at low WHSV of 5.40 h^{-1} temperature has a strong effect as compared to that at WHSV of 21.60 h^{-1}.

In the case of HY, temperature and WHSV were major factors to predict acrolein yield over HY. In this case, high temperature seems to favor acrolein yield. For example,

Table 4.10: Significant model coefficients to predict acrolein yield over different catalysts

Factors	Acrolein yield (g/100 g feed)			
	HZSM-5	HY	Silica-alumina	γ-alumina
Intercept	-11.25	-124.15	88.59	63.42
T	0.05	0.65	0.19	-0.18
C	-0.09	0	-1.36	0.79
W	-0.27	-1.48	0.37	-2.62
T^2	0	-8.23E-04	0	0
C^2	0	0	0	0
W^2	0	-0.08	0	0
T*C	0	0	-3.25 E-03	0
T*W	0	-7.95 E-03	0	0.01
C*W	0	0	0	-0.05
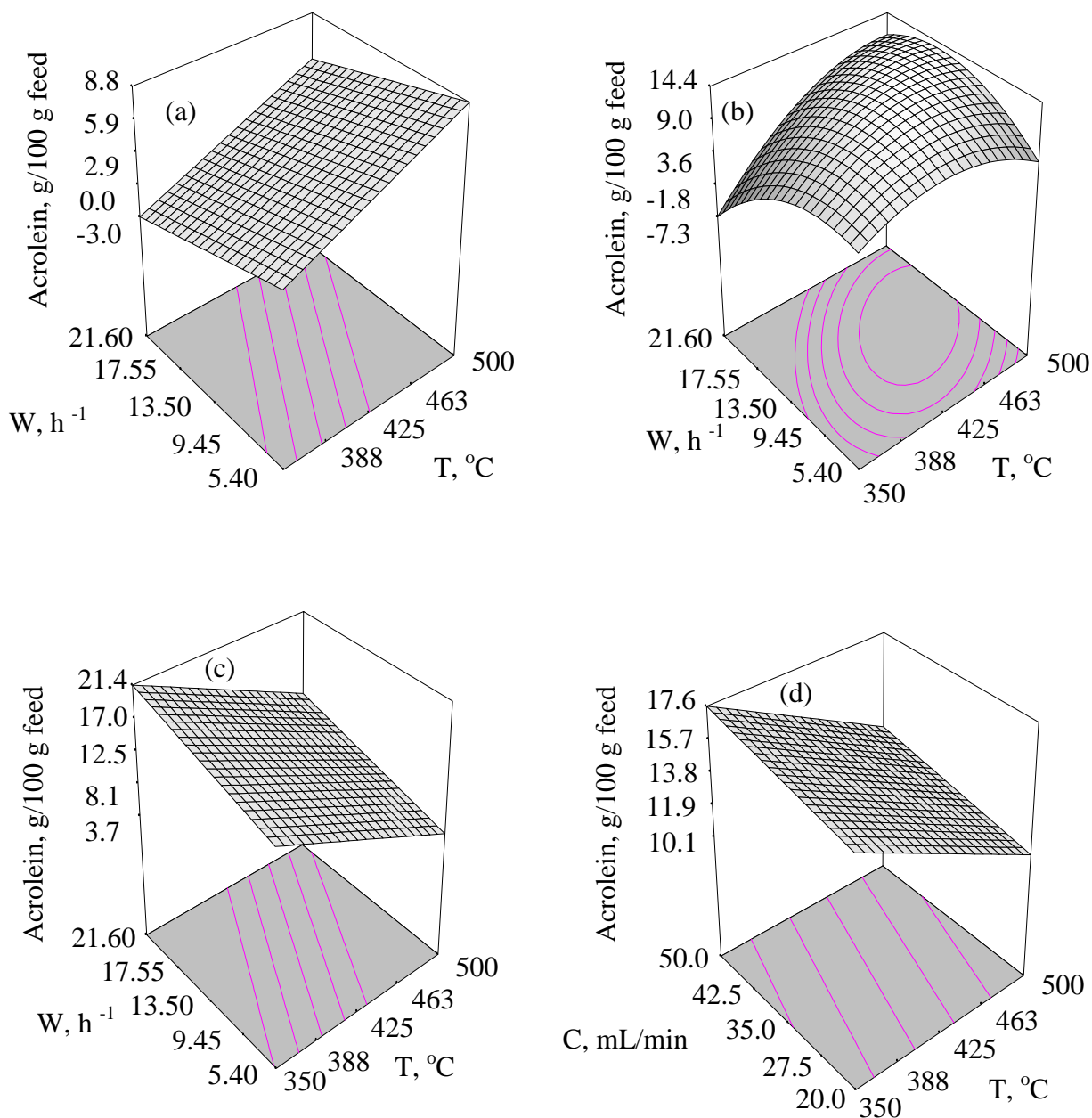
Figure 4.11: Response surface for acrolein yield: (a) effect of temperature and WHSV at carrier gas flow rate at of 35mL/min using HZSM-5; (b) effect of temperature and WHSV at carrier gas flow rate of 35 mL/min using HY; (c) effect of temperature and WHSV at carrier gas flow rate of 35 mL/min using silica-alumina; (d) effect of temperature and carrier gas flow rate at WHSV of 13.50 h $^{-1}$ using γ-alumina

at 500 $^{\mathrm{o}}$C with increase in WHSV from 5.40 to 21.60 h $^{-1}$ acrolein yield increased from 4 to 13.8 g/ 100 g feed as shown in Figure 4.11 (b).

In the case of silica-alumina, temperature, WHSV and interaction of temperature and carrier gas flow rate were significant parameters to predict acrolein yield. It was observed that acrolein yield decreased from 8.1 to 3.7 g/100 g feed with increase in temperature from 350 to 500 $^{\mathrm{o}}$C at WHSV of 5.40 h $^{-1}$ as shown in Figure 4.11 (c). Acrolein yield increased from 3.7 to 21.4 g/100 g feed at 350 $^{\mathrm{o}}$C with increase in WHSV from 5.40 to 21.60 h $^{-1}$. Low temperature and high WHSV seems to favor acrolein yield in this case. For example, at 500 $^{\mathrm{o}}$C when WHSV was increased from 5.40 to 21.60 h $^{-1}$ acrolein yield increased from 4 to 9.5 g/100 g feed.

In the case of γ-alumina, temperature, interaction of temperature and carrier gas flow rate, interaction of carrier gas flow rate and WHSV were significant factors to predict acrolein yield. It was observed that acrolein yield decreased from 17.6 to 12 g/100 g feed with increase in temperature from 350 to 500 $^{\mathrm{o}}$C at carrier gas flow rate of 50 mL/min as shown in Figure 4.11 (d). It was also observed that low temperature and high carrier gas flow rate seemed to favor acrolein yield in this case.

The predicted and experimental maximum acrolein yield at optimum conditions with different catalysts is shown in Table 4.11. It was observed that maximum acrolein (~ 25 g/100 g feed) was produced with γ-alumina at 380 $^{\mathrm{o}}$C, WHSV of 8.68 h $^{-1}$ and carrier gas flow rate of 44 mL/min. At the same temperature and high WHSV of 18.32 h $^{-1}$ and medium carrier gas flow rate (26 mL/min) acrolein produced was ~19 g/100 g feed. However, with HY and HZSM-5 less acrolein was produced even at higher temperature of 470 $^{\mathrm{o}}$C as shown in Table 4.11.

Table 4.11: Optimum operating conditions for maximum acrolein yield over different catalysts

Catalyst	Temperature (^{o}C)	Carrier gas flow rate (mL/min)	WHSV (h^{-1})	Acrolein yield (g/100 g feed)	
				Predicted	Experimental
HZSM-5	470	26	8.68	7.3	9.8
HY	470	44	18.32	13.4	15.4
Silica-alumina	380	26	18.32	18.8	18.8
γ-alumina	380	44	8.68	23.8	25.3

To summarize, γ-alumina was the best catalyst to obtain maximum acrolein yield (25.3 g/100 g feed) at temperature of 380 ^{o}C, carrier gas flow rate of 44 mL/min and WHSV of 8.68 h^{-1}.

4.2.3.3 Formaldehyde yield

Formaldehyde constituted up to 9 g/100 g feed of the liquid product (see Appendix F3). The model coefficients to predict formaldehyde yield with different catalysts are given in Table 4.12.

It was proposed that formaldehyde was formed through ionic as well as free radical pathways. Similar to acetaldehyde yield, formation of formaldehyde was favored at intermediate temperature (from 425 to 470 ^{o}C). Interestingly, for the large pore size catalysts such as silica-alumina and γ-alumina optimum temperature for maximum formaldehyde formation was as low as 380 ^{o}C. It was because further increase in temperature favored formation of acetaldehyde as discussed in 4.2.3.1 and it caused decrease in formaldehyde yield with these catalysts. The proposed reaction pathways and the effect of pore size of different catalysts on formation of formaldehyde are discussed below.

In the case of HZSM-5, temperature and carrier gas flow rate were significant parameters to predict formaldehyde yield (see Appendix G; Table G5). It was observed that formaldehyde yield increased with increase in temperature at all carrier gas flow rates and it was 4.3 g/100 g feed at 500 ^{o}C and 20 mL/min as shown in Figure 4.12 (a). It was because in case HZSM-5, liquid product yield has increasing trend with increase in temperature as shown in Figure 4.8 (a) and (b).

Table 4.12: Significant model coefficients to predict formaldehdye production over different catalysts

Factors	Formaldehyde yield (g/100 g feed)			
	HZSM-5	HY	Silica-alumina	Γ-alumina
Intercept	-40.37	-137.57	-38.15	-8.23
T	0.16	0	0.27	0
C	0.03	0	0.15	0.60
W	0.62	0.88	-2.03	0.41
T^2	-1.59E-04	-7.6E-04	-4.13E-04	0
C^2	0	0	0	-7.99E-03
W^2	-0.02	-0.03	0	-0.12
T*C	0	0	0	0
T*W	0	0	4.59E-03	0
C*W	0	0	0	0
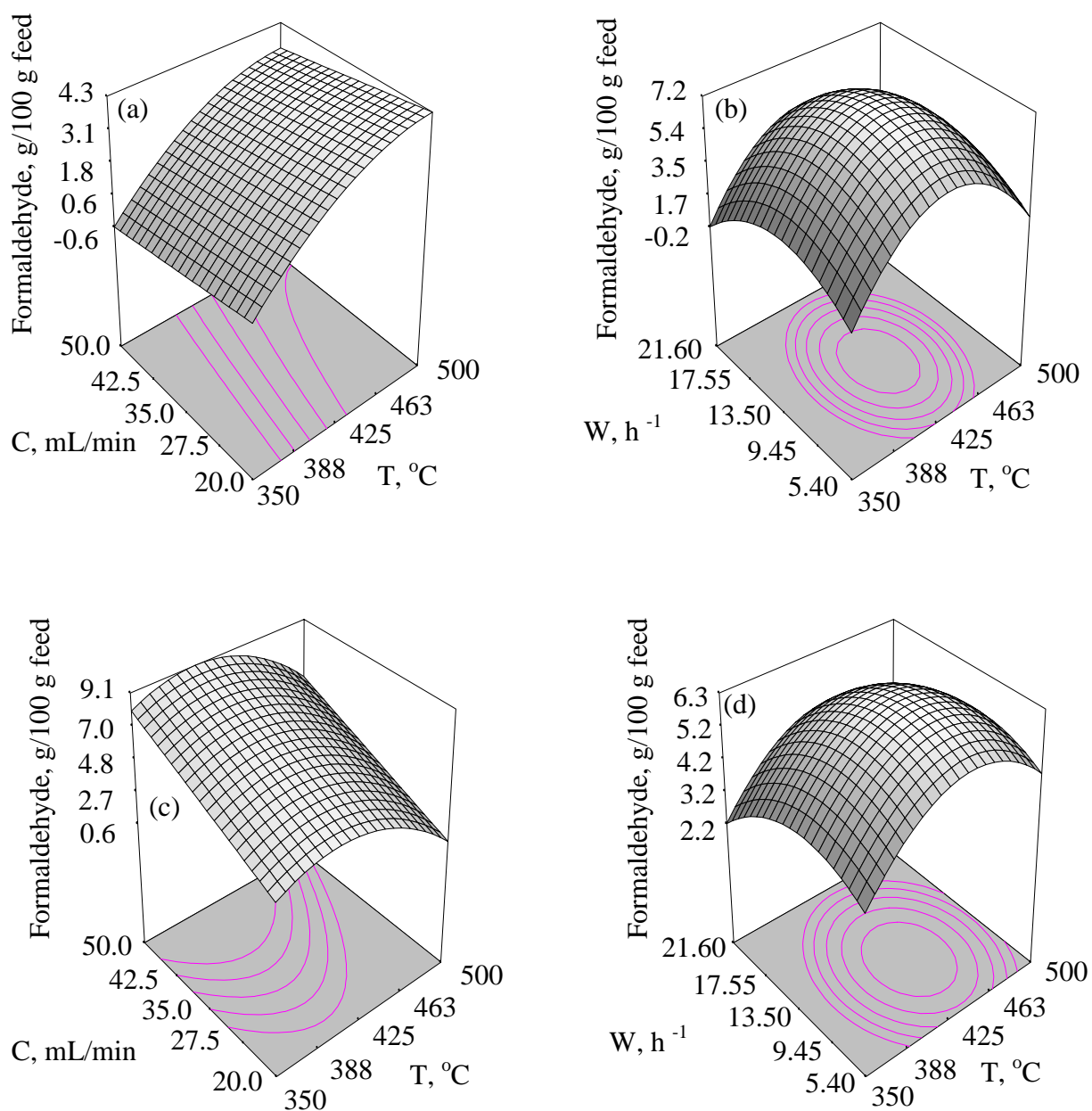
Figure 4.12: Response surface for formaldehyde yield: (a) effect of temperature and carrier gas flow rate at WHSV of 13.50 h $^{-1}$ using HZSM-5; (b) effect of temperature and WHSV at carrier gas flow rate of 35 mL/min using HY; (c) effect of temperature and carrier gas flow rate at WHSV of 13.50 h $^{-1}$ using silica-alumina; (d) effect of temperature and WHSV at carrier gas flow rate of 35 mL/min using γ-alumina

In the case of HY, interaction of temperature and WHSV was significant parameter to predict formaldehyde yield (see Appendix G; Table G5). It was observed that intermediate temperature of 425 to 470 ^{o}C and WHSV from 13.50 to 17.55 h $^{-1}$ favored formaldehyde yield as shown in Figure 4.12 (b). In case of HY, glycerol conversion was as high as 98 wt% when the operating temperature was 425 ^{o}C. It seems that the diffusion limitations are overcome at this temperature. Therefore, with further increase in temperature formation of formaldehyde takes place as per the proposed reaction pathways. For example, it was observed that with increase in operating temperature up to 425 ^{o}C at WHSV of 5.40 h $^{-1}$ and carrier gas flow rate of 35 mL/min formation of formaldehyde has increasing trend. However, with further increase in temperature formation of formaldehyde has a decreasing trend. This indicated that higher temperature would favor acetaldehyde formation in case of HY as observed in Figure 4.10 (b).

In the case of silica-alumina, temperature and carrier gas flow rate were significant factors to predict formaldehyde yield. It was observed that at 350 ^{o}C formaldehyde yield increased from 0.6 to 8.1 g/100 g feed with increase in carrier gas flow rate from 20 to 50 mL/min as shown in Figure 4.12 (c). Furthermore, at 500 ^{o}C when the carrier gas flow rate was increased from 20 to 50 mL/min formaldehyde yield increased from 0.6 to 4.8 g/100 g feed. From the above observation it seems that temperature (from 350 to 425 ^{o}C) and high carrier gas flow rate (50 mL/min) favored formaldehyde yield in case of silica-alumina. Further increase in temperature favored acetaldehyde formation in this case as shown in Figure 4.12 (c).

The response surface to predict formaldehyde yield in case of γ-alumina is shown in Figure 4.12 (d). Formaldehdye yield has an increasing trend with increase in

temperature up to 425 $^\circ$C and carrier gas flow rate of 35 mL/min. However with further increase in temperature to 500 $^\circ$C, formaldehyde yield has a decreasing trend. This could be due to increased production of acetaldehyde at higher temperature in case of γ-alumina as shown in Figure 4.12 (d).

The predicted and experimental maximum formaldehyde yield at optimum conditions with different catalysts is shown in Table 4.13. It was observed that maximum formaldehyde (~ 9 g/100 g feed) was produced with silica-alumina at 380 $^\circ$C, WHSV of 8.68 h^{-1} and carrier gas flow rate of 44 mL/min. With HY and HZSM-5 formaldehyde yield was less (from 3 to 7 g/100 g feed) even at temperature as high as 470 $^\circ$C.

Table 4.13: Optimum operating conditions for maximum formaldehyde yield over different catalyst

Catalyst	Temperature (^{o}C)	Carrier gas flow rate (mL/min)	WHSV (h^{-1})	Formaldehyde yield (g/ 100g feed)	
				Predicted	Experimental
HZSM-5	470	26	18.32	3.6	3.8
HY	425	35	13.50	7.2	7.5
Silica-alumina	380	44	8.68	9.2	8.9
γ-alumina	380	26	13.50	5.2	5.4

4.2.3.4 Acetol yield

Acetol (hydroxyl-acetone) finds applications in cosmetic industry as skin tanning agent. Acetol detected in the liquid product ranged from 1 to 9 g/100 g feed (see Appendix F4). The model coefficients to predict acetol yield with different catalysts is shown in Table 4.14.

It was proposed that acetol was formed through ionic pathways which are feasible at lower temperature. Therefore, the formation of acetol should be favored at low temperature.

It was observed that temperature and WHSV were significant factors to predict acetol yield in case of HZSM-5 (see Appendix G; Table G6). Acetol yield increased with increase in temperature and it was 11.1 g/100 g feed at 500 ^{o}C at WHSV of 5.4 h $^{-1}$ as shown in Figure 4.13 (a). It was because the liquid product yield has an increasing trend with increase in temperature (see Figure 4.8 (a)) due to smaller pore size of HZSM-5 which would lead to higher acetol yield with increase in temperature.

In the case of HY temperature and interaction of WHSV and temperature were significant parameters to predict acetol yield. It was observed that with simultaneous increase in temperature and WHSV acetol yield was 12 g/100 g feed at 500 ^{o}C and WHSV of 21.60 h $^{-1}$ as shown in Figure 4.13 (b).

In the case of silica-alumina, temperature and interaction of WHSV and carrier gas flow rate were significant parameters to predict acetol formation. It was observed that the acetol yield decreased from 8.2 to 0.5 g/100 g feed with increase in temperature from 350 to 500 ^{o}C at WHSV of 21.60 h $^{-1}$ shown in Figure 4.13 (c). Also at WHSV of

Table 4.14: Significant model coefficients to predict acetol yield over different catalysts

| Factors	Acetol yield (g/100 g feed)			
	HZSM-5	HY	Silica-alumina	γ-alumina
Intercept	-19.57	-87.99	49.17	18.54
T	0.06	+0.42	-0.05	-0.04
C	0	0.16	0.74	0
W	-0.13	-0.57	-1.74	0.25
T^2	0	-5.68E-04	0	0
C^2	0	0	0	0
W^2	0	-0.09	0	0
T*C	0	0	0	0
T*W	0	7.20E-03	0	0
C*W	0	0	0.05	0
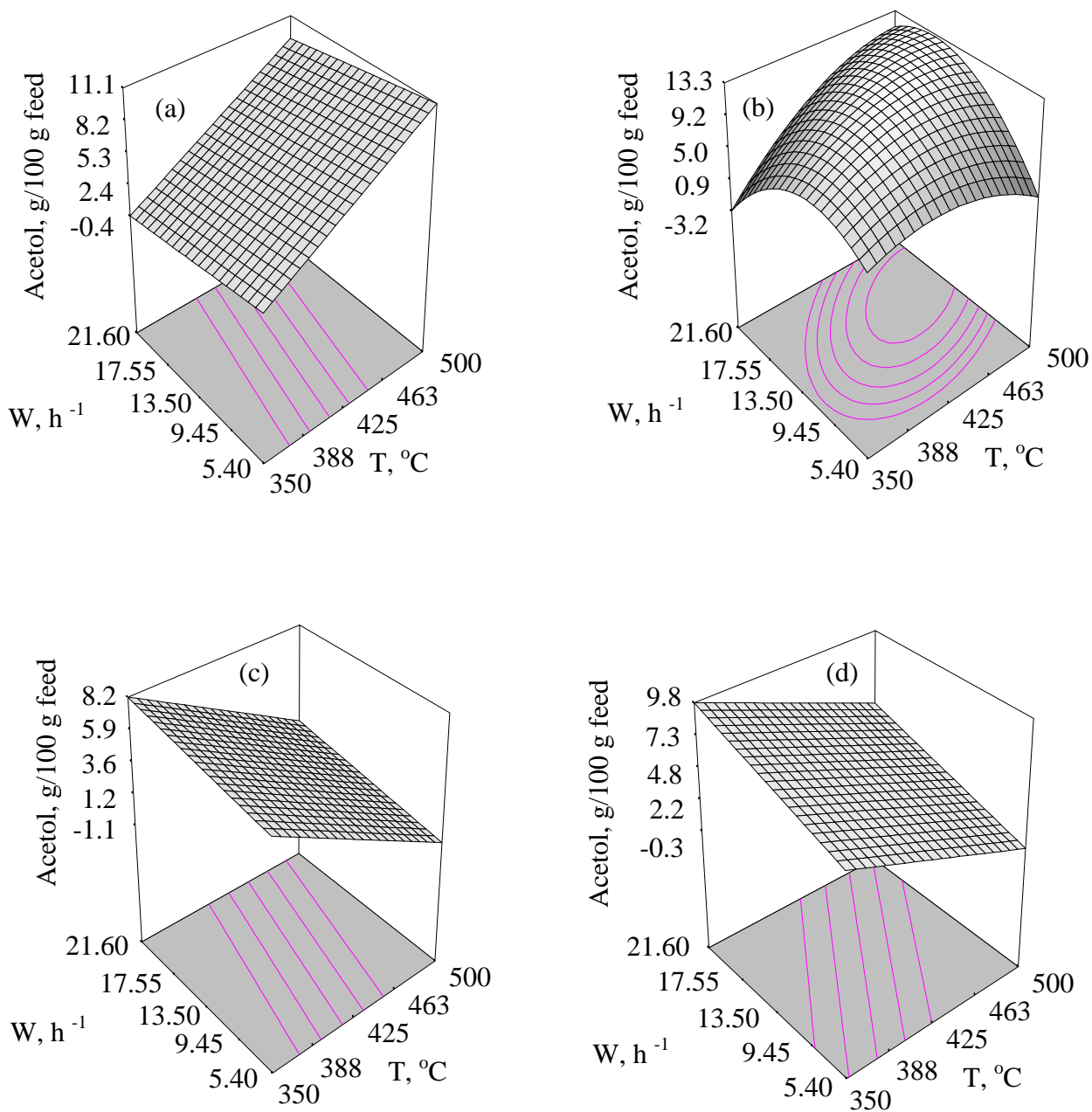
Figure 4.13: Response surface for acetol yield: (a) effect of temperature and WHSV at carrier gas flow rate at of 35 mL/min using HZSM-5; (b) effect of temperature and WHSV at carrier gas flow rate of 35 mL/min using HY; (c) effect of temperature and WHSV at carrier gas flow rate of 35 mL/ min using silica-alumina; (d) effect of temperature and WHSV at carrier gas flow rate of 35 mL/min using γ-alumina

5.40 h $^{-1}$ acetol yield decreased from 6.3 to 0.6 g/100 g feed when temperature was increased from 350 to 500 ^{o}C.

Temperature and WHSV were significant factors to predict acetol yield in the case of γ-alumina. It was observed that acetol yield decreased from 9.8 to 3 g/100 g feed with increase in temperature from 350 to 500 ^{o}C when WHSV was maintained constant at 21.60 h $^{-1}$ as shown in Figure 4.13 (d).

Observed trends for acetol formation in case of silica-alumina and γ-alumina are explained by the proposed reaction pathways. It was proposed that acetol was formed through ionic pathways which dominate at lower temperature. Thus, with the large pore size (absence of diffusion limitations) catalysts such as silica-alumina and γ-alumina, low temperature favored acetol formation.

The predicted and experimental maximum acetol yield at optimum conditions with various catalysts is shown in Table 4.15. Maximum acetol (~ 15 g/100 g feed) was produced with HY at 470 ^{o}C and WHSV of 18.32 h $^{-1}$. At the same temperature, carrier gas flow rate and WHSV of 8.68 h $^{-1}$, ~9 g/100 g feed of acetol was produced in case of HZSM-5 Interestingly, with silica-alumina and γ-alumina acetol yield was comparable to that for HY at lower temperature of 380 ^{o}C, carrier gas flow rate 44 mL/min and WHSV of 18.32 h $^{-1}$.

In conclusion, HY was the best catalyst for maximum acetol yield at temperature of 470 ^{o}C, carrier gas flow rate of 44 mL/min and WHSV of 18.32 h $^{-1}$.

Table 4.15: Optimum operating conditions for maximum acetol yield over different catalysts

Catalyst	Temperature (^{o}C)	Carrier gas flow rate (mL/min)	WHSV (h^{-1})	Acetol yield (g/ 100g feed)	
				Predicted	Experimental
HZSM-5	470	44	8.68	8.8	8.9
HY	470	44	18.32	14.2	14.7
Silica-alumina	380	44	18.32	8.4	8.8
γ-alumina	380	35	18.32	8.8	8.5

4.2.4 Statistical analysis of experimental data for gas product yield

The main objective of this research work was to maximize the liquid product yield, thus a lower range (350 to 500 $^{\circ}$C) of temperature was chosen. However, it was observed that small amount of gas was produced along with liquid and char product. The gas product mainly consisted of CO, CO_2, CH_4 and C_2+ hydrocarbons (see Appendix A, B, C and D). In this research, the gas product yield (g/100 g feed) was calculated as follows:

$$G = \left(\frac{G_T}{F}\right)*100 \tag{4.5}$$

Where,   G   =   Gas product yield, g/100 g feed

          G_T =   Gas collected, g

          F   =   Glycerol fed, g

Gas product yields over different catalysts are given in Appendix E2.

The model coefficients to predict gas product yield using different catalysts are given in Table 4.16. Temperature and WHSV were significant factors to predict gas production using different catalysts (see Appendix G; Table G7). It was proposed that gaseous products such as CO, CO_2, CH_4 and hydrocarbons were formed by free radical pathways (see Figure 4.7) which dominate at high temperature. A general trend of increased gas product yield at high temperature was observed for different catalysts. This is explained by the proposed reaction pathways where gaseous products are formed by predominantly free radical pathways.

The surface response to predict gas product yield using HZSM-5 is shown in Figure 4.14 (a). Low amount of gas product (from 0.2 to 3 g/100 g feed) was obtained using HZSM-5. It was observed that at WHSV of 5.40 h $^{-1}$ when the temperature was

Table 4.16: Significant model coefficients to predict gas product yield over different catalysts

Factors	Gas product yield (g/100 g feed)			
	HZSM-5	HY	Silica-alumina	γ-alumina
Intercept	-2.65	19.98	-156.67	-5.38
T	0.01	-0.07	0.37	0.03
C	0	0	2.73	0
W	-0.09	-1.25	4.23	-0.15
T^2	0	1.46E-04	0	0
C^2	0	0	0	0
W^2	0	0.04	0	0
T*C	0	0	-5.53E-03	0
T*W	0	-6.81E-04	-8.15 E-03	0
C*W	0	0	-0.03	0
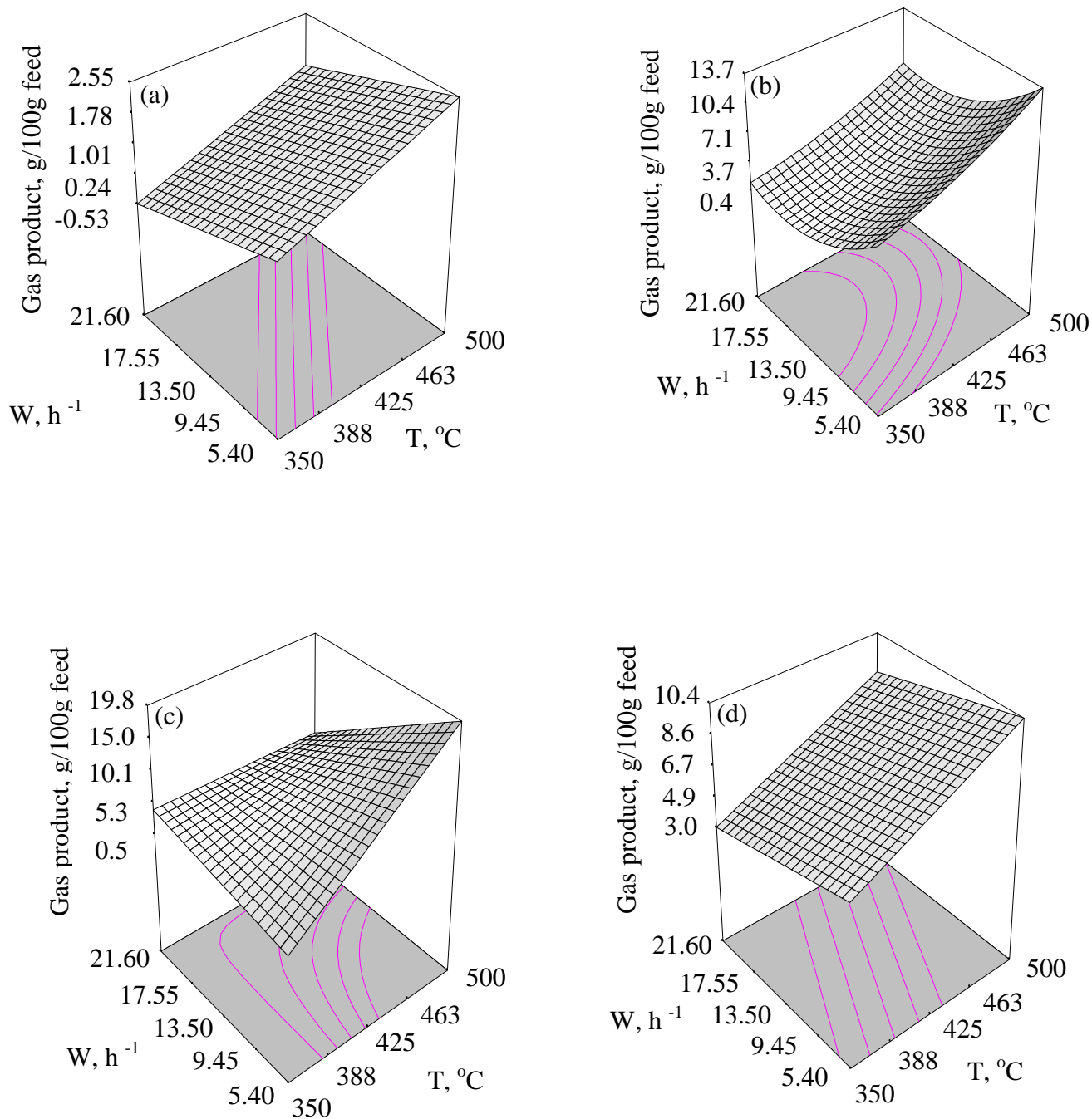
Figure 4.14: Response surface for gas production: (a) effect of temperature and WHSV at carrier gas flow rate at of 35 mL/min using HZSM-5; (b) effect of temperature and WHSV at carrier gas flow rate of 35 mL/min using HY; (c) effect of temperature and WHSV at carrier gas flow rate of 35 mL/ min silica-alumina; (d) effect of temperature and WHSV at carrier gas flow rate of 35 mL/min using γ-alumina

increased from 350 to 500 ^{o}C the gas product yield increased from 0.24 to 2.55 g/100 g feed and from 0.4 to 13.7 g/100 g feed for HZSM-5 and HY, respectively (see Figure 4.14 (b). Also at 500 ^{o}C gas product yield was almost 7 g/100 g feed even with decrease in WHSV from 21.60 to 13.50 h $^{-1}$ however with further increase in WHSV to 5.40 h $^{-1}$ gas product increased to 13.7 g/ 100 g feed. It would appear that temperature was the main parameter to predict gas product yield in case of HY.

Surface responses for gas product yield in the case of silica-alumina and γ-alumina are shown in Figure 4.14 (c) and (d). It was observed that at WHSV of 5.40 h $^{-1}$ when temperature was increased from 350 to 500 ^{o}C gas product yield increased from 0.5 to 19.8 g/100 g feed and from 3.0 to 10.4 g/100 g feed for silica-alumina and γ-alumina, respectively. Furthermore, for γ-alumina the gas product decreased from 10.4 to 7 g/100 g feed when WHSV was increased from 5.40 to 21.60 h $^{-1}$ at 500 ^{o}C.

The predicted and experimental gas product yields at optimum conditions with different catalysts are shown in Table 4.17. Under optimum conditions to maximize the liquid product yield, gas product yield ranged from 2 to 6 g/100 g feed. Silica-alumina and γ-alumina produced higher gas product yield at low temperature of 380 ^{o}C as compared to HZSM-5 and HY.

Table 4.17: Optimum operating condition for minimum gas product yield over different catalysts

Catalyst	Temperature (^{o}C)	Carrier gas flow rate (mL/min)	WHSV (h^{-1})	Gas product yield (g/ 100g feed)	
				Predicted	Experimental
HZSM-5	470	26	8.68	1.9	1.8
HY	425	50	13.50	3.4	5.9
Silica-alumina	380	26	8.68	1.3	2.6
γ-alumina	380	44	8.68	6.0	6.3

4.2.5 Statistical analysis of experimental data for char and residue product yield

Char is one of the by-products of cracking reaction (Gates 1979). It was desired to minimize the char and residue in this research work. It was proposed that formation of coke could be the result of direct condensation followed by polymerization of glycerol molecule on the acidic surface (see Figure 4.7). In this research work char and residue yield (g/100 g feed) was calculated as follows:

$$C_R = \left(\frac{C_T}{F}\right) * 100 \qquad (4.6)$$

Where, C_R = Char and residue product yield, g/100 g feed

C_T = Char and residue collected, g

F = Glycerol fed, g

Char and residue product yield over different catalysts is given in Appendix E3.

The model coefficients to predict char and residue yield in case of different catalysts are shown in Table 4.18. The response surfaces to predict char and residue yield using different catalysts are shown in Figure 4.15.

In the case of HZSM-5 it was observed that char and residue yield decreased from 8.0 to 1.2 g/100 g feed with decrease in WHSV from 5.40 to 21.60 h^{-1} at 500 ^{o}C as shown in Figure 4.15 (a). In case of HY, char and residue yield decreased from 10.4 to 7 g/100 g feed when temperature was increased from 350 to 500 ^{o}C at WHSV of 21.60 h^{-1} as shown in Figure 4.15 (b). More char and residue yield was obtained at high temperature in case of silica-alumina than HY. For example, at 500 ^{o}C with increase in WHSV from 5.40 to 21.60 h^{-1}, the char and residue yield decreased from 10.1 to 4.2 g/100 g feed as shown in Figure 4.15 (c). In the case of γ-alumina, at WHSV of 21.60 h^{-1} char and residue yield increased from 3.8 to 7.1 g/100 g feed with increase in

Table 4.18: Significant model coefficients* to predict char and residue over different catalysts

| Factors	Char and residue (g/100 g feed)			
	HZSM-5	HY	Silica-alumina	γ-alumina
Intercept	82.23	37.34	13.14	12.69
T	-0.17	-0.02	3.90E-03	-0.03
C	-0.88	-0.62	0	-0.08
W	-3.60	-1.46	-0.33	-0.36
T^2	0	0	0	0
C^2	0	0	0	0
W^2	-0.05	0	0	0
T*C	2.36E-03	0	0	4.31E-04
T*W	4.97E-03	0	0	1.62E-03
C*W	0	-0.05	0	-8.12E-03

* see Appendix G; Table G8
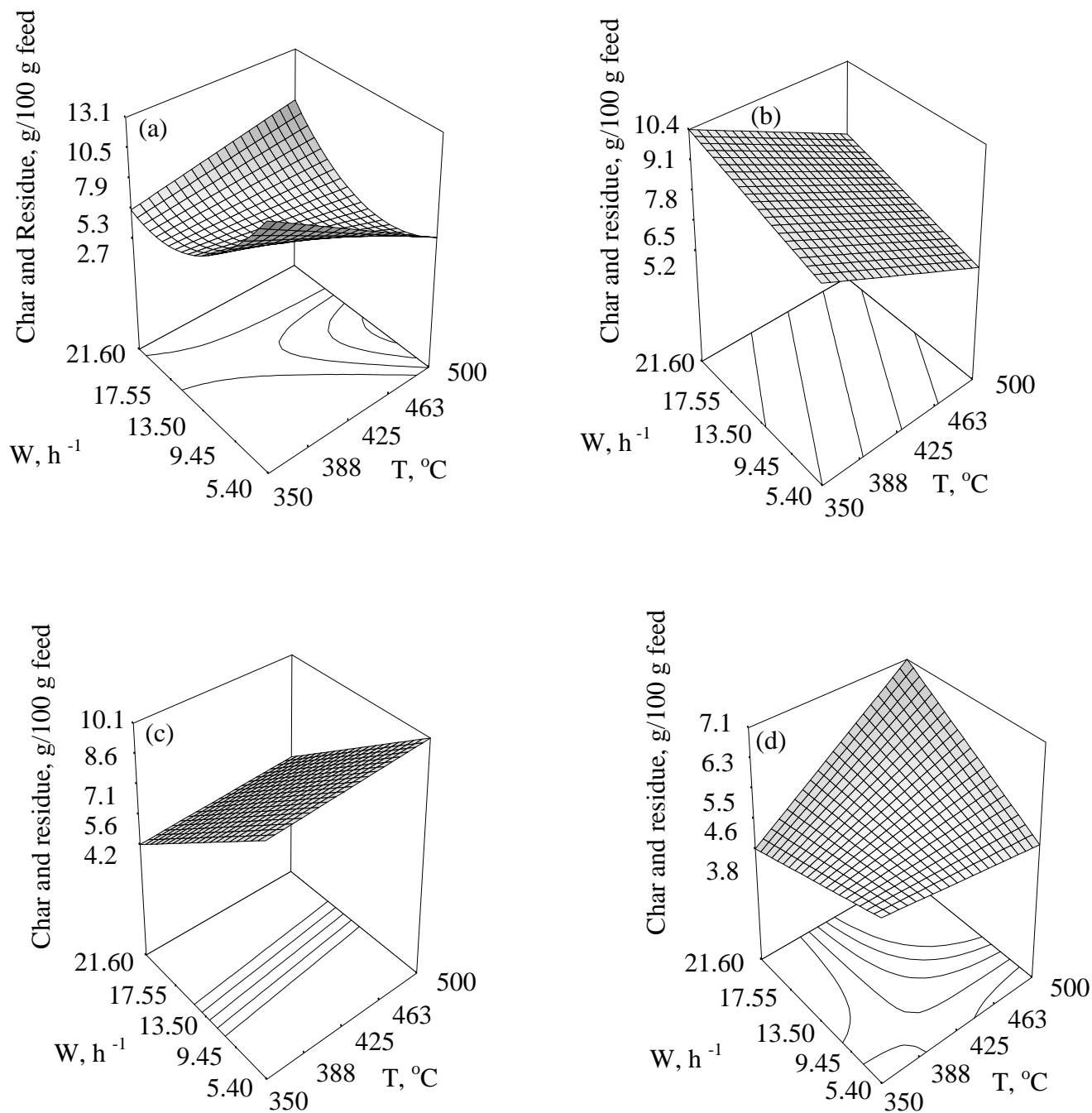
Figure 4.15: Response surface for char and residue: (a) effect of temperature and WHSV at carrier gas flow rate at of 35 mL/min using HZSM-5; (b) effect of temperature and WHSV at carrier gas flow rate of 35 mL/min using HY; (c) effect of temperature and WHSV at carrier gas flow rate of 35 mL/min using silica-alumina; (d) effect of temperature and WHSV at carrier gas flow rate of 35 mL/min using γ-alumina

temperature from 350 to 500 ^{o}C as shown in Figure 4.15 (d).

In the present research work, it was desirable to minimize char and residue yield while producing maximum liquid product. The optimum operating condition to minimize the char and residue using different catalyst is shown in Table 4.19.

In conclusion, HZSM-5 produced minimum char at higher temperature. This was because of it unique pore size which resist char production (Sang et al., 2004).

Table 4.19: Predicted and experimental minimum char and residue yield under optimum conditions over different catalysts

Catalyst	Temperature (^{o}C)	Carrier gas flow rate (mL/min)	WHSV (h^{-1})	Char and residue yield (g/ 100g feed)	
				Predicted	Experimental
HZSM-5	470	26	8.68	3.6	4.2
HY	425	50	13.50	4.5	6.0
Silica-alumina	380	26	18.32	5.7	6.2
γ-alumina	380	44	8.68	4.7	4.2

4.3 Effect of physiochemical properties of catalysts on optimum glycerol conversion, liquid product yield and acetaldehyde, acrolein, formaldehyde and acetol yields

In this section the effects of catalyst physiochemical properties on glycerol conversion, liquid product yield and acetaldehyde, acrolein, formaldehyde and acetol yields are discussed.

4.3.1 Effect of catalyst acidity

Acidity of the catalysts has major effect on the glycerol conversion, liquid product yield and acetaldehyde, acrolein, formaldehyde and acetol yields. The observed trend of total acidity (see Table 4.20) from most to least acidic was HZSM-5>HY>silica-alumina>γ-alumina. The effect of total acidity on glycerol conversion is given in Figure 4.16 (a). Glycerol conversion did not change significantly (~100 wt%) when the total acidity was increased from $1.7x10^4$ to $5.5x10^4$ a.u. However, it decreased to 78.8 wt% when total acidity was increased further to $7.0x10^4$ a.u. (HZSM-5). It was because during the cracking reaction the glycerol molecules were adsorbed on the surface of catalysts. After the reaction the products were not easily desorbed from relatively strong acid sites. This resulted in lower glycerol conversion in case of HZSM-5.

A similar trend was observed for the liquid product yield (see Figure 4.16(b)). Liquid product yield varied in the range from 80.9 to 83.6 g/100 g feed when the total acidity increased from $1.7x10^4$ to $5.5x10^4$ a.u. Liquid product yield decreased significantly when the total acidity increased to $7.0x10^4$ a.u. This was because liquid product yield was a function of glycerol conversion (see Equation 4.4). The decrease in glycerol conversion is responsible for decrease in liquid product yield at higher acidity.

Table 4.20: Total acidity and optimum production of acetaldehyde, acrolein, formaldehyde and acetol

Catalyst	Total acidity (a.u.)	Optimum liquid components (g/100 g feed)			
		Acetaldehyde	Acrolein	Formaldehdye	Acetol
HZSM-5	70248	11.2	9.8	3.8	8.9
HY	55295	17.8	15.4	7.5	14.7
Silica-alumina	21518	24.5	18.6	8.9	8.8
γ-alumina	17529	15.1	25.4	5.4	8.5
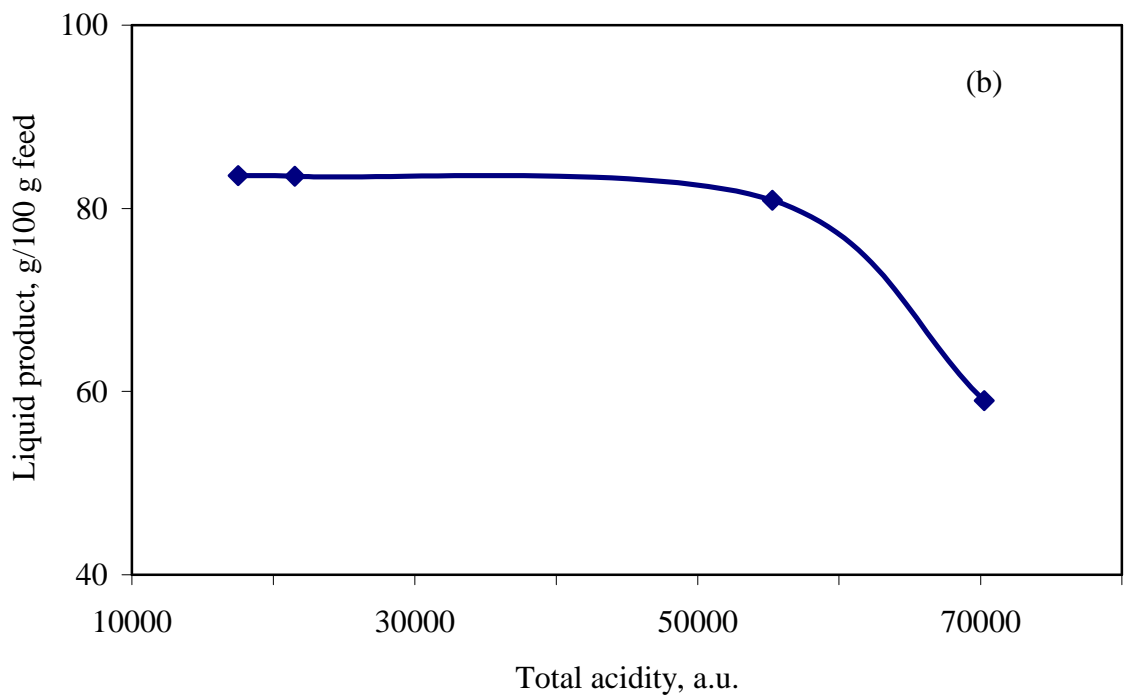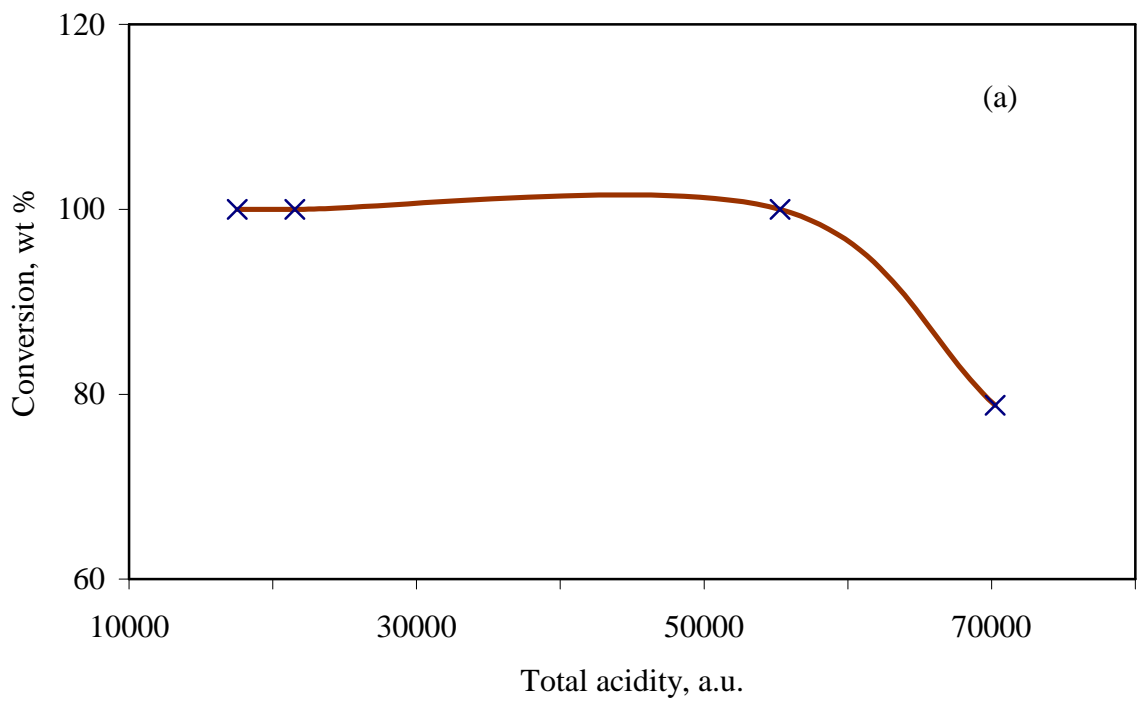
Figure 4.16: Effect of total acidity of catalysts on the optimum (a) glycerol conversion (b) optimum liquid product yield

straight forward trend was observed between formation of individual liquid components and total acidity. However, trend of increasing acetaldehyde, acrolein and formaldehyde yield with decrease in total acidity was observed (see Table 4.20).

4.3.2 Effect of catalyst pore size

The effects of pore size on glycerol conversion and liquid product yield are given in Figure 4.17 As shown in this figure, glycerol conversion and liquid product yield depends not only on acidity but also on the pore sizes of the catalysts. However, excessive pore size does not have any significant effect on glycerol conversion and liquid product yield as evident from Figure 4.17 (a) and (b).

The effect of pore size on the production of acetaldehyde, acrolein, formaldehyde and acetol is shown in Figure 4.18. Pore size had different effects on individual liquid components. For example, maximum acetaldehyde yield was obtained at 3.15 nm (silica-alumina). On the other hand, maximum acrolein and acetol yield were obtained for catalysts with average pore sizes of 11.2 nm (γ-alumina) and 0.74 nm (HY), respectively (see Figure 4.18). Moreover maximum formaldehyde yield was obtained at 0.74 nm and no significant change in formaldehyde yield was obtained with further increase in pore size.

4.3.3 Scanning electron microscope (SEM)

Catalysts were characterized using SEM before the reaction. The images obtained for different catalysts before and after the reaction are shown in Figure 4.19 and 4.20. It was observed that there was coke deposition and agglomeration of catalyst particles after the reaction. Interestingly, there was not much difference in surface texture in case of HZSM-5 before and after the reaction.
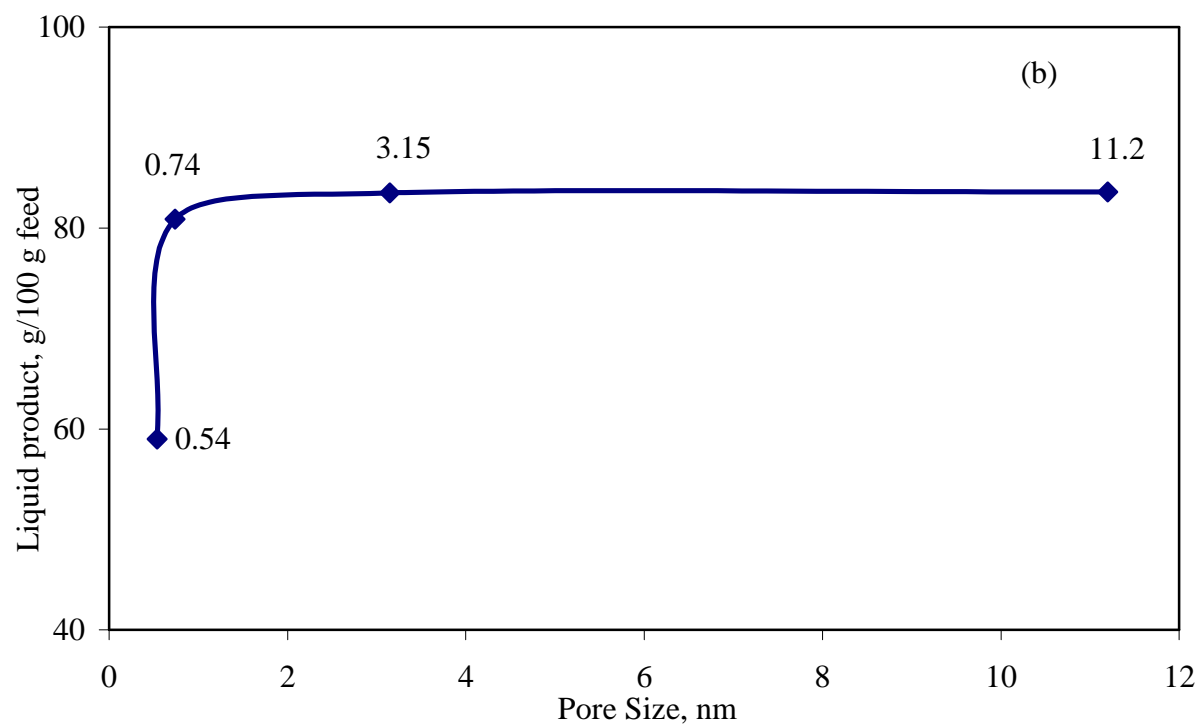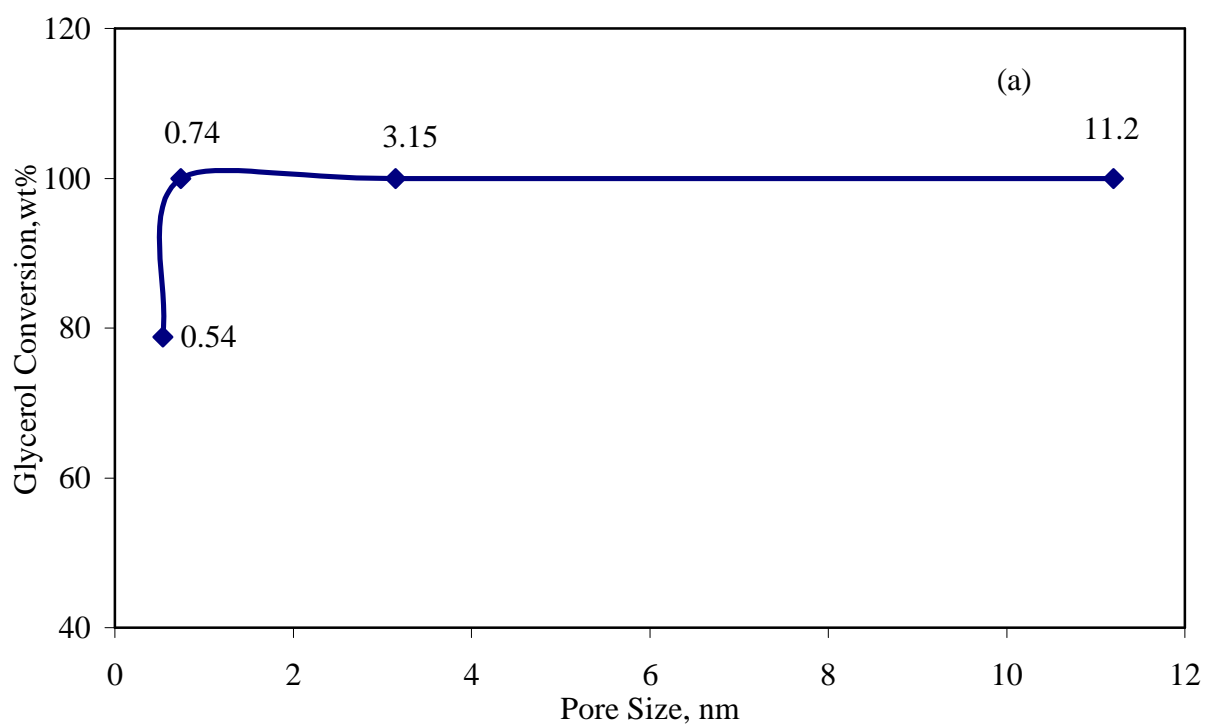
Figure 4.17: Effect of pore size on (a) optimum glycerol conversion (b) optimum liquid product yield
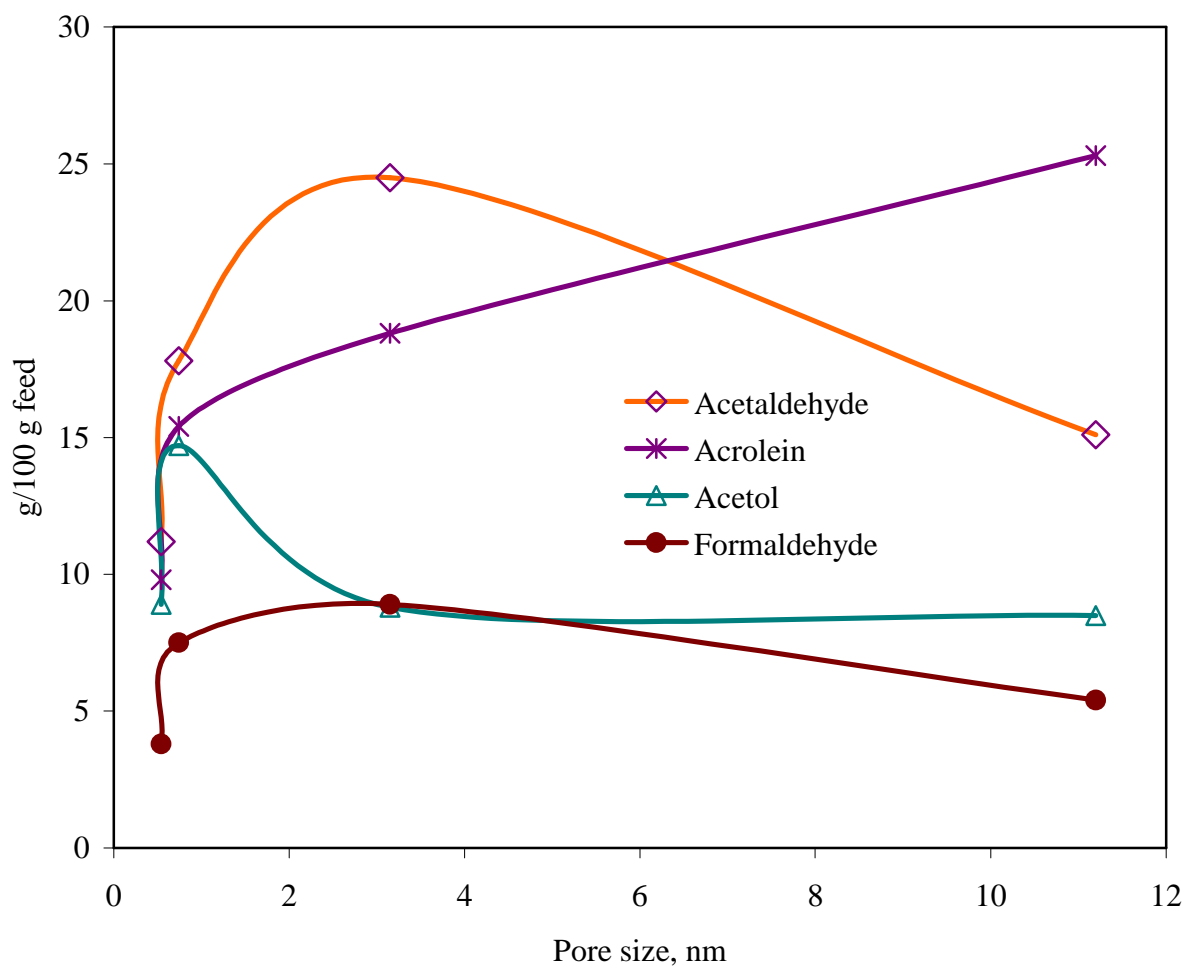
Figure 4.18: Effect of catalyst pore size on optimum yield of acetaldehyde, acrolein, formaldehyde and acetol
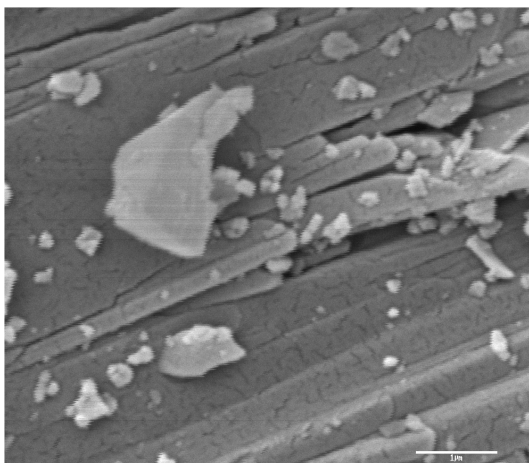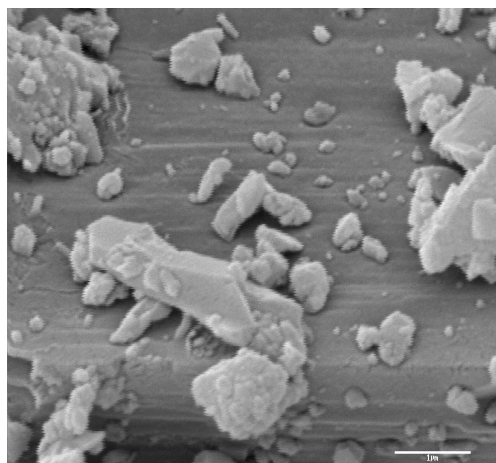
a) Fresh HZSM-5   b) Spent HZSM-5
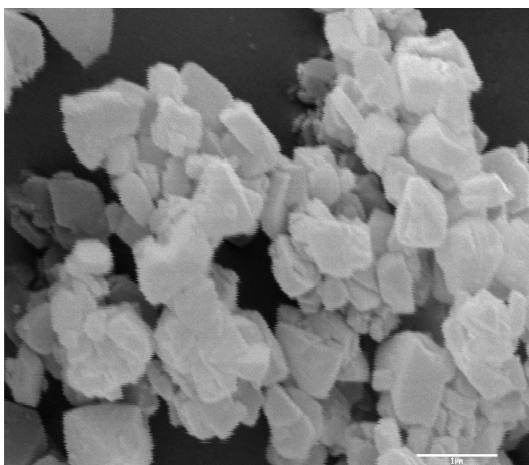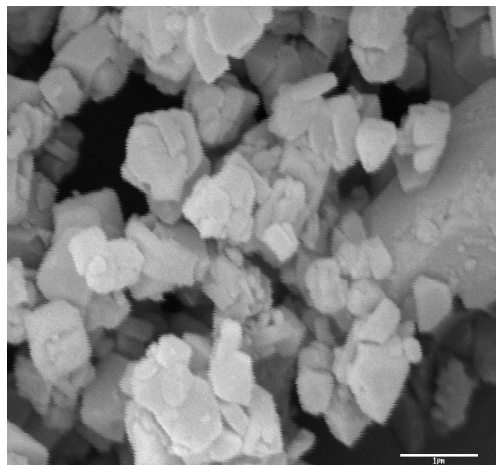
a) Fresh HY   b) Spent HY

Figure 4.19: Scanning electron micrographs for (a) fresh HZSM-5 (b) spent HZSM-5 (c) fresh HY (d) spent HY
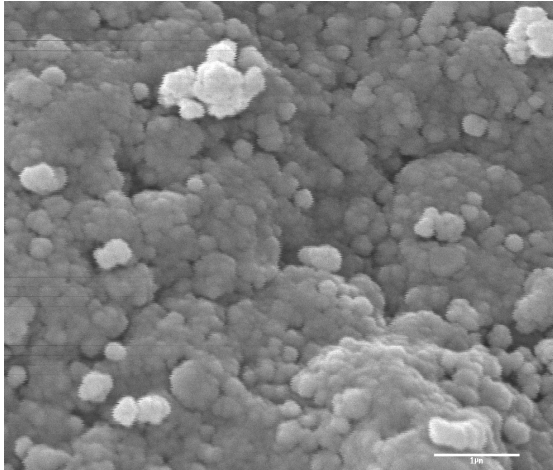
(a) Fresh silica-alumina
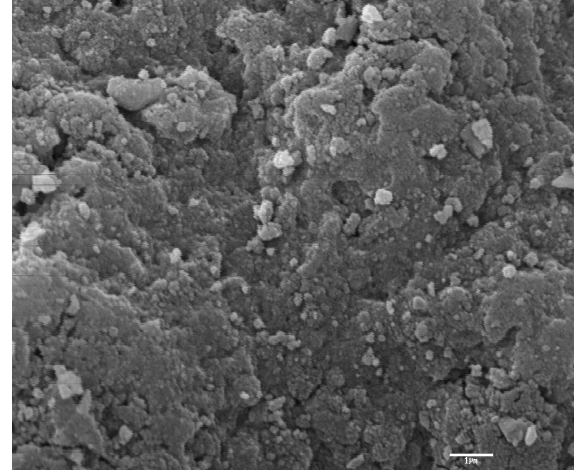
(b) Spent silica-alumina
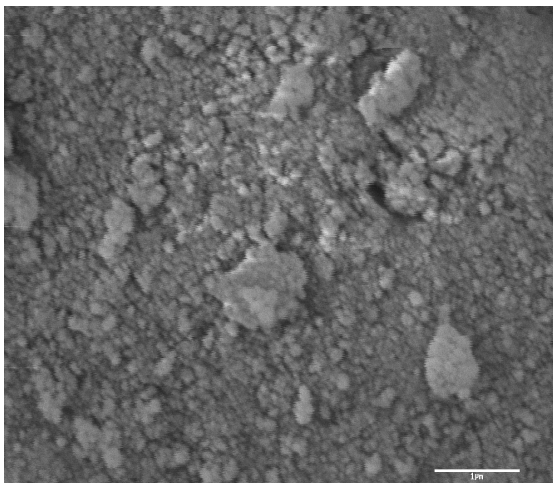
(c) Fresh gamma alumina
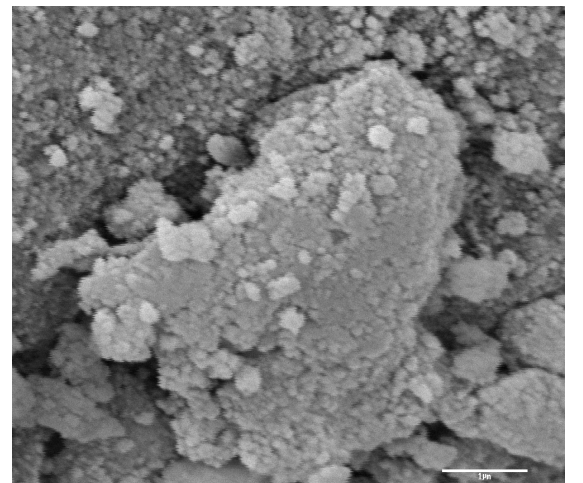
(d) Spent gamma alumina

Figure 4.20: Scanning electron micrographs for (a) fresh silica-alumina (b) spent silica-alumina (c) fresh γ-alumina (d) spent γ-alumina

4.4   Implication of experimental results

The findings of this research indicate that glycerol can be used for the production of acetaldehyde, acrolein, formaldehyde and acetol. Main use of acetaldehyde is in silvering of mirrors. In addition, it is also used as intermediate in the synthesis of other chemicals such as acetic acid and n-butyl alcohol, perfumes and solvent in rubber industry. Acrolein is used primarily as intermediate in the manufacture of acrylic acid. Another important application of acrolein is as aquatic algaecide (http://www.inchem.org). Formaldehyde is used in plastic industry for the production of bakelite. In addition, it is widely used in manufacture of inks and wrinkle free clothing (http://www.the-innovation-group.com). Acetol (hydroxyl-acetone) is used in cosmetic industry as main constituent of skin tanning creams.

The separation of individual liquid components is important to impart market value to them. Individual liquid components can be separated using distillation column as the boiling point data for the components present in liquid product has wide range as shown in Table 4.21.

A study was also carried out to estimate (see Table 4.22) the possible value addition to glycerol by production of liquid chemicals. In this study price differential was calculated based on the bulk prices (Chemical Market Reporter, 2005) of glycerol and major components present in the liquid product, excluding the production and capital cost. It was interesting to observe that based on the optimum production of components for $100 input there was a potential to produce about $182 in return. Thus, there is strong potential to produce value added liquid chemicals from glycerol using catalytic treatment.

Table 4.21: Boiling points of different components present in liquid product

Components	Boiling point (°C)	Freezing Point (°C)
Acetaldehyde	21	-40
Acetic acid	117-118	40
Acetol	145-146	56
Acetone	56	-17
Allyl alcohol	96-98	22
Acrolein (2-propenal)	53	-29
Formaldehyde	-19	--
Glycerol formal	192-193	93
IPA	82	12
Phenol	182	79
Propionic acid	141	54
Water	100	0

Table 4.22: Estimation of possible value addition based on bulk prices of chemicals produced in catalytic treatment of glycerol

Basis: 100 Kg of glycerol

Components	Price, A ($/Kg)	Optimum production of components, B (Kg)	Price calculation for products, C = A*B/100*100 ($)
Glycerol	0.40		
Acetaldehyde	1.30	24.50	31.85
Acrolein	2.57	25.30	65.02
Formaldehyde	0.60	8.90	5.35
Acetol	0.72	14.44	10.40
		Total = 73.14	**Total = 112.61**

Selling price of glycerol = 0.40*100 = $40.00

Selling price of products = $112.61

Value addition = (112.61 – 40.00)/40.00*100 = 182 %

5   CONCLUSIONS AND RECOMMENDATIONS

5.1   Conclusions

1. Complete conversion of glycerol was obtained with silica-alumina and γ-alumina at all experimental conditions. The optimum operating conditions to obtain the maximum glycerol conversion over HZSM-5 (78.8 wt%) and HY (100 wt%) were 470 ^{o}C, 26 mL/min and WHSV of 8.68 h $^{-1}$.

2. Silica-alumina and γ-alumina produced the highest liquid product yield (~ 83 g/ 100 g feed) at 380 ^{o}C, WHSV of 8.68 h $^{-1}$ and carrier gas flow rate of 26 and 44 mL/min respectively.

3. The highest liquid product yields over HY (80.9 g/100 g feed) was obtained at temperature of 425 ^{o}C, carrier gas flow rate of 50 mL/min and WHSV of 13.50 h $^{-1}$ and over HZSM-5 (59.0 g/100 g feed) at temperature of 470 ^{o}C, carrier gas flow rate of 26 mL/min and WHSV of 8.68 h $^{-1}$.

4. The highest acetaldehyde yield (24.5 g/100 g feed) was obtained with silica-alumina at the optimum conditions of temperature 470 ^{o}C, carrier gas flow rate 44 mL/min and WHSV 18.32 h $^{-1}$.

5. The highest acrolein yield (25.3 g/100 g feed) was obtained with γ-alumina at the optimum conditions of temperature 380 ^{o}C, carrier gas flow rate 44 mL/min and WHSV 8.68 h $^{-1}$.

6. The highest formaldehyde yield (~9 g/100 g feed) was obtained with silica-alumina at the optimum conditions of temperature 380 $^{\circ}$C, carrier gas flow rate 44 mL/min and WHSV 8.68 h^{-1}.

7. The highest acetol yield (14.7 g/100 g feed) was obtained with HY at the optimum conditions of temperature 470 $^{\circ}$C, carrier gas flow rate 44 mL/min and WHSV 18.32 h^{-1}.

8. The gas product yield obtained under optimum conditions for maximum liquid product yield ranged from 2 to 6 g/ 100 g feed.

9. The char and residue yield obtained under optimum conditions for maximum liquid product ranged from 3 to 6g/ 100 g feed.

10. Optimum conversion increased from 80 to 100 wt% and optimum liquid product increased from 59 to 83.3 g/100 g feed when the pore size of catalyst was increased from 0.54 in case of HZSM-5 to 0.74 nm in case of HY; beyond which the effect pore of size was minimal.

5.2 Recommendations

1. Crude glycerol should be used as feed under the optimized conditions for each catalyst.

2. Catalyst such as H-mordenite (pore size 0.67 nm) with pore size in between HZSM-5 and HY should be used to evaluate the effects of pore size on optimum glycerol conversion as well as liquid product yield.

3. Kinetic study should be performed to evaluate the rates of reactions for formation of acetaldehyde, acrolein, formaldehyde and acetol.

4. Process specific catalyst can be designed for the catalytic conversion of crude glycerol to selectively produce acetaldehyde, acrolein, formaldehyde and acetol.

5. Pilot plant study of the catalytic treatment of glycerol should be performed.

6. A process should be developed to separate individual components from the liquid product.

6 REFERENCES

Akpanudoh, N.S., K. Gobin and G. Manos, "Catalytic Degradation of Plastic Waste to Liquid Fuels Over Commercial Catalysts: Effect of Polymer to Catalyst Ratio/Acidity Content", Journal of Molecular Catalysis A: Chemical **235,** 67-73 (2005).

Adjaye, J. D., S.P.R. Katikaneni and N.N. Bakhshi, "Catalytic Conversion of Biofuel to Hydrocarbons: Effect of Mixtures of HZSM-5 and Silica-Alumina Catalysts on Product Distribution", Fuel Processing Technology **48,** 115-143 (1996).

Anand, R., R. Maheshwari, K.U. Gore, S.S. Khaire and V.R. Chumbhale, "Isopopylation of Naphthalene Over Modified Faujasites: Effect of Steaming Temperature on Activity and Selectivity", Applied Catalysis A: General **249,** 265-272 (2003).

Anderson, J.R., K. Foger, T. Mole, R.A. Rajadhyaksha and J. V. Sanders, "Reactions on ZSM-5-type Zeolite Catalysts", Journal of Catalysis **58,** 114 (1979).

Antal, M.J., W.S.L. Mok, J.C. Roy and A.T. Raissi, "Pyrolytic Sources of Hydrocarbons from Biomass", Journal of Analytical and Applied Pyrolysis **8**, 291-303 (1985).

Argauer, R.J. and R. Landolt, "Crystalline Zeolite ZSM-5 and Method Of Preparing the Same", US Patent **3702886,** (1972).

Barnwal, B.K. and M.P. Sharma, "Prospects of Biodiesel Production from Vegetable Oils in India", Renewable and Sustainable Energy Reviews **9,** 363-378 (2005).

Bhatia, S., "Zeolite Catalysts Principles and Applications", CRC Press, Florida (1989), pp. 15-17; pp. 84; pp. 87**.**

Buhler, W., E. Dinjus, H.J. Ederer, A. Kruse and C. Mas, "Ionic Reactions and Pyrolysis of Glycerol as Competing Reaction Pathways in near- and Supercritical Water", Journal of Supercritical Fluids **22,** 37–53 (2002).

Bungay, H.R., "Confessions of a Bioenergy Advocate", Trends in Biotechnology **22,** 67-71 (2004).

Campbell, I., "Principles of Reactions on Solid Catalysts Biomass Catalysts and Liquid Fuels", Holt, Rinehart and Winston Publishing Corporation, (1983), pp. 106-121.

Chandrawar, K.H, S.B. Kulkarni and P. Ratnaswamy, "Alkylation of Benzene and Ethanol over ZSM-5 Zeolites", Applied Catalysis **4,** 287 (1982).

Chaudhari, S. T. and N. N. Bakhshi, "Steam Gasification of Chars and Bio-oil", Report to Bioenergy Development Program Renewable Energy Branch, Energy, Mines and Resources Canada, Ottawa, Canada, February (2002), pp. 396-436.

Chen, N.Y. "Hydrophobic Properties of Zeolites", Journal of Physical Chemistry **80,** 60 (1976).

Claude, S., "Research on New Outlets for Glycerol – Recent Developments in France", 52nd International Congress and Expo of DGF, Magdeburg, Germany, September 13-15 (1998).

Cortright, R.D, R.R. Davda and J.A. Dumesic, "Hydrogen from Catalytic Reforming of Biomass-Derived Hydrocarbons in Liquid Water", Nature **418**, 964-967 (2002).

Czernik, S., R. French, C. Feik and E. Chornet, "Production of Hydrogen from Biomassderived Liquids", Proceedings of the 2000 DOE Hydrogen Program Review (2000).

Dabbagh, H., M. Yalfani and B. Davis, "An XRD and Fourier Transformed Infrared Spectroscopy Investigation of Single and Mixed γ-alumina and Thorium Oxide", Journal of Molecular Catalysis A: Chemical **238,** 72-77 (2005).

Dalai, A.K., N.N. Bakhshi, X. Lang, M.J. Reaney, P.B. Hertz and J. Munson, "Production of Diesel Fuel Lubricity Additives from Various Vegetable Oils", Annual Interim Report for Canodev Research Inc. April (2000).

Derouane, E.G., J.B. Nagy, P.Dejaifve, J.H.C. Van hoof, B.P. Speckman, J.C. Vedrine, C. Naccache, "Elucidation of the Mechanism of Conversion of Methanol and Ethanol to Hydrocarbons on a New Type of Synthetic Zeolite" Journal of Catalysis **53**, 40 (1978).

Digne, M., P. Sautet, P. Raybaud, P. Euzenc, H. Toulhoat, "Use of DFT to Achieve a Rational Understanding of Acid–Basic Properties of γ -alumina Surfaces", Journal of Catalysis **226**, 54–68 (2004).

Falamaki, C., M. Edrissi, M. Sohrabi, "Studies on the Crystallization Kinetics of Zeolite ZSM-5 With 1,6-Hexanediol as a Structure-Directing Agent ", Zeolite **19**, 2 (1997).

Fordham, P, M. Besson and P. Gallezot, "Selective Catalytic Oxidation of Glyceric Acid to Tartronic and Hydroxypyruvic Acids", Applied Catalysis A: General **133,** LI79-LI84 (1995).

Furrer, R.M., Master's Thesis "Direct Conversion of Plant Tall Oils and De-pitched Tall Oil to Fuels and Chemicals Using HZSM-5 Catalyst", University of Saskatchewan (1988).

Gutiérrez, G., A. Taga and B. Johansson, "Theoretical structure determination of γ-Al_2O_3", Physical Reviews B **65,** 012101 (2001).

Garcia, R, M Besson and P Gallezot, "Chemoselective Catalytic Oxidation of Glycerol with Air on Platinum Metals", Applied Catalysis A: General **127,** 165-176 (1995).

Gates, B.C., J.R. Kazert and G. Schuit, "Chemistry of Catalytic Processes", McGraw Hill (1979), pp. 5-7; pp. 85-89.

Grieken, R., J.L Van Sotelo, J.M Menendez and J.A. Melero, "Anomalous Crystallization Mechanism in the Synthesis of Nanocrystalline ZSM-5", Microporous and Mesoporous Materials **39**, 135-147 (2000).

Haas, M.J., "Improving Economics of Biodiesel Production Through the Use of Low Value Lipids as Feedstocks: Vegetable Oil Soapstack", Fuel Processing Technology **86,** 1087-1096 (2005).

http://www.canola-council.org/ as on 25/5/2004.

http://www.chemicalmarketreporter.com accessed July 2005.

http://www.inchem.org/documents/ehc/ehc/ehc127.htm accessed July 2005.

http://www.the-innovation-group.com/ChemProfiles/Formaldehyde.htm accessed July 2005.

Huber, G.W., J.W. Shabaker and J.A. Dumesic, "Raney Ni-Sn Catalyst for H_2 Production from Biomass-Derived Hydrocarbons", Science **30**, 2075 (2003).

Jacobs, P., H.K. Beyer and J. Valyon, "Properties of the End Members in the Pentasil-Family of Zeolites: Characterization as Adsorbents", Zeolites **1,** 161-168 (1981).

Katikaneni, S.P.R., J.D. Adjaye and N.N. Bakhshi, "Studies on the Catalytic Conversion of Canola Oil to Hydrocarbons, Influence of Hybrid Catalysts and Steam", Energy Fuels **9,** 599-609 (1995).

Katikaneni, S.P.R., J.D. Adjaye, R. O. Idem and N. N. Bakhshi, "Performance of Various Cracking Catalysts in the Conversion of Canola Oil to Fuels and Chemicals in a Fluidized Bed Reactor", JAOCS **75,** 381-391 (1998).

Kumar, N., V. Nieminen, K. Demirkan, T. Salmi, D.Y. Murzin and E. Laine, "Effect of Synthesis Time and Mode of Stirring on Physico-Chemical and Catalytic Properties of ZSM-5 Zeolite Catalysts", Applied Catalysis A: General **235**, 113 (2002).

Lewandowski, M. and Z. Sarbak, "The Effects of Boron Addition to Hydrodesulphurization and Hydrodenitrogenation Activity of NiMo/Al$_2$O$_3$ catalysts", Fuel **79,** 487 (2000).

Ma, F. and M.A. Hanna, "Biodiesel Production: a Review", Bioresource Technology **70**, 1-15(1999).

McMorn, P., G. Roberts and G.H. Hutchings, "Oxidation of Glycerol with Hydrogen Perxode Using Silicalite and Aluminophosphate Catalysts", Catalysis Letters **63,** 193-197 (1999).

Molina, R., A. Schutz and G. Poncelet, "Transformation of m-xylene over Aluminium Pillared Clays and Ultrastable Zeolite Y", Journal of Catalysis **145,** 79 -85 (1994).

Nam, I. and G.F. Froment, "Catalyst deactivation by site coverage through multi site reaction mechanisms", Journal of Catalysis, 108, 271 (1987).

Neher, A., T. Haas, D. Arntz. H. Klenk and W. Girke, "Process for the Production of Acrolein", US Patent **5387720,** (1995).

Noordin, M.Y., V.C. Venkatesh, S. Sharif, S. Elting and A. Abdullah, "Application of Response Surface Methodology in Describing the Performance of Coated Tools When Turning AISI 1045 Steel", Journal of Material Processing Technology **145**, 46-58 (2004).

Oslon, D.H., G.T. Kokotalio, S.L. Lawton and W.M. Meier, "Crystal Structure and Structure Related Properties of HZSM-5", Journal of Physical Chemistry **85**, 2238-43 (1981).

Peterson, C., G. Moller, R. Haws, X. Zhang, J. Thompson and D. Reece, "Optimization of a Batch Type Ethyl Ester Process from Ethyl Ester Process Scale-Up and Biodegradability of Biodiesel", report for the United States Department of Agriculture (1997).

Pinto, H. P., R. M. Nieminen and Simon D. Elliott, "*Ab initio* Study of γ-Al$_2$O$_3$ Surfaces", Physical Review **B 70**, 125402 (2004).

Plyuto, Y.V., I. Babich, L. Sharanda, A. Marco de Wit and J. Mol, "Thermolysis of Ru(acac)$_3$ Supported on Silica and Alumina", Thermochimica Acta **335,** 87-91 (1999).

Prakash, C.B., "A Critical Review of Biodiesel as a Transportation Fuel in Canada, Report to Transportation System Branch", Air Pollution Prevention Directorate, Environment Canada, March 25 (1998).

Prasad, Y.S., N.N. Bakhshi, J.F. Matthews and R.L. Eager, "Catalytic Conversion of Canola Oil to Fuels and Chemical Feed Stock, Part I. Effect of Process Conditions on Performance of HZSM-5 Catalyst", Canadian Journal of Chemical Engineering **64,** 278-284 (1986).

Rajagopal, S., T. L. Grimm, D. J. Collins and R. Miranda, "Denitrogenation of Piperidine on Alumina, Silica, and Silica-Aluminas: The Effect of Surface Acidity", Journal of Catalysis **137,** 453-461 (1992).

Reding, G., T. Maurer and B. Czarnetzki, "Comparing Synthesis Routes to Nano-Crystalline Zeolite ZSM-5", Microporous and Mesoporous Materials **57**, 83-92 (2003).

Rinaldi, R. and U. Schuchardt, "Factor Responsible for the Activity of Alumina Surfaces in Catalytic Epoxidation of Cis-Cyclooctene with Aqueous H$_2$O$_2$", Journal of Catalysis **227,** 109-116 (2004).

Sang, S., F. Chang, A. liu, C. He, Y. He and L. Xu, "Difference of ZSM-5 Zeolites Synthesized with Various Templates", Catalysis Today **93-95,** 729-734 (2004).

Sato, S., R. Takahashi, T. Sodesawa, C. Kobayashi, A. Miura and K. Ogura, "Variations in Structure and Acidity of Silica-Alumina During Steaming Process", Physical Chemistry Chemical Physics **3**, 885-891 (2001).

Satterfield, C. N., "Heterogeneous Catalysis in Industrial Practice 2nd ed.", McGraw Hill (1991), pp. 143.

Smith, C., "Biodiesel Revolution Gathering Momentum", www.straight.com accessed on August 10, 2005

Stein, Y.S. and M.J. Antal Jr., "A Study of the Gas-Phase Pyrolysis of Glycerol", Journal of Analytical and Applied Pyrolysis **4**, 283-296 (1983).

Szostak, R., "Handbook of Molecular Sieves", Van Nostrand Reinhold New York (1992), pp. 519.

Thiruchitrambalam, V., Master's Thesis "Hydrogen and Syn gas Production from Glycerol Using Pyrolysis and Steam Gasification", University of Saskatchewan (2004).

Thomas, M., Y. Beauchamp, Y. A. Youssef and J. Masounave, "An Experimental Design for Surface Roughness and Built-up Edge Formation in Lathe Dry Turning", International Journal of Quality Science **2,** 3 167-180 (1997).

Védrine, J. C., A. Auroux, P. Dejaifve, V. Ducarme, H. Hoser and S. Zhou, "Catalytic and Physical Properties of Phosphorus-modified ZSM-5 Zeolite", Journal of Catalysis **73**, 147-160 (1982).

Wang, D., D. Montané and E. Chornet, "Catalytic Steam Reforming of Biomass-Derived Oxygenates: Acetic Acid and Hydroxyacetaldehyde", Applied Catalysis A: General **143,** 245-270 (1996).

Wolverton, C. and K. C. Hass, "Phase Stability and Structure of Spinel-based Transition Aluminas", Physical Reviews B **63**, 024102 (2000).

Xu, X., Y. Matsumura, J. Stenberg and M.J. Antal, Jr., "Carbon-Catalyzed Gasification of Organic Feedstocks in Supercritical Water", Ind. Eng. Chem. Res. **35**, 2522-2530 (1996).

Zhang, Y., M. A. Dube, DD. McLean and M. Kates, "Biodiesel Production from Waste Cooking Oil: 2. Economic Assessment and Sensitivity Analysis", Bioresource Technology **90,** 229-240 (2003).

Zhong, Li, K. Xie and R. C.T. Slade, "Studies on the Interaction CuCl and HY Zeolite for Preparing Hetergeneous Cu Catalyst", Applied catalysis A**:** General **202,** 107-115 (2001).

7   APPENDICES

Appendix A: Experimental results for glycerol conversion over HZSM-5

Table A1: Comparison of liquid, gas and char product under different experimental conditions for glycerol conversion over HZSM-5

Exp #	Experimental Conditions			Glycerol fed (g)	Conversion (wt%)	Total Liquid Product (g)	Gas Product (g)	Char and residue (g)	Total Product (g)	Wt% of total Products			Un-accounted (wt%)	Mass balance (wt%)
	T (°C)	CGF (mL/min)	WHSV (h⁻¹)							Gas	Liquid	Char and residue		
1	380	26	8.68	4.87	41.0	4.05	0.02	0.38	4.45	0.50	90.97	8.54	8.60	91.4
2	425	35	13.50	4.92	52.6	4.34	0.04	0.13	4.51	0.82	96.30	2.88	8.30	91.7
3	425	35	13.50	4.89	46.3	4.37	0.03	0.22	4.62	0.74	94.50	4.76	5.50	94.5
4	380	26	18.32	4.53	27.0	3.84	0.01	0.25	4.1	0.27	93.63	6.10	9.50	90.5
5	500	35	13.50	4.57	60.8	4.09	0.09	0.11	4.29	2.17	95.26	2.56	6.10	93.9
6	470	26	18.32	4.40	56.8	3.92	0.05	0.12	4.09	1.20	95.87	2.93	7.00	93.0
7	470	44	18.32	5.00	68.3	4.06	0.06	0.41	4.53	1.42	89.54	9.04	9.40	90.6
8	470	44	8.68	4.61	67.6	3.85	0.08	0.28	4.21	1.81	91.53	6.66	8.70	91.3
9	350	35	13.50	4.94	24.9	4.28	0.02	0.3	4.6	0.36	93.11	6.53	6.90	93.1
10	380	44	18.32	4.89	28.2	4.32	0.02	0.18	4.52	0.45	95.57	3.98	7.60	92.4
11	425	35	13.50	5.09	44.0	4.57	0.04	0.22	4.57	0.86	93.30	4.53	5.10	94.9
13	470	26	8.68	4.65	78.8	3.98	0.08	0.2	4.26	1.93	93.40	4.70	8.40	91.6
14	425	35	5.40	4.27	73.3	3.17	0.14	0.31	3.62	3.80	87.60	8.60	5.39	94.6
15	380	44	8.68	4.05	37.2	3.21	0.02	0.38	3.61	0.62	88.86	10.52	10.80	89.2
16	425	50	13.50	4.60	45.2	3.8	0.05	0.34	4.19	1.08	90.79	8.12	8.90	91.1
18	425	20	13.50	4.57	57.7	4.07	0.04	0.11	4.22	0.97	96.42	2.61	7.70	92.3
20	425	35	21.60	4.75	39.2	4.05	0.04	0.35	4.45	1.04	91.08	7.87	6.30	93.7

Table A2: Composition of liquid product from glycerol conversion over HZSM-5

Compound (wt %)	Experiment number																	
	1	2	3	4	5	6	7	8	9	10	11	13	14	15	16	18	20
Acetaldehyde	4.98	7.59	8.51	2.90	17.59	13.46	13.09	14.06	2.15	1.76	8.72	17.35	17.41	2.67	5.00	11.45	5.67
Acetone	0.22	0.47	0.53	0.89	0.84	0.78	0.70	0.44	1.57	0.36	0.21	1.16	1.14	0.42	0.23	0.60	0.25
Acrolein	4.80	5.04	5.89	2.43	10.10	7.46	10.33	10.91	1.65	1.05	7.00	15.24	14.12	2.63	2.40	11.33	3.99
Formaldehyde	5.00	7.47	8.51	3.35	6.62	8.27	7.38	4.46	2.93	2.65	7.72	5.27	5.02	2.15	5.71	6.01	7.89
IPA	0.20	0.26	0.49	0.46	0.23	0.34	0.25	0.24	0.82	0.20	0.25	0.26	0.16	0.23	0.20	0.25	0.45
Allyl Alcohol	4.31	8.32	6.77	5.33	3.71	5.82	5.52	1.99	1.60	5.28	6.42	2.56	0.33	2.14	5.92	4.63	12.03
Acetol	13.51	16.80	15.21	13.38	17.16	16.34	18.06	15.15	5.30	10.82	14.94	14.39	13.04	12.17	15.91	12.81	16.93
Acetic Acid	1.19	1.04	1.14	0.96	0.49	0.85	0.48	0.55	0.62	0.83	0.81	0.61	0.19	0.93	0.96	0.82	0.90
Propionic Acid	3.45	2.84	2.45	3.06	1.50	2.52	1.46	1.72	2.09	2.44	2.21	1.83	1.47	2.86	2.91	2.38	2.41
Glycerol Formal	5.00	1.82	2.63	5.41	2.13	1.53	1.07	1.84	4.86	3.10	2.45	1.13	1.69	4.57	2.50	3.35	2.62
Phenol	0.39	0.23	0.29	0.31	0.04	0.18	0.10	0.05	0.22	0.24	0.15	0.14	0.04	0.38	0.27	0.16	0.27
Water	46.96	23.53	29.73	42.26	28.63	27.00	26.74	32.43	41.89	50.41	29.27	27.00	32.50	50.65	33.83	25.28	30.78
Unknowns	10.00	24.59	17.86	19.24	10.96	15.48	14.81	16.16	34.30	20.86	19.84	13.06	12.90	18.21	24.17	20.94	15.81
Total	100.00	100.00	100.00	100.00	100.00	100.00	100.00	100.00	100.00	100.00	100.00	100.00	100.00	100.00	100.00	100.00	100.00

113

Table A3: Composition of gas product from glycerol conversion over HZSM-5

EXP #	Experimental Conditions			Gas Product (g)	gas mL/g feed	CO	CO2	CH4	C2+
	T (°C)	CGF (mL/min)	WHSV (h⁻¹)					mol %	
1	380	26	8.68	0.02	3.1	61.5	26.8	2.2	9.4
2	425	35	13.50	0.04	5.0	53.3	29.9	2.6	14.3
3	425	35	13.50	0.03	4.8	59.9	20.0	2.4	17.6
4	380	26	18.32	0.01	1.6	60.2	25.6	2.8	11.4
5	500	35	13.50	0.09	13.0	54.3	17.3	4.3	24.1
6	470	26	18.32	0.05	7.5	55.7	19.4	2.8	22.0
7	470	44	18.32	0.06	8.5	48.7	24.5	3.5	23.3
8	470	44	8.68	0.08	11.1	53.2	22.7	3.6	20.5
9	350	35	13.50	0.02	1.7	-	87.4	-	12.5
10	380	44	18.32	0.02	2.1	-	83.9	-	16.1
11	425	35	13.50	0.04	5.4	53.7	20.1	2.6	23.6
13	470	26	8.68	0.08	12.3	55.5	18.3	4.0	22.2
14	425	35	5.40	0.14	7.7	59.5	13.0	4.6	23.1
15	380	44	8.68	0.02	4.0	68.4	14.2	-	17.4
16	425	50	13.50	0.05	6.5	51.4	30.4	1.9	16.3
18	425	20	13.50	0.04	6.0	50.2	26.3	3.0	20.8
20	425	35	21.60	0.04	5.9	39.8	41.3	1.8	17.2

Appendix B: Experimental results for glycerol conversion over HY

Table B1: Comparison of liquid, gas and char product under different experimental conditions for glycerol conversion over HY

Exp #	Experimental Conditions			Glycerol fed (g)	Conversion (wt%)	Total Liquid Product (g)	Gas Product (g)	Char and residue (g)	Total Product (g)	Wt% of total Products			Un-accounted (wt%)	Mass balance (wt%)
	T (^{o}C)	CGF (mL/min)	WHSV (h^{-1})							Gas	Liquid	Char and residue		
1	380	26	8.68	5.18	79.1	4.17	0.21	0.51	4.88	4.2	85.4	10.4	5.8	94.2
2	425	35	13.50	4.89	92.7	3.84	0.18	0.41	4.43	4.0	86.7	9.3	9.4	90.6
3	425	35	13.50	5.5	95.3	4.47	0.18	0.32	4.97	3.6	89.9	6.4	9.6	90.4
4	380	26	18.32	4.59	59.2	3.8	0.06	0.35	4.21	1.5	90.2	8.3	8.3	91.7
5	500	35	13.50	4.91	98.0	3.69	0.37	0.43	4.49	8.3	82.1	9.6	8.6	91.4
6	470	26	18.32	4.68	95.7	3.84	0.23	0.26	4.32	5.2	88.8	6.0	7.7	92.3
7	470	44	18.32	5.04	95.8	3.86	0.28	0.41	4.55	6.1	84.9	9.0	9.7	90.3
8	470	44	8.68	5.24	99.6	4.23	0.35	0.17	4.76	7.5	88.9	3.6	9.2	90.8
9	350	35	13.50	5.29	66.7	4.5	0.06	0.41	4.97	1.2	90.5	8.2	6.0	94.0
10	380	44	18.32	5.26	76.3	3.96	0.08	0.75	4.79	1.7	82.6	15.6	8.9	91.1
13	470	26	8.68	4.61	100.0	3.57	0.43	0.35	4.35	9.9	82.1	8.0	5.6	94.4
14	425	35	5.40	4.53	99.3	3.37	0.47	0.31	4.15	11.3	81.2	7.5	8.4	91.6
15	380	44	8.68	4.79	88.0	3.82	0.17	0.38	4.37	3.9	87.4	8.7	8.8	91.2
16	425	50	13.50	5.29	98.5	4.36	0.20	0.32	4.88	4.2	89.3	6.6	7.8	92.2
18	425	20	13.50	4.78	95.1	3.89	0.15	0.42	4.47	3.5	87.1	9.4	6.5	93.5
20	425	35	21.60	4.8	71.1	3.98	0.12	0.35	4.45	2.7	89.4	7.9	7.3	92.7

Table B2: Composition of liquid product from glycerol conversion over HY

Compound (wt %)	Experiment number																	
	1	2	3	4	5	6	7	8	9	10	11	13	14	15	16	18	20
Acetaldehyde	10.40	14.60	16.19	5.36	24.08	19.71	19.09	19.35	5.48	7.73	18.23	21.52	12.79	15.80	17.15	12.04	10.40
Acetone	0.20	0.49	0.48	0.10	1.05	0.64	0.68	1.11	0.11	0.24	0.87	0.90	0.31	0.41	0.39	0.35	0.20
Acrolein	15.68	17.08	17.73	7.76	16.27	18.46	17.10	16.38	11.78	9.26	15.05	13.88	15.41	17.01	19.10	12.26	15.68
Formaldehyde	8.76	6.72	9.84	7.99	4.71	5.53	5.95	6.58	7.67	10.67	6.52	9.55	1.99	10.57	8.83	8.06	8.76
IPA	0.33	0.29	0.41	0.28	0.20	0.24	0.34	0.26	0.11	0.41	0.32	0.68	0.52	0.40	0.34	0.30	0.33
Allyl Alcohol	1.35	0.92	1.26	1.30	0.69	0.94	0.95	0.53	1.52	1.76	0.40	0.37	1.17	1.25	0.92	0.92	1.35
Acetol	12.72	12.51	17.05	12.15	15.77	14.32	20.36	12.78	11.50	15.22	9.94	7.23	14.51	17.85	12.37	12.79	12.72
Acetic Acid	0.66	0.14	0.08	0.62	0.04	0.09	0.09	0.64	0.88	0.89	0.69	1.39	0.42	0.66	0.50	0.46	0.66
Propionic Acid	1.87	0.53	0.24	1.80	0.04	0.28	0.33	0.03	2.26	2.21	0.40	0.81	1.22	0.24	0.46	1.47	1.87
Glycerol Formal	2.87	1.01	0.98	2.19	0.26	0.42	0.46	0.24	3.87	3.18	0.18	0.48	2.40	0.88	1.19	1.35	2.87
Phenol	0.16	0.11	0.07	0.21	0.10	0.09	0.11	0.09	0.28	0.21	0.11	0.12	0.09	0.08	0.10	0.10	0.16
Water	31.08	29.65	23.28	36.98	29.88	28.77	28.06	31.01	27.88	29.59	32.66	36.58	31.55	26.61	28.00	31.27	31.08
Unknowns	13.92	15.96	12.40	23.24	6.92	10.48	6.50	11.00	26.64	18.61	14.62	6.49	17.63	8.25	10.66	18.63	13.92
Total	100.00	100.00	100.00	100.00	100.00	100.00	100.00	100.00	100.00	100.00	100.00	100.00	100.00	100.00	100.00	100.00	100.00

Table B3: Composition of gas product from glycerol conversion over HY

EXP #	Experimental Conditions			Gas Product (g)	gas mL/g feed	CO	CO2	CH4	C2+
	T (°C)	CGF (mL/min)	WHSV (h⁻¹)				mol %		
1	380	26	8.68	0.21	24.1	39.3	47.8	1.1	11.2
2	425	35	13.50	0.18	25.7	59.1	11.7	4.5	24.7
3	425	35	13.50	0.18	23.4	61.5	10.0	4.3	24.0
4	380	26	18.32	0.06	9.8	63.0	10.2	1.6	25.2
5	500	35	13.50	0.37	57.4	55.4	6.6	12.3	25.7
6	470	26	18.32	0.23	35.6	59.0	7.1	8.7	25.1
7	470	44	18.32	0.28	36.1	49.8	21.7	7.1	21.4
8	470	44	8.68	0.35	49.7	52.0	7.7	10.3	29.8
9	350	35	13.50	0.06	8.0	65.2	9.9	1.3	23.7
10	380	44	18.32	0.08	10.3	54.9	20.5	1.6	23.0
13	470	26	8.68	0.43	67.7	54.8	8.8	9.2	27.3
14	425	35	5.40	0.47	75.1	57.3	10.0	6.9	25.7
15	380	44	8.68	0.17	24.5	61.6	11.2	2.1	25.1
16	425	50	13.50	0.20	27.5	62.8	8.9	4.5	23.7
18	425	20	13.50	0.15	23.8	64.8	6.7	4.1	24.4
20	425	35	21.60	0.12	17.8	65.8	8.3	3.3	22.5

Appendix C: Experimental results for glycerol conversion over silica-alumina

Table C1: Comparison of liquid, gas and char product under different experimental conditions for glycerol conversion over silica-alumina

Exp #	Experimental Conditions			Glycerol fed (g)	Conversion (wt%)	Total Liquid Product (g)	Gas Product (g)	Char and residue (g)	Total Product (g)	Wt% of total Products			Un-accounted (wt%)	Mass balance (wt%)
	T (°C)	CGF (mL/min)	WHSV (h^{-1})							Gas	Liquid	Char and residue		
1	380	26	8.68	5.42	99.9	4.53	0.15	0.31	4.99	3.0	90.8	6.2	8.0	92.0
2	425	35	13.50	5.00	100.0	3.87	0.35	0.34	4.55	7.6	85.0	7.4	8.9	91.1
4	380	26	18.32	5.27	100.0	4.37	0.21	0.3	4.88	4.2	89.6	6.2	7.5	92.5
5	500	35	13.50	5.06	99.7	3.73	0.57	0.37	4.67	12.2	79.9	7.9	7.7	92.3
6	470	26	18.32	5.32	100.0	4.03	0.60	0.29	4.92	12.3	81.9	5.9	7.5	92.5
7	470	44	18.32	5.12	100.0	4.36	0.09	0.22	4.67	1.9	93.4	4.7	8.8	91.2
8	470	44	8.68	4.61	99.7	3.3	0.60	0.44	4.24	14.2	77.8	8.0	7.9	92.1
9	350	35	13.50	4.71	98.4	3.8	0.16	0.34	4.3	3.6	88.5	7.9	8.8	91.2
10	380	44	18.32	4.94	100.0	4.13	0.18	0.25	4.56	4.0	90.5	5.5	7.7	92.3
11	425	35	13.50	4.39	100.0	3.5	0.36	0.3	4.15	8.3	84.4	7.2	5.6	94.4
13	470	26	8.68	5.23	100.0	3.47	0.87	0.5	4.84	17.9	71.8	10.3	7.5	92.5
14	425	35	5.40	4.48	100.0	3.4	0.35	0.43	4.18	8.3	81.4	10.3	6.7	93.3
15	380	44	8.68	5.05	100.0	4.00	0.38	0.33	4.65	6.8	86.1	7.1	8.0	92.0
16	425	50	13.50	4.2	100.0	3.38	0.24	0.25	3.87	6.2	87.3	6.5	7.8	92.2
18	425	20	13.50	4.71	100.0	3.63	0.25	0.47	4.35	5.7	83.5	10.8	7.7	92.3
20	425	35	21.60	4.61	99.1	3.77	0.21	0.25	4.23	4.9	89.2	5.9	8.3	91.7

118

Table C2: Composition of liquid product from glycerol conversion over silica-alumina

Compound (wt %)	Experiment number															
	1	2	4	5	6	7	8	9	10	11	13	14	15	16	18	20
Acetaldehyde	17.71	25.59	23.68	27.64	28.05	28.75	29.54	12.44	17.96	21.47	24.59	27.80	19.61	27.47	26.57	20.82
Acetone	0.28	1.22	0.69	7.90	8.09	1.79	2.09	0.79	1.21	1.12	0.66	2.15	1.32	2.19	2.30	1.74
Acrolein	21.27	14.62	22.64	10.20	10.73	14.58	8.51	19.99	19.76	15.80	9.27	12.19	17.36	19.55	17.16	20.20
Formaldehyde	8.09	10.39	2.41	4.45	4.74	8.01	7.23	7.47	9.52	8.01	4.70	8.36	11.27	11.41	7.77	6.76
IPA	0.46	0.25	0.59	0.09	0.36	0.18	0.14	0.38	0.47	0.30	0.18	0.21	1.10	0.31	0.35	0.33
Allyl Alcohol	0.75	0.24	5.11	0.22	0.21	0.25	0.23	0.90	0.73	0.38	0.23	0.21	0.01	0.06	0.07	0.57
Acetol	12.44	2.88	1.00	0.43	0.92	3.07	0.54	9.69	10.53	6.88	4.04	0.34	5.45	2.56	6.37	9.56
Acetic Acid	0.57	0.09	0.03	0.90	0.71	0.97	1.44	0.73	0.51	0.88	0.52	1.47	0.75	0.48	0.78	0.54
Propionic Acid	0.31	0.20	0.69	0.04	0.04	0.02	0.04	0.46	0.07	0.02	0.01	0.02	0.01	0.02	0.02	0.07
Glycerol Formal	1.73	0.19	0.55	0.22	0.15	0.13	0.16	2.08	0.81	0.87	0.51	0.48	0.19	0.14	0.59	1.18
Phenol	0.11	0.17	0.00	0.13	0.11	0.16	0.11	0.22	0.14	0.19	0.11	0.16	0.19	0.11	0.14	0.16
Water	21.80	35.05	25.84	34.63	32.46	32.82	40.70	31.16	28.50	35.14	37.32	37.18	31.83	31.44	29.65	26.72
Unknowns	14.48	9.12	16.76	13.14	13.44	9.26	9.26	13.68	9.80	8.94	17.86	9.43	10.91	4.25	8.23	11.37
Total	100.00	100.00	100.00	100.00	100.00	100.00	100.00	100.00	100.00	100.00	100.00	100.00	100.00	100.00	100.00	100.00

Table C3: Composition of gas product from glycerol conversion over silica-alumina

EXP #	Experimental Conditions			Gas product (g)	Gas mL/g feed	H_2	CO	CO_2	CH_4	C_2+
	T (^{o}C)	CGF (mL/min)	WHSV (h^{-1})			mol %				
1	380	26	8.68	0.15	19.8	-	75.3	10.0	1.9	12.7
2	425	35	13.50	0.35	49.7	-	69.5	11.6	3.2	15.7
4	380	26	18.32	0.21	28.8	-	76.0	9.0	1.9	13.0
5	500	35	13.50	0.57	86.5	-	62.2	4.4	10.4	18.9
6	470	26	18.32	0.60	86.3	3.2	65.5	6.5	10.1	17.9
7	470	44	18.32	0.09	12.5	-	66.5	9.5	6.2	16.9
8	470	44	8.68	0.60	95.4	-	60.0	8.7	7.8	23.3
9	350	35	13.50	0.16	22.9	-	69.5	18.6	0.9	11.0
10	380	44	18.32	0.18	26.4	-	74.3	9.7	1.7	14.4
11	425	35	13.50	0.35	56.9	-	69.3	11.6	3.3	15.8
13	470	26	8.68	0.87	124.8	-	57.2	7.1	13.0	22.5
14	425	35	5.40	0.35	56.1	-	69.3	11.6	3.2	15.8
15	380	44	8.68	0.32	43.8	-	69.0	15.1	1.3	14.5
16	425	50	13.50	0.24	41.4	-	71.8	9.8	2.4	16.0
18	425	20	13.50	0.25	37.8	-	67.6	9.3	3.7	19.3
20	425	35	21.60	0.21	31.3	-	65.4	14.2	2.4	17.9

Appendix D: Experimental results for glycerol conversion over γ-alumina

Table D1: Comparison of liquid, gas and char product under different experimental conditions for glycerol conversion over γ-alumina

Exp #	Experimental Conditions			Glycerol fed (g)	Conversion (wt%)	Total Liquid Product (g)	Gas Product (g)	Char and residue (g)	Total Product (g)	Wt% of total Products			Un-accounted (wt%)	Mass balance (wt%)
	T (°C)	CGF (mL/min)	WHSV (h^{-1})							Gas	Liquid	Char and residue		
1	380	26	8.68	5.05	100.0	4.21	0.22	0.21	4.64	4.7	90.8	4.5	8.1	91.9
2	425	35	13.50	4.74	100.0	3.82	0.30	0.26	4.31	6.9	87.1	5.9	7.5	92.5
4	380	26	18.32	4.21	99.6	3.62	0.21	0.21	4.04	5.2	89.6	5.2	4.0	96.0
5	500	35	13.50	5.19	100.0	3.9	0.61	0.28	4.79	12.7	81.5	5.8	7.8	92.2
6	470	26	18.32	4.73	99.1	3.78	0.25	0.29	4.32	5.8	87.5	6.7	8.7	91.3
7	470	44	18.32	4.55	100.0	3.59	0.34	0.28	4.21	8.1	85.3	6.7	7.5	92.5
8	470	44	8.68	4.7	99.9	3.69	0.41	0.25	4.35	9.5	84.8	5.7	7.4	92.6
9	350	35	13.50	4.64	99.7	3.9	0.23	0.2	4.33	5.2	90.1	4.6	6.8	93.2
10	380	44	18.32	4.7	99.2	3.84	0.29	0.19	4.33	6.8	88.8	4.4	8.0	92.0
11	425	35	13.50	4.71	100.0	3.84	0.31	0.24	4.39	7.1	87.4	5.5	6.8	93.3
13	470	26	8.68	4.77	100.0	3.73	0.43	0.2	4.36	10.0	85.0	4.6	8.5	91.5
14	425	35	5.40	4.3	100.0	3.5	0.31	0.21	4.02	7.8	87.0	5.2	6.5	93.5
15	380	44	8.68	4.5	100.0	3.76	0.28	0.22	4.26	6.6	88.2	5.2	5.3	94.7
16	425	50	13.50	4.55	100.0	3.57	0.38	0.21	4.16	9.2	85.7	5.0	8.5	91.5
18	425	20	13.50	4.43	100.0	3.51	0.31	0.25	4.06	7.6	86.3	6.2	8.4	91.6
20	425	35	21.60	4.88	100.0	4.02	0.20	0.25	4.45	4.4	90.0	5.6	8.9	91.1

Table D2: Composition of liquid product from glycerol conversion over γ-alumina

Compound (wt %)	Experiment number															
	1	2	4	5	6	7	8	9	10	11	13	14	15	16	18	20
Acetaldehyde	10.62	9.13	5.95	20.07	12.08	12.29	14.97	10.01	6.95	10.94	14.61	10.51	9.18	9.88	8.13	8.12
Acetone	2.46	2.39	0.40	3.41	1.52	1.54	1.78	2.20	1.76	2.20	5.16	2.60	1.60	1.95	3.01	2.21
Acrolein	19.88	15.55	18.17	15.15	18.01	13.70	15.40	16.90	12.12	16.69	14.43	11.58	30.23	21.64	16.34	21.12
Formaldehyde	6.57	3.76	4.72	6.97	3.97	5.18	6.00	6.44	4.79	6.81	4.85	4.78	6.28	5.28	2.88	4.68
IPA	0.24	0.17	0.19	0.27	0.20	0.22	0.23	0.20	0.14	0.44	0.21	0.33	0.10	0.20	0.14	0.18
Allyl Alcohol	0.57	0.46	1.15	0.38	0.60	0.43	0.33	0.52	1.05	0.50	0.34	0.33	1.56	0.67	0.52	0.80
Acetol	4.98	7.32	13.04	0.75	0.90	4.15	5.36	4.39	10.47	2.48	2.35	1.59	10.31	9.74	6.87	12.26
Acetic Acid	0.62	0.49	0.81	0.66	0.46	0.53	0.79	0.56	0.68	0.79	0.67	0.60	0.90	0.48	0.47	0.49
Propionic Acid	0.02	0.05	0.08	0.04	0.02	0.03	0.04	0.02	0.02	0.02	0.03	0.01	0.11	0.06	0.03	0.03
Glycerol Formal	0.39	0.35	1.23	0.13	0.38	0.21	0.36	0.41	0.82	0.35	0.19	0.17	0.48	0.49	0.32	0.66
Phenol	0.60	0.43	0.72	0.23	0.32	0.27	0.47	0.56	0.51	0.66	0.39	0.37	0.61	0.39	0.34	0.39
Water	31.88	33.31	22.54	35.56	30.89	35.17	37.82	34.26	31.97	32.74	38.43	37.62	32.02	29.13	30.75	28.07
Unknowns	21.18	26.57	30.99	16.39	30.66	26.27	16.43	23.54	28.73	25.37	18.35	29.51	6.62	20.09	30.20	20.99
Total	100.00	99.98	99.99	100.00	100.00	99.99	99.98	100.00	100.00	100.00	100.00	100.00	100.00	100.00	100.00	100.00

Table D3: Composition of gas product from glycerol conversion over γ-alumina

EXP #	Experimental Conditions			Gas Product (g)	Gas mL/g feed	CO	CO2	CH4	C2+
	T (^{o}C)	CGF (mL/min)	WHSV (h^{-1})			mol %			
1	380	26	8.68	0.22	31.0	71.9	16.4	1.9	9.8
2	425	35	13.50	0.30	45.4	66.4	16.1	3.3	14.3
4	380	26	18.32	0.21	36.1	73.0	16.0	1.9	9.1
5	500	35	13.50	0.61	88.0	65.8	9.9	9.0	15.2
6	470	26	18.32	0.25	37.7	65.8	15.9	4.7	13.5
7	470	44	18.32	0.34	54.4	67.6	13.2	5.4	13.7
8	470	44	8.68	0.41	62.8	64.6	15.2	5.4	14.8
9	350	35	13.50	0.23	34.9	72.7	15.5	2.0	9.8
10	380	44	18.32	0.30	44.4	69.8	18.4	2.0	9.9
11	425	35	13.50	0.31	46.9	66.4	15.8	3.4	14.4
13	470	26	8.68	0.43	65.3	63.7	15.4	5.6	15.2
14	425	35	5.40	0.31	51.0	65.4	16.4	3.2	14.8
15	380	44	8.68	0.28	44.9	72.4	15.9	1.9	9.7
16	425	50	13.50	0.38	59.9	67.5	15.0	2.9	14.6
18	425	20	13.50	0.31	49.1	68.1	15.8	3.3	12.8
20	425	35	21.60	0.20	28.6	69.8	14.8	3.0	12.4

Appendix E: Liquid, gas and char product yield results

Appendix E1: Liquid product yield under different experimental conditions using different catalysts

Exp #	Experimental Conditions			Liquid product (g/100 g feed)			
	T (°C)	CGF (mL/min)	WHSV (h^{-1})	HZSM-5	HY	Silica-alumina	γ-alumina
1	380	26	8.68	24.2	59.6	83.5	83.4
2	425	35	13.50	40.8	71.2	77.4	80.6
3	425	35	13.50	35.6	76.6	--	--
4	380	26	18.32	11.8	42.0	82.9	85.6
5	500	35	13.50	50.3	73.2	73.4	75.1
6	470	26	18.32	45.9	77.8	75.8	79.0
7	470	44	18.32	49.5	72.4	85.2	78.9
8	470	44	8.68	51.1	80.3	71.3	78.4
9	350	35	13.50	11.5	51.8	79.1	83.7
10	380	44	18.32	16.5	51.6	83.6	80.9
11	425	35	13.50	33.8	--	79.7	81.5
13	470	26	8.68	64.4	77.4	66.3	78.2
14	425	35	5.40	47.5	73.7	75.9	81.4
15	380	44	8.68	16.4	67.7	79.2	83.6
16	425	50	13.50	27.8	80.9	80.5	78.4
18	425	20	13.50	46.8	76.4	77.1	79.0
20	425	35	21.60	24.5	54.0	80.9	82.0

Appendix E2: Gas product yield (g/100 g feed) under different experimental conditions using different catalysts

Exp #	Experimental Conditions			Gas product (g/100 g feed)			
	T (^{o}C)	CGF (mL/min)	WHSV (h^{-1})	HZSM-5	HY	Silica-alumina	γ-alumina
1	380	26	8.68	0.49	3.96	2.71	4.34
2	425	35	13.50	0.75	3.64	6.90	6.41
3	425	35	13.50	0.70	3.27	--	--
4	380	26	18.32	0.22	1.41	3.93	5.04
5	500	35	13.50	1.97	7.60	11.28	11.70
6	470	26	18.32	1.09	4.81	11.30	5.26
7	470	44	18.32	1.20	5.52	1.70	7.47
8	470	44	8.68	1.65	6.68	13.10	8.74
9	350	35	13.50	0.32	1.15	3.31	4.87
10	380	44	18.32	0.41	1.59	3.64	6.17
11	425	35	13.50	0.79	--	8.11	6.62
13	470	26	8.68	1.78	9.33	16.56	9.10
14	425	35	5.40	3.28	10.38	7.79	7.21
15	380	44	8.68	0.49	3.55	7.52	6.27
16	425	50	13.50	0.98	3.84	5.74	8.44
18	425	20	13.50	0.88	3.14	5.27	6.93
20	425	35	21.60	0.84	2.50	4.45	4.02

Appendix E3: Char and residue yield (g/100 g feed) under different experimental conditions using different catalysts

Exp #	Experimental Conditions			Char and residue (g/100 g feed)			
	T (°C)	CGF (mL/min)	WHSV (h^{-1})	HZSM-5	HY	Silica-alumina	γ-alumina
1	380	26	8.68	7.80	9.85	5.72	4.16
2	425	35	13.50	2.64	8.38	6.80	5.49
3	425	35	13.50	4.50	5.82	--	--
4	380	26	18.32	5.52	7.63	5.69	4.99
5	500	35	13.50	2.41	8.76	7.31	5.39
6	470	26	18.32	2.73	5.56	5.45	6.13
7	470	44	18.32	8.20	8.13	4.30	6.15
8	470	44	8.68	6.07	3.24	9.54	5.32
9	350	35	13.50	6.07	7.75	7.22	4.31
10	380	44	18.32	3.68	14.26	5.06	4.04
11	425	35	13.50	4.32	--	6.83	5.10
13	470	26	8.68	4.30	7.59	9.56	4.19
14	425	35	5.40	7.26	6.84	9.60	4.88
15	380	44	8.68	9.38	7.93	6.53	4.89
16	425	50	13.50	7.39	6.05	5.95	4.62
18	425	20	13.50	2.41	8.79	9.98	5.64
20	425	35	21.60	7.37	7.29	5.42	5.12

Appendix F: Acetaldehyde, acrolein, formaldehyde and acetol yields over different catalysts

Appendix F1: Acetaldehyde yield (g/100 g feed) under different experimental conditions using different catalysts

Exp #	Experimental Conditions			Acetadehdye (g/100 g feed)			
	T (°C)	CGF (mL/min)	WHSV (h^{-1})	HZSM-5	HY	Silica-alumina	γ-alumina
1	380	26	8.68	1.2	6.2	14.8	8.9
2	425	35	13.50	3.1	10.4	19.8	7.4
3	425	35	13.50	3.0	12.4	--	--
4	380	26	18.32	0.3	2.3	19.6	5.1
5	500	35	13.50	8.8	17.6	20.3	15.1
6	470	26	18.32	6.2	15.3	21.3	9.5
7	470	44	18.32	6.5	13.8	24.5	9.7
8	470	44	8.68	7.2	15.5	21.1	11.7
9	350	35	13.50	0.2	2.8	9.8	8.4
10	380	44	18.32	0.3	4.0	15.0	5.6
11	425	35	13.50	2.9	--	17.1	8.9
13	470	26	8.68	11.2	14.1	16.3	11.4
14	425	35	5.40	6.7	15.9	21.1	8.6
15	380	44	8.68	0.4	8.7	15.5	7.7
16	425	50	13.50	1.4	12.8	22.1	7.8
18	425	20	13.50	5.4	13.1	20.5	6.4
20	425	35	21.60	1.4	6.5	16.8	6.7

Appendix F2: Acrolein yield (g/100 g feed) under different experimental conditions using different catalysts

Exp #	Experimental Conditions			Acrolein (g/100 g feed)			
	T (°C)	CGF (mL/min)	WHSV (h⁻¹)	HZSM-5	HY	Silica-alumina	γ-alumina
1	380	26	8.68	1.2	9.4	17.8	16.6
2	425	35	13.50	2.1	12.2	11.3	12.5
3	425	35	13.50	2.1	13.6	--	--
4	380	26	18.32	0.3	3.3	18.8	15.6
5	500	35	13.50	5.1	11.9	7.5	11.4
6	470	26	18.32	3.4	14.4	8.1	14.2
7	470	44	18.32	5.1	12.4	12.4	10.8
8	470	44	8.68	5.6	13.2	6.1	12.1
9	350	35	13.50	0.2	6.1	15.8	14.2
10	380	44	18.32	0.2	4.8	16.5	9.8
11	425	35	13.50	2.4	--	12.6	13.6
13	470	26	8.68	9.8	11.7	6.2	11.3
14	425	35	5.40	6.8	10.2	9.3	9.4
15	380	44	8.68	0.4	10.4	13.8	25.3
16	425	50	13.50	0.7	13.8	15.7	17.0
18	425	20	13.50	5.3	14.6	13.2	12.9
20	425	35	21.60	1.0	6.62	16.3	17.3

Appendix F3: Formaldehyde yield (g/100 g feed) under different experimental conditions using different catalysts

Exp #	Experimental Conditions			Formaldehdye (g/100 g feed)			
	T (^{o}C)	CGF (mL/min)	WHSV (h^{-1})	HZSM-5	HY	Silica-alumina	γ-alumina
1	380	26	8.68	1.2	5.2	6.8	5.5
2	425	35	13.50	3.0	4.8	8.0	3.0
3	425	35	13.50	3.0	7.5	--	--
4	380	26	18.32	0.4	3.4	2.0	4.0
5	500	35	13.50	3.3	3.5	3.3	5.2
6	470	26	18.32	3.8	4.3	3.6	3.1
7	470	44	18.32	3.7	4.3	6.8	4.1
8	470	44	8.68	2.3	5.3	5.2	4.7
9	350	35	13.50	0.3	4.0	5.9	5.4
10	380	44	18.32	0.4	5.5	8.0	3.9
11	425	35	13.50	2.6	--	6.4	5.6
13	470	26	8.68	3.4	5.1	3.1	3.8
14	425	35	5.40	0.7	7.0	6.3	3.9
15	380	44	8.68	0.4	1.4	8.9	5.3
16	425	50	13.50	1.6	8.6	9.2	4.1
18	425	20	13.50	2.8	6.8	6.0	2.3
20	425	35	21.60	1.9	4.4	5.5	3.8

Appendix F4: Acetol yield (g/100 g feed) under different experimental conditions using different catalysts

Exp #	Conditions			Acetol (g/100 g feed)			
	T (°C)	CGF (mL/min)	WHSV (h^{-1})	HZSM-5	HY	Silica-alumina	γ-alumina
1	380	26	8.68	3.27	7.58	10.4	4.2
2	425	35	13.50	6.9	8.91	2.2	5.9
3	425	35	13.50	5.4	13.1	--	--
4	380	26	18.32	1.6	5.1	0.8	11.2
5	500	35	13.50	8.6	11.5	0.3	0.6
6	470	26	18.32	7.5	11.1	0.7	0.7
7	470	44	18.32	8.9	14.7	2.6	3.3
8	470	44	8.68	7.7	10.3	0.4	4.2
9	350	35	13.50	0.6	6.0	7.7	3.7
10	380	44	18.32	1.8	7.9	8.8	8.5
11	425	35	13.50	5.0	--	5.5	2.0
13	470	26	8.68	9.3	7.7	2.7	1.8
14	425	35	5.40	7.7	5.3	0.3	1.3
15	380	44	8.68	2.0	9.8	4.3	8.6
16	425	50	13.50	4.4	14.4	2.1	7.6
18	425	20	13.50	6.0	9.5	4.9	5.4
20	425	35	21.60	4.1	6.9	7.7	10.1

Appendix G: ANOVA Table for different responses

Table G1: **Analysis of variance showing the effect of variables on glycerol conversion over HZSM-5 and HY**

Source Of Variation	Sum Of Squares	Degree Of Freedom	Mean Square	F Value	Prob>F
HZSM-5					
Model	3680.89	3	1226.96	27.77	< 0.0001
T	2884.48	1	2884.48	65.29	< 0.0001
C	39.83	1	39.83	0.90	0.3565
W	756.58	1	756.58	17.21	0.0008
Residual	706.9	16	44.18		
Pure Error	53.76	5	10.75		
Total	4387.90	19			
HY					
Model	2634.46	9	292.72	35.80	< 0.0001
A	1458.65	1	1458.65	178.39	< 0.0001
C	72.28	1	72.28	8.84	0.0140
W	555.84	1	555.84	67.98	< 0.0001
T2	238.40	1	238.40	29.16	0.0003
C2	15.63	1	15.63	1.91	0.1968
W2	134.91	1	134.91	16.50	0.0023
T*C	86.46	1	86.46	10.57	0.0087
T*W	69.03	1	69.03	8.44	0.0157
C*W	9.46	1	9.46	1.16	0.3073
Residual	81.77	10	8.18		
Pure Error	5.44	5	1.09		
Total	2716.23	19			

Table G2: **Analysis of variance showing the effect of variables on Liquid product yield over different catalysts**

Source Of Variation	Sum Of Squares	Degree Of Freedom	Mean Square	F Value	Prob>F
HZSM-5					
Model	3661.86	3	1220.62	47.14	< 0.0001
T	3145.24	1	3145.24	121.46	< 0.0001
C	146.66	1	146.66	5.66	0.0301
W	369.96	1	369.96	14.29	0.0016
Residual	414.34	16	25.90		
Pure Error	27.19	5	5.44		
Total	4076.20	19			
HY					
Model	2208.34	5	441.67	28.46	< 0.0001
T	1107.62	1	1107.62	71.38	< 0.0001
W	404.57	1	404.57	26.07	0.0002
T2	365.74	1	365.74	23.57	0.0003
W2	299.41	1	299.41	19.29	0.0006
T*W	85.81	1	85.81	5.53	0.0339
Residual	217.25	14	15.52		
Pure Error	21.27	5	4.25		
Total	2425.59	19			
Silica-alumina					
Model	330.64	6	55.11	17.63	< 0.0001
T	118.25	1	118.25	37.84	< 0.0001
C	19.98	1	19.98	6.39	0.0252
W	92.85	1	92.85	29.71	0.0001
T*C	40.50	1	40.50	12.96	0.0032
T*W	48.02	1	48.02	15.37	0.0018
C*W	11.04	1	11.04	3.53	0.0827
Residual	40.63	13	3.13		
Pure Error	2.87	5	0.57		
Total	371.27	19			
γ-alumina					
Model	99.94	9	11.10	36.39	< 0.0001
T	83.68	1	83.68	274.20	< 0.0001
C	0.14	1	0.14	0.45	0.5211
W	1.96	1	1.96	6.41	0.0322
T2	2.65	1	2.65	8.69	0.0163
C2	6.53	1	6.53	21.38	0.0012
W2	1.99	1	1.99	6.54	0.0309
T*C	6.56	1	6.56	21.48	0.0012
T*W	2.95	1	2.95	9.66	0.0125
C*W	7.51	1	7.51	24.62	0.0008
Residual	2.75	9	0.31		
Pure Error	0.45	5	0.090		
Total	102.69	18			

Table G3: **Analysis of variance showing the effect of variables on acetaldehyde yield over different catalysts**

Source Of Variation	Sum Of Squares	Degree Of Freedom	Mean Square	F Value	Prob>F
HZSM-5					
Model	164.74	3	54.91	41.40	< 0.0001
T	137.62	1	137.62	103.76	< 0.0001
C	9.25	1	9.25	6.97	0.0178
W	17.87	1	17.87	13.48	0.0021
Residual	21.22	16	1.33		
Pure Error	0.015	5	3.0E-03		
Total	185.97	19			
HY					
Model	346.09	5	69.22	77.15	< 0.0001
T	286.30	1	286.30	319.12	< 0.0001
W	11.10	1	11.10	12.37	0.0038
T2	7.69	1	7.69	8.58	0.0117
W2	17.37	1	17.37	19.37	0.0007
T*W	8.22	1	8.22	9.16	0.0097
Residual	11.66	13	0.90		
Pure Error	3.15	5	0.63		
Total	357.75	18			
Silica-alumina					
Model	120.92	3	40.31	7.97	0.0018
T	93.40	1	93.40	18.46	0.0006
C	3.45	1	3.45	0.68	0.4212
C2	24.07	1	24.07	4.76	0.0444
Residual	80.94	16	5.06		
Pure Error	4.78	5	0.96		
Total	201.85	19			
γ-alumina					
Model	90.15	5	18.03	46.27	< 0.0001
T	51.18	1	51.18	131.34	< 0.0001
C	0.31	1	0.31	0.80	0.3854
W	12.20	1	12.20	31.31	< 0.0001
T2	22.69	1	22.69	58.22	< 0.0001
C2	2.26	1	2.26	5.79	0.0305
Residual	5.46	14	0.39		
Pure Error	1.24	5	0.25		
Total	95.60	19			

Table G4: Analysis of variance showing the effect of variables on acrolein yield over different catalysts

Source Of Variation	Sum Of Squares	Degree Of Freedom	Mean Square	F Value	Prob>F
HZSM-5					
Model	98.25	3	32.75	17.76	< 0.0001
T	66.26	1	66.26	35.93	< 0.0001
C	9.02	1	9.02	4.89	0.0419
W	22.98	1	22.98	12.46	0.0028
Residual	29.50	16	1.84		
Pure Error	0.088	5	0.018		
Total	127.75	19			
HY					
Model	204.97	5	40.99	43.28	< 0.0001
T	82.05	1	82.05	86.63	< 0.0001
W	18.54	1	18.54	19.57	0.0006
T2	39.02	1	39.02	41.19	< 0.0001
W2	49.31	1	49.31	52.06	< 0.0001
T*W	23.32	1	23.32	24.63	0.0002
Residual	204.97	5	40.99		
Pure Error	1.58	5	0.32		
Total	218.23	19			
Silica-alumina					
Model	224.33	4	56.08	25.17	< 0.0001
T	167.74	1	167.74	75.29	< 0.0001
C	0.39	1	0.39	0.18	0.6811
W	42.86	1	42.86	19.24	0.0005
T*C	13.34	1	13.34	5.99	0.0272
Residual	33.42	15	2.23		
Pure Error	1.17	5	0.23		
Total	257.75	19			
γ-alumina					
Model	128.89	5	25.78	3.63	0.0257
T	40.23	1	40.23	5.67	0.0320
C	3.74	1	3.74	0.53	0.4797
W	0.18	1	0.18	0.025	0.8773
T*W	41.22	1	41.22	5.81	0.0303
C*W	43.52	1	43.52	6.14	0.0266
Residual	99.32	14	7.09		
Pure Error	0.59	5	0.12		
Total	228.21	19			

Table G5: **Analysis of variance showing the effect of variables on formaldehyde yield over different catalysts**

Source Of Variation	Sum Of Squares	Degree Of Freedom	Mean Square	F Value	Prob>F
HZSM-5					
Model	24.83	5	4.97	22.72	< 0.0001
T	18.36	1	18.36	83.99	< 0.0001
C	1.19	1	1.19	5.44	0.0352
W	0.66	1	0.66	3.03	0.1036
T2	1.46	1	1.46	6.66	0.0218
W2	3.54	1	3.54	16.18	0.0013
Residual	3.06	14	0.22		
Pure Error	0.12	5	0.024		
Total	27.89	19			
HY					
Model	41.62	4	10.40	5.18	0.0080
T	0.51	1	0.51	0.26	0.6207
W	1.15	1	1.15	0.57	0.4608
T2	33.29	1	33.29	16.58	0.0010
W2	9.56	1	9.56	4.76	0.0454
T*W	41.62	4	10.40	5.18	0.0080
Residual	30.12	15	2.01		
Pure Error	7.36	5	1.47		
Total	71.73	19			
Silica-alumina					
Model	54.77	5	10.95	12.10	0.0001
T	9.49	1	9.49	10.49	0.0060
C	25.73	1	25.73	28.43	0.0001
W	1.88	1	1.88	2.07	0.1718
T2	9.91	1	9.91	10.95	0.0052
T*W	7.76	1	7.76	8.58	0.0110
Residual	12.67	14	0.90		
Pure Error	2.24	5	0.45		
Total	67.44	19			
γ-alumina					
Model	9.93	4	2.48	8.09	0.0013
C	1.55	1	1.55	5.04	0.0414
W	1.28	1	1.28	4.16	0.0608
C2	5.63	1	5.63	18.35	0.0008
W2	2.28	1	2.28	7.42	0.0165
Residual	4.30	14	0.31		
Pure Error	0.63	4	0.16		
Total	14.23	18			

Table G6: **Analysis of variance showing the effect of variables on acetol yield over different catalysts**

Source Of Variation	Sum Of Squares	Degree Of Freedom	Mean Square	F Value	Prob>F
HZSM-5					
Model	112.08	2	56.04	75.76	< 0.0001
T	106.76	1	106.76	144.32	< 0.0001
W	5.32	1	5.32	7.19	0.0158
Residual	12.58	17	0.74		
Pure Error	2.44	5	0.49		
Total	124.66	19			
HY					
Model	162.85	6	27.14	23.52	< 0.0001
T	38.30	1	38.30	33.19	< 0.0001
C	27.96	1	27.96	24.23	0.0003
W	2.72	1	2.72	2.35	0.1490
T2	18.55	1	18.55	16.07	0.0015
W2	61.69	1	61.69	53.46	< 0.0001
T*W	19.13	1	19.13	16.57	0.0013
Residual	15.00	13	1.15		
Pure Error	13.54	5	2.71		
Total	177.86	19			
Silica-alumina					
Model	114.14	4	28.54	7.34	0.0018
T	67.32	1	67.32	17.32	0.0008
C	0.77	1	0.77	0.20	0.6616
W	4.37	1	4.37	1.12	0.3059
C*W	41.68	1	41.68	10.72	0.0051
Residual	58.30	15	3.89		
Pure Error	8.02	5	1.60		
Total	172.44	19			
γ-alumina					
Model					
T	64.59	2	32.30	6.85	0.0066
W	44.46	1	44.46	9.43	0.0069
Residual	80.15	17	4.71		
Pure Error	8.53	5	1.71		
Total	144.75	19			

Table G7: Analysis of variance showing the effect of variables on gas product yield over different catalysts

Source Of Variation	Sum Of Squares	Degree Of Freedom	Mean Square	F Value	Prob>F
HZSM-5					
Model	5.76	2	2.88	12.95	0.0004
T	3.47	1	3.47	15.61	0.0010
W	2.29	1	2.29	10.30	0.0051
Residual	3.78	17	0.22		
Pure Error	5.48E-03	5	1.09E-03		
Total	9.54	19			
HY					
Model	108.22	5	21.64	36.95	< 0.0001
T	52.11	1	52.11	88.97	< 0.0001
W	40.24	1	40.24	68.70	< 0.0001
T2	1.22	1	1.22	2.08	0.1712
W2	15.13	1	15.13	25.82	0.0002
T*W	0.17	1	0.17	0.29	0.5973
Residual	8.20	14	0.59		
Pure Error	0.092	5	0.018		
Total	116.42	19			
Silica-alumina					
Model	236.06	6	39.34	21.60	< 0.0001
T	107.21	1	107.21	58.85	< 0.0001
C	4.40	1	4.40	2.41	0.1443
W	45.53	1	45.53	25.00	0.0002
T*C	38.63	1	38.63	21.21	0.0005
T*W	24.50	1	24.50	13.45	0.0028
C*W	15.79	1	15.79	8.67	0.0114
Residual	23.68	13	1.82		
Pure Error	1.43	5	0.29		
Total	259.75	19			
γ-alumina					
Model	37.13	2	18.56	13.39	0.0003
T	29.99	1	29.99	21.63	0.0002
W	7.14	1	7.14	5.15	0.0365
Residual	23.56	17	1.39		
Pure Error	0.058	5	0.012		
Total	60.69	19			

Table G8: Analysis of variance showing the effect of variables on char and residue yield over different catalysts

Source Of Variation	Sum Of Squares	Degree Of Freedom	Mean Square	F Value	Prob>F
HZSM-5					
Model	66.96	6	11.16	8.81	0.0006
T	9.30	1	9.30	7.34	0.0179
C	17.27	1	17.27	13.62	0.0027
W	3.83	1	3.83	3.02	0.1056
W2	20.41	1	20.41	16.11	0.0015
T*C	7.03	1	7.03	5.55	0.0349
T*W	9.12	1	9.12	7.19	0.0188
Residual	16.47	13	1.27		
Pure Error	2.52	5	0.50		
Total	83.43	19			
HY					
Model	47.74	4	11.94	5.13	0.0083
T	13.25	1	13.25	5.70	0.0306
C	0.21	1	0.21	0.089	0.7699
W	4.37	1	4.37	1.88	0.1904
C*W	29.92	1	29.92	12.87	0.0027
Residual	34.87	15	2.32		
Pure Error	4.49	5	0.90		
Total	82.61	19			
Silica-alumina					
Model	38.52	3	12.84	20.55	< 0.0001
T	0.38	1	0.38	0.60	0.4498
C	8.64	1	8.64	13.82	0.0021
W	30.77	1	30.77	49.26	< 0.0001
Residual	9.37	15	0.62		
Pure Error	0.010	5	2.01E-03		
Total	47.89	18			
γ-alumina					
Model	5.19	6	0.87	7.41	0.0013
T	2.24	1	2.24	19.17	0.0007
C	0.045	1	0.045	0.39	0.5446
W	0.73	1	0.73	6.24	0.0267
T*C	0.23	1	0.23	2.01	0.1797
T*W	0.97	1	0.97	8.34	0.0127
C*W	0.97	1	0.97	8.34	0.0127
Residual	1.52	13	0.12		
Pure Error	0.096	5	0.019		
Total	6.71	19			

Appendix H1: Calibration curves for flow meter and syringe pump
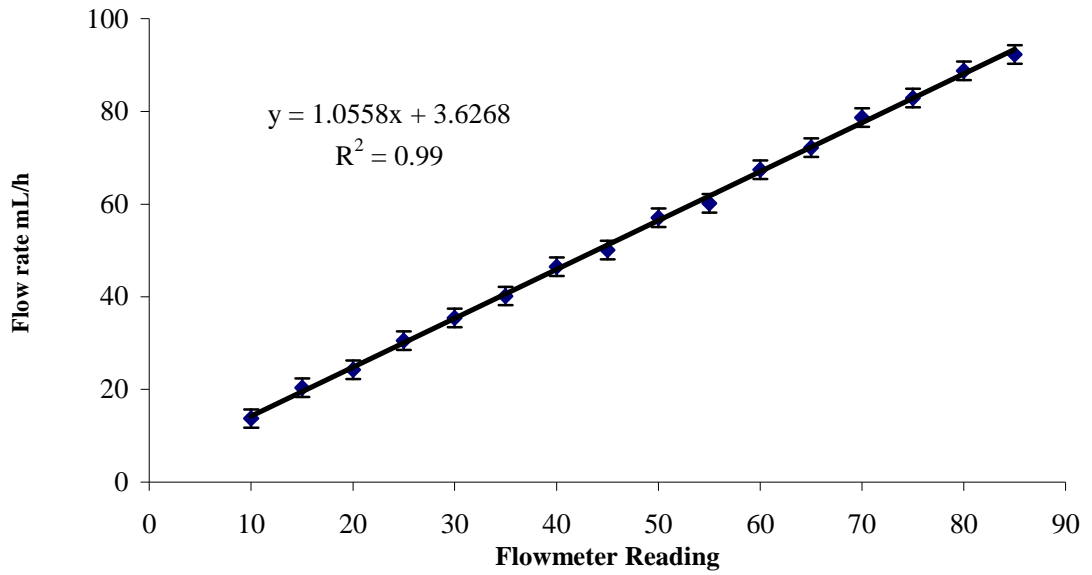
Figure: Calibration curve for flow meter
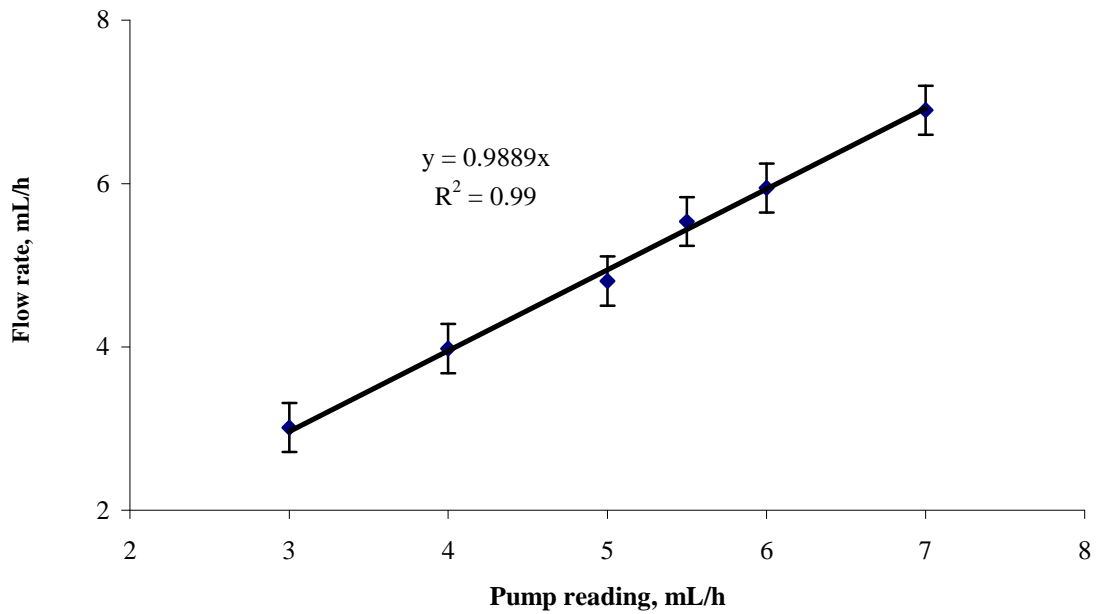
Figure: Calibration curve for syringe pump

Appendix H2: GC calibration curves for gaseous and liquid products

$y = -3E\text{-}15x^2 + 4E\text{-}10x$

$R^2 = 0.99$
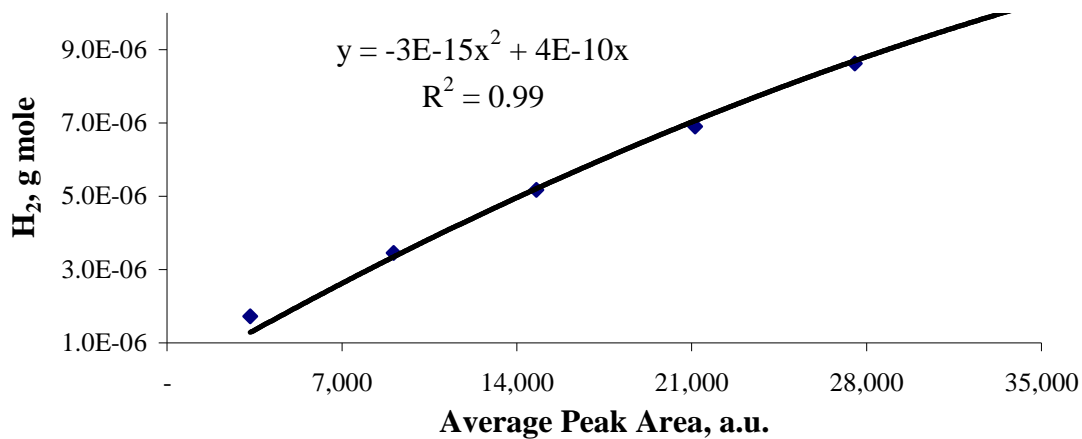
Figure: GC calibration curve for hydrogen

$y = 9E\text{-}12x$

$R^2 = 0.99$
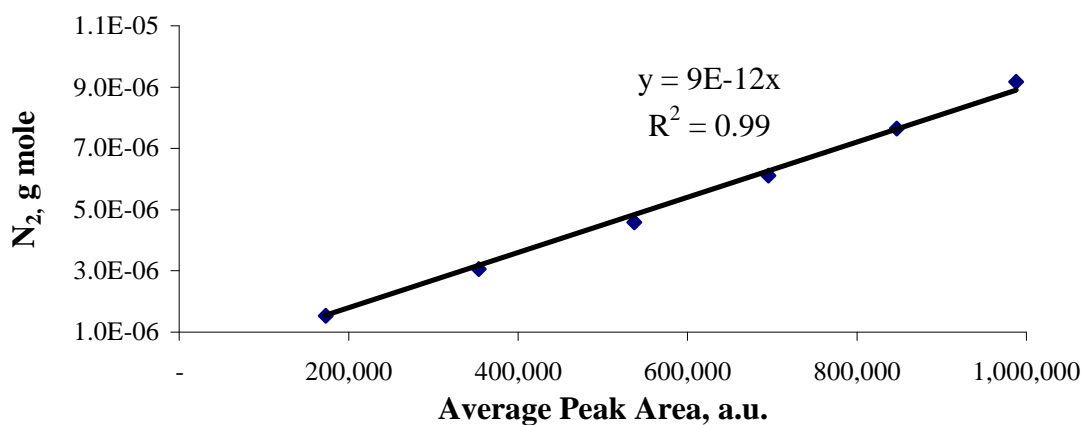
Figure: GC calibration curve for nitrogen

$y = 7E\text{-}12x$

$R^2 = 0.99$
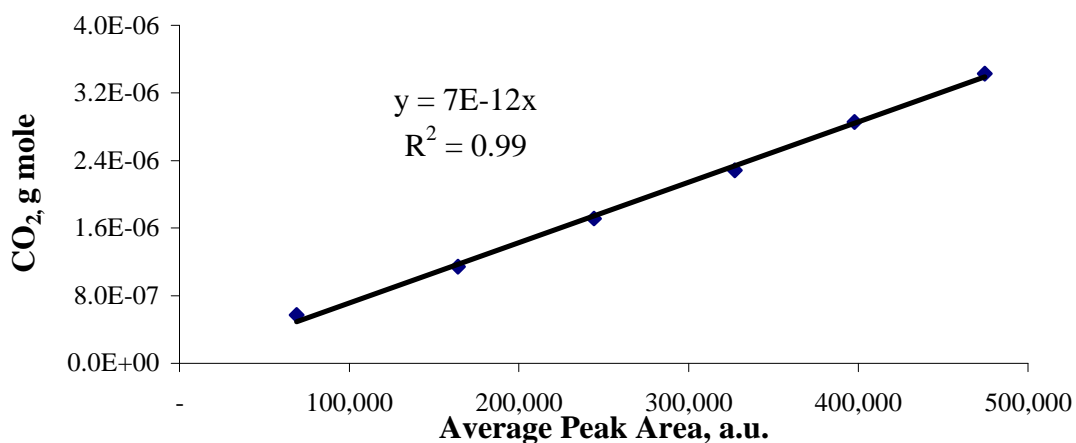
Figure: GC calibration curve for carbon di-oxide
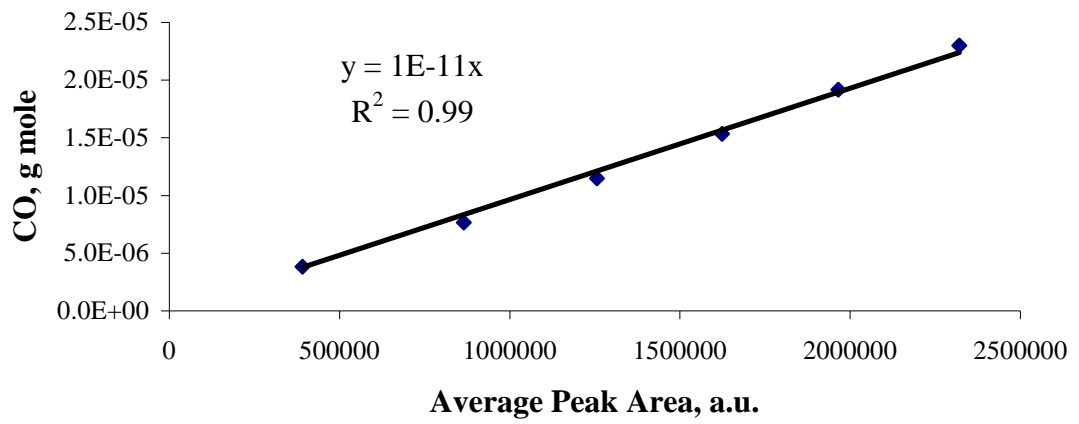
Figure: GC calibration curve for carbon monooxide
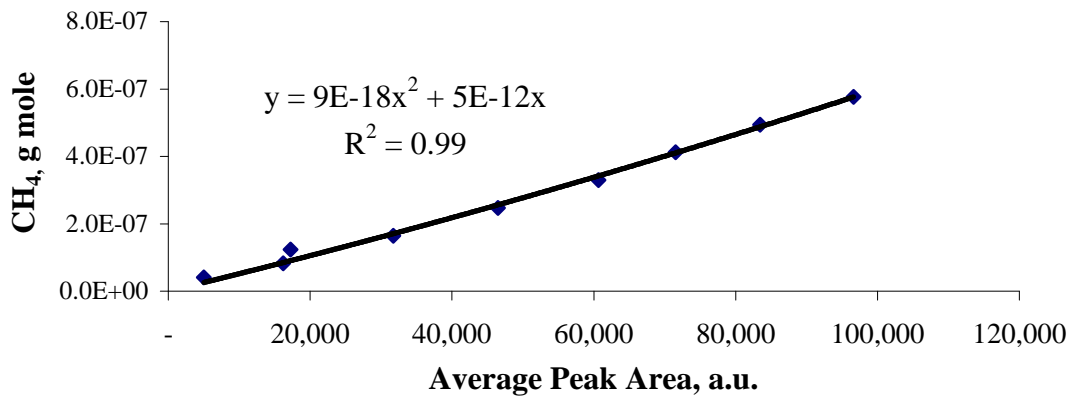
Figure: GC calibration curve for methane
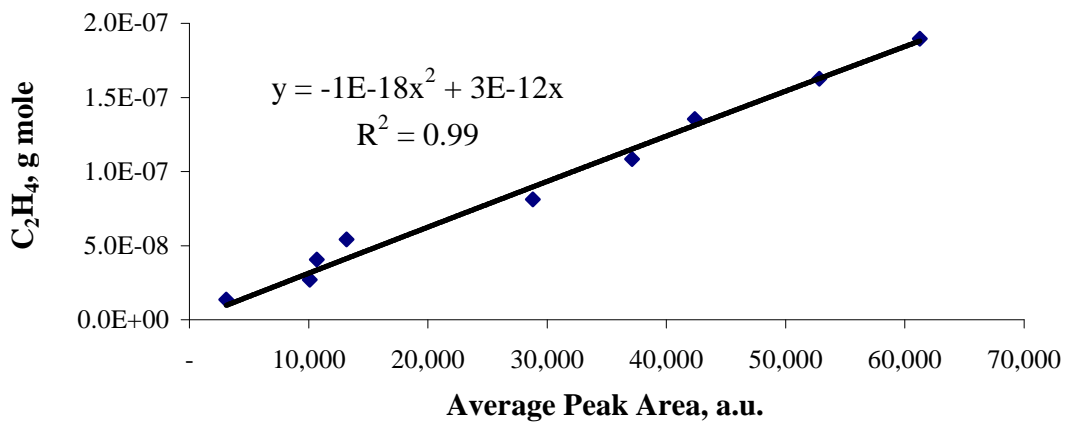
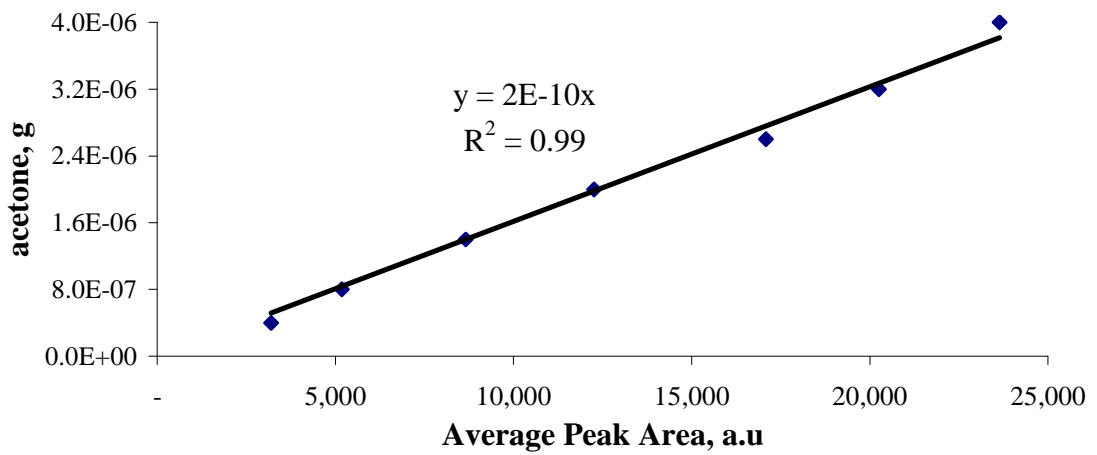Figure: GC calibration curve for ethene
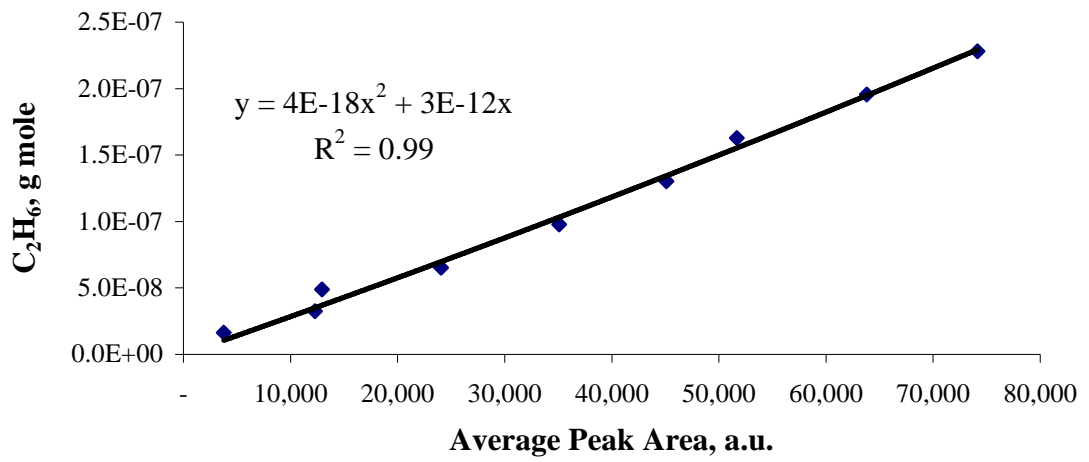
Figure: GC calibration curve for ethane
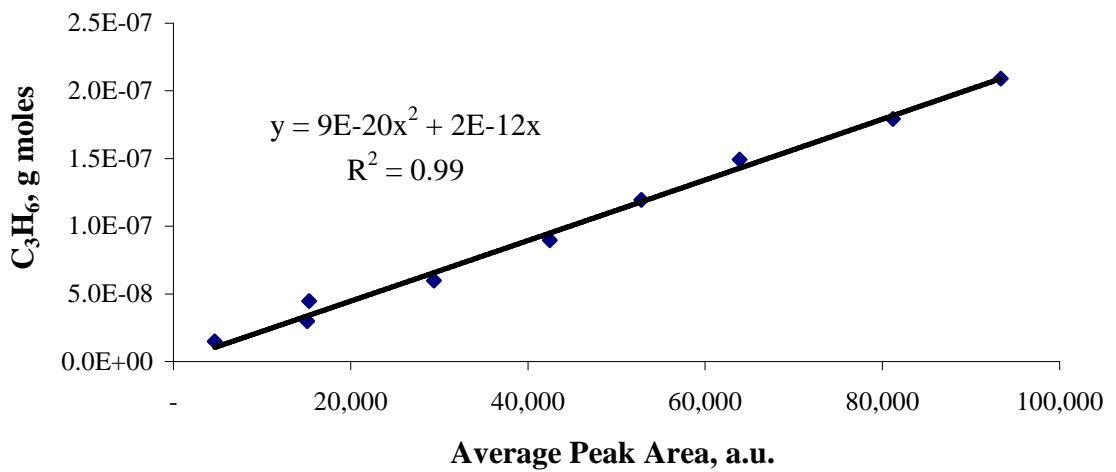
Figure: GC calibration curve for ethyne
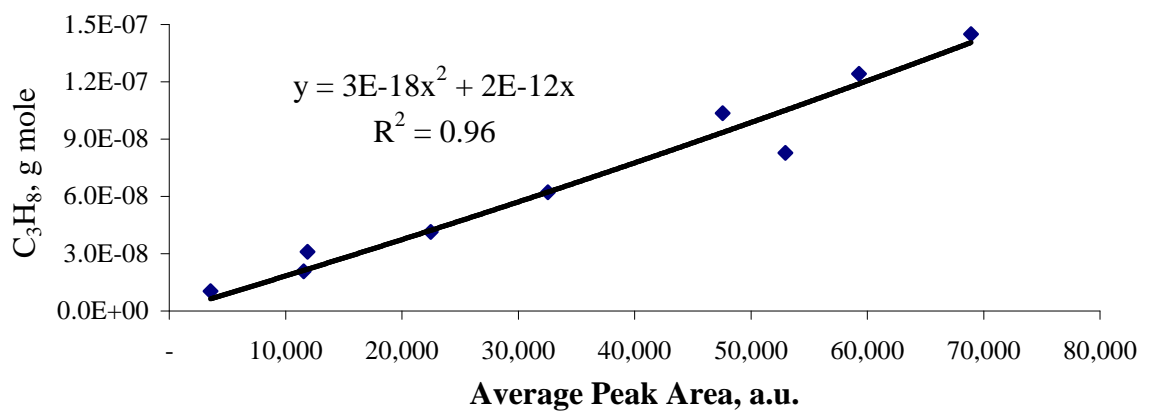
Figure: GC calibration curve for propane
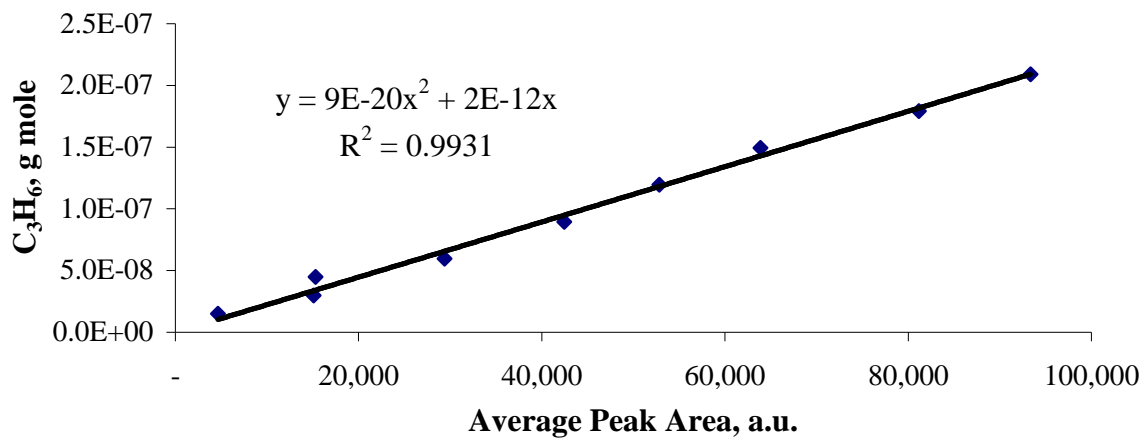
Figure: GC calibration curve for propylene
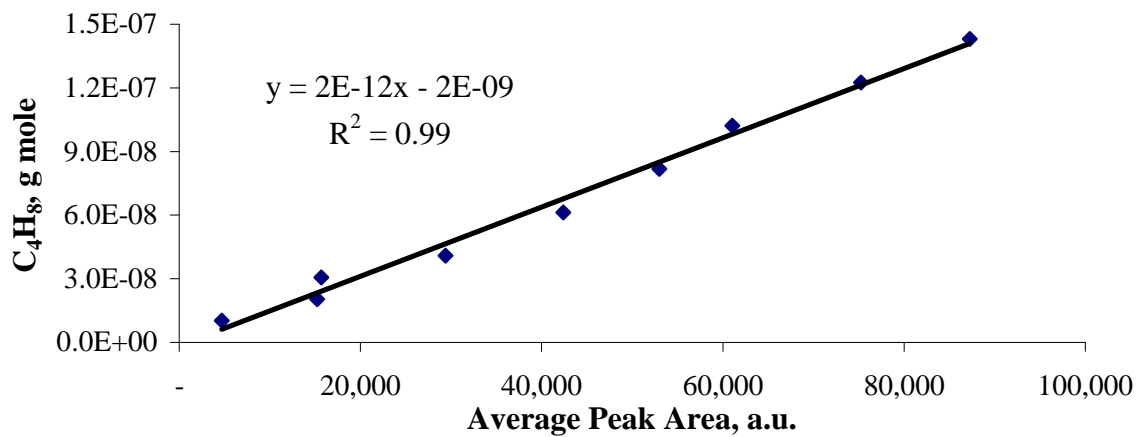
Figure: GC calibration curve for butane
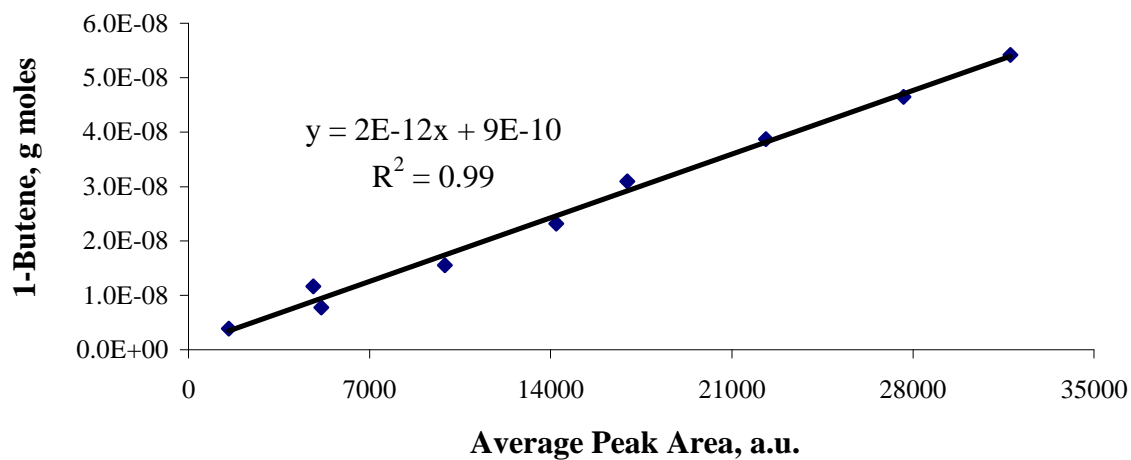
Figure: GC calibration curve for 1-butene
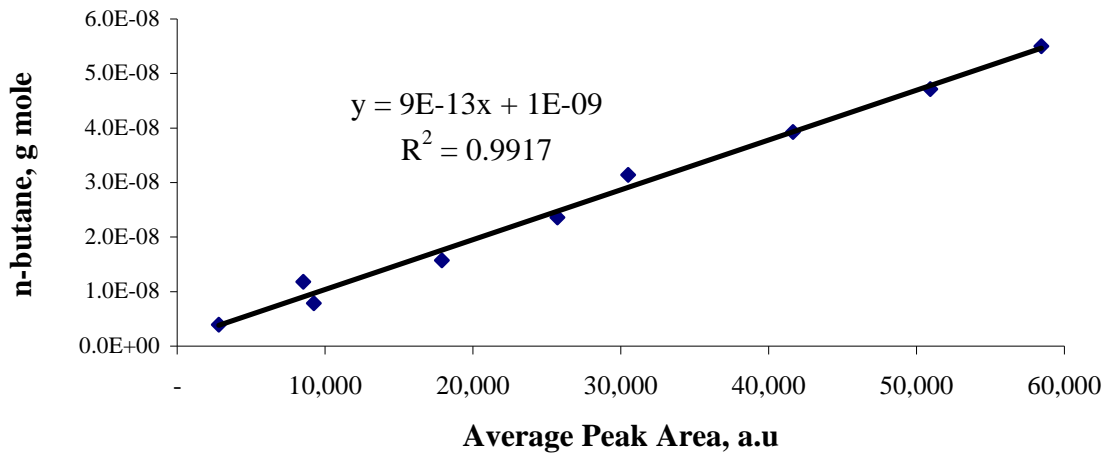
Figure: GC calibration curve for n-butane

$y = 9E\text{-}13x + 1E\text{-}09$

$R^2 = 0.9917$
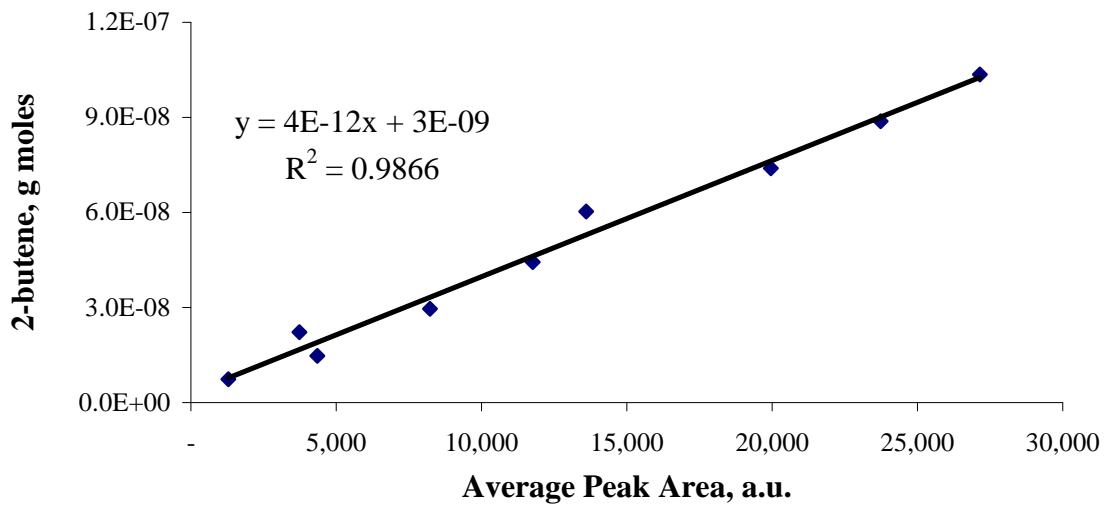
Figure: GC calibration curve for 2-butene

$y = 4E\text{-}12x + 3E\text{-}09$

$R^2 = 0.9866$
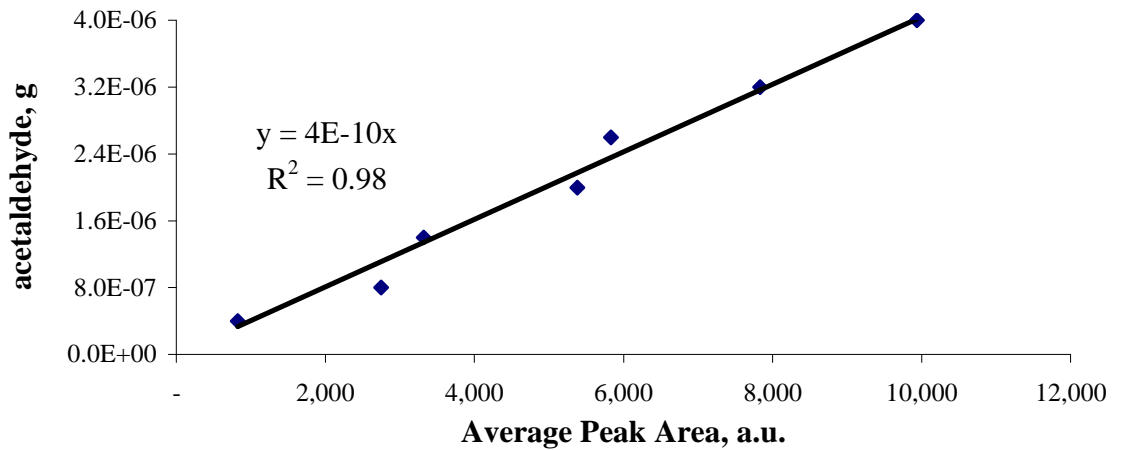
Figure: GC calibration curve for acetaldehyde

$y = 4E\text{-}10x$

$R^2 = 0.98$
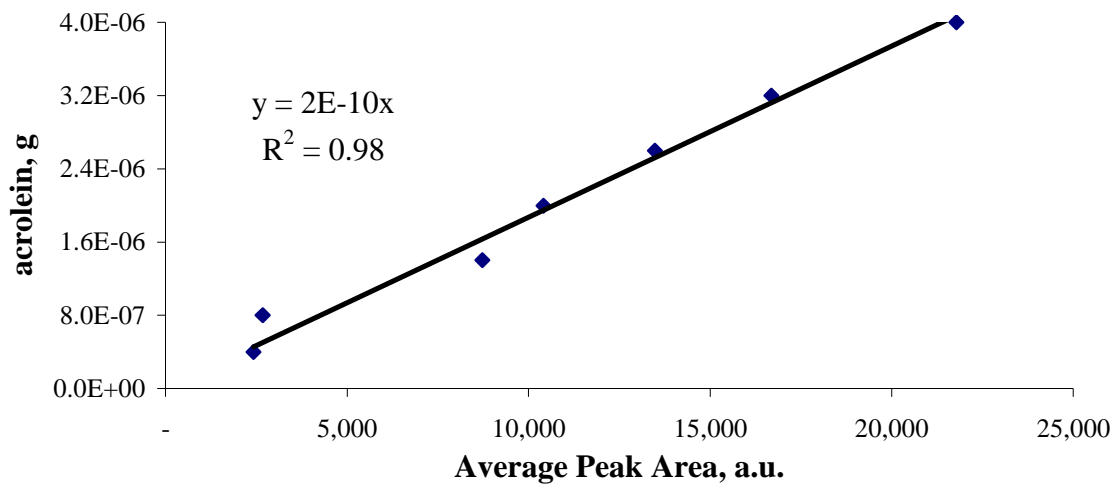
Figure: GC calibration curve for acrolein
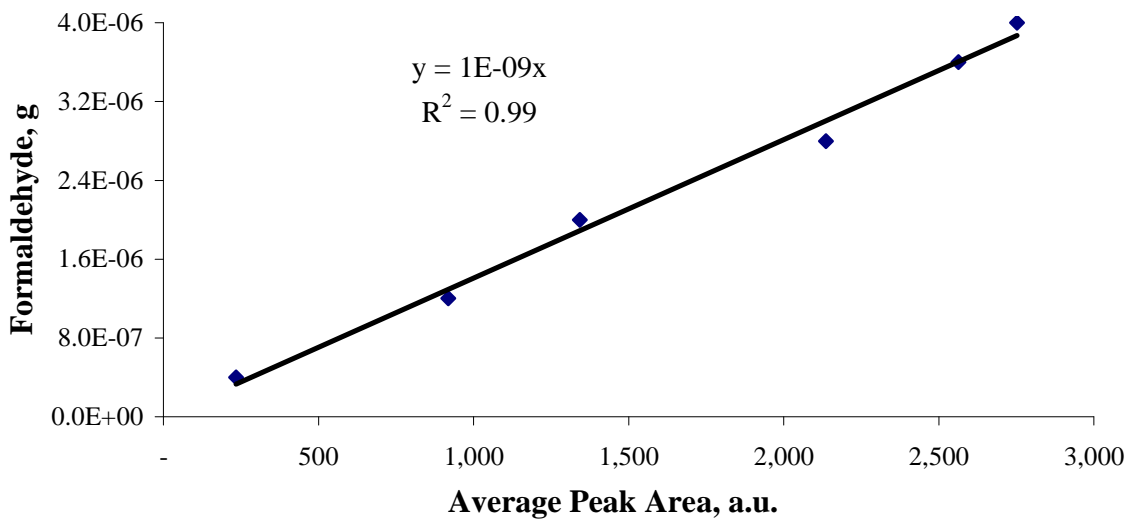
Figure: GC calibration curve for formaldehyde
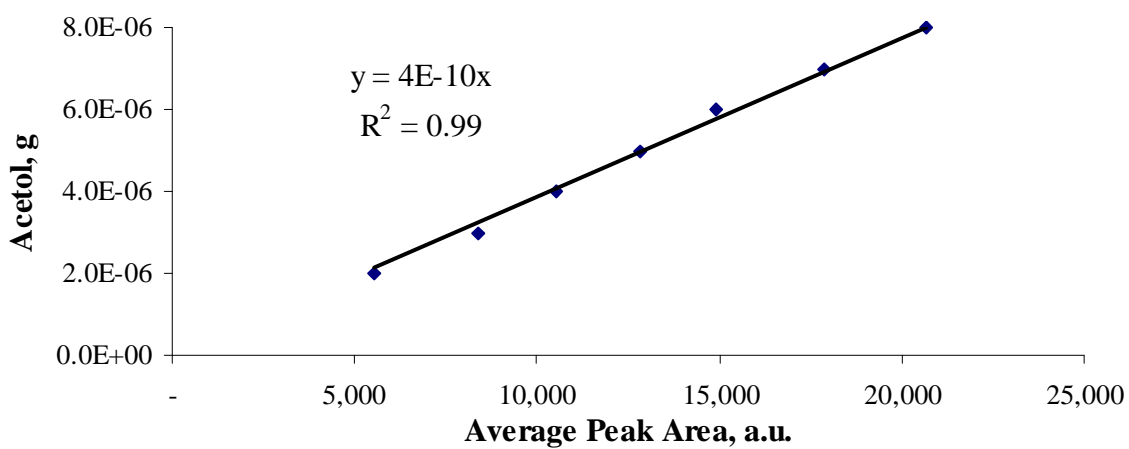
Figure: GC calibration curve for acetol
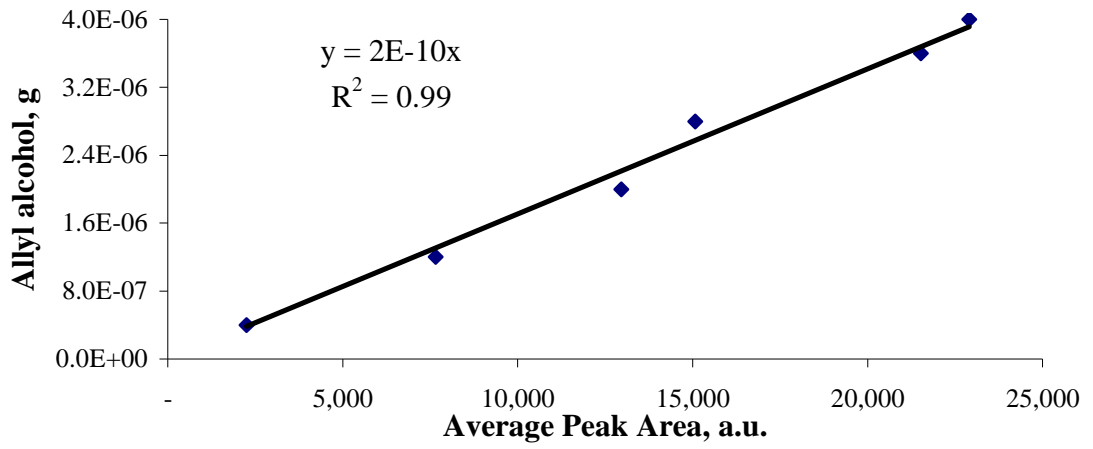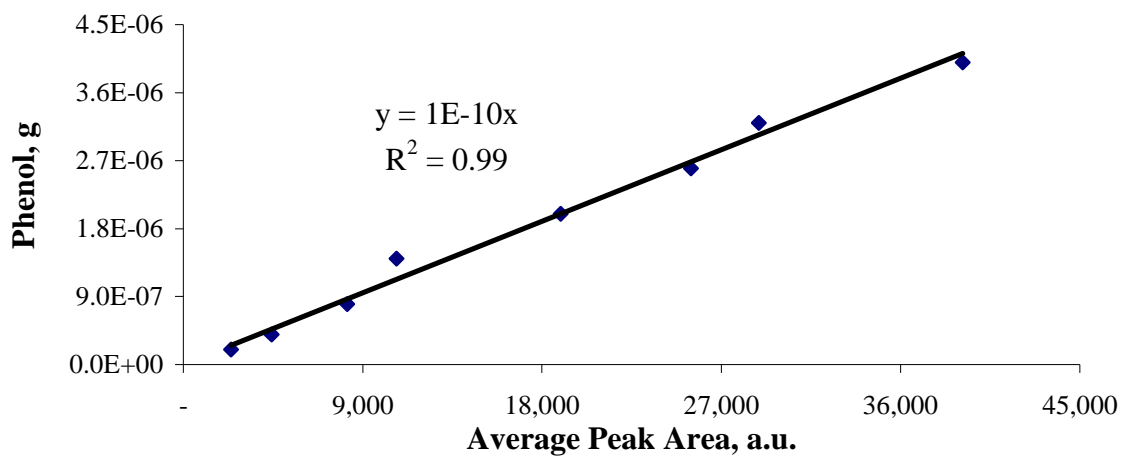
Figure: GC calibration curve for allyl alcohol

Figure: GC calibration curve for acetone
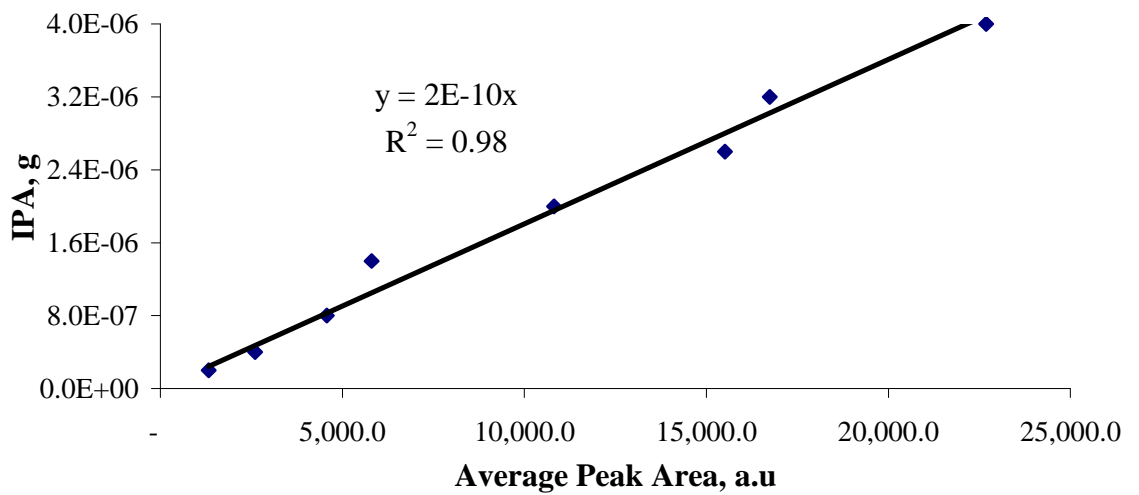
Figure: GC calibration curve for Isopropyl alcohol (IPA)
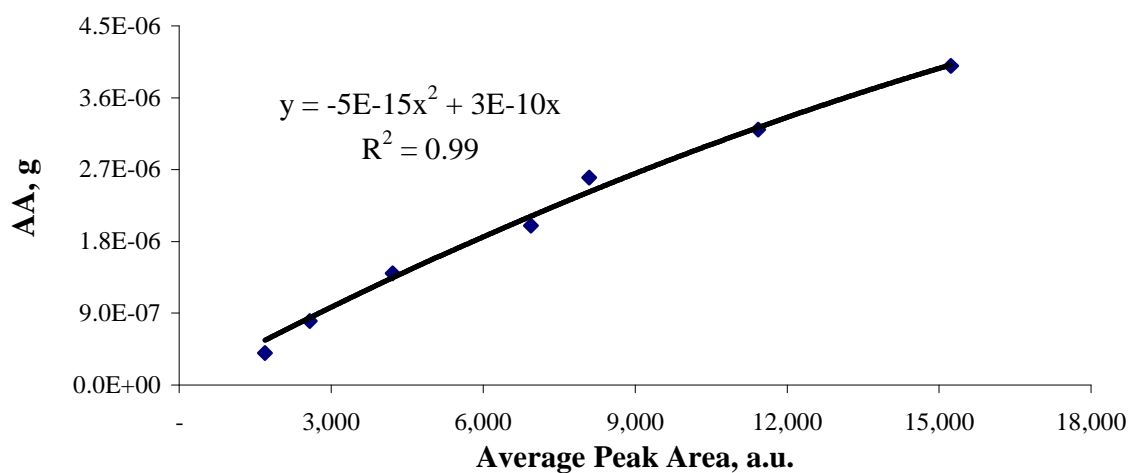
Figure: GC calibration curve for phenol

$y = 1E\text{-}10x$

$R^2 = 0.99$

Figure: GC calibration curve for Acetic Acid (AA)

$y = -5E\text{-}15x^2 + 3E\text{-}10x$

$R^2 = 0.99$
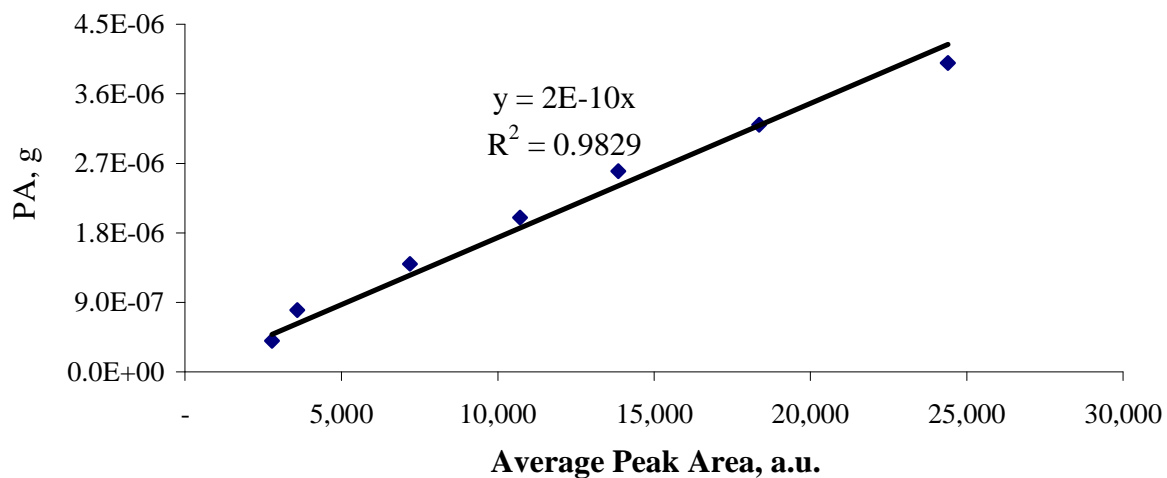
Figure: GC calibration curve for Propionic Acid (PA)
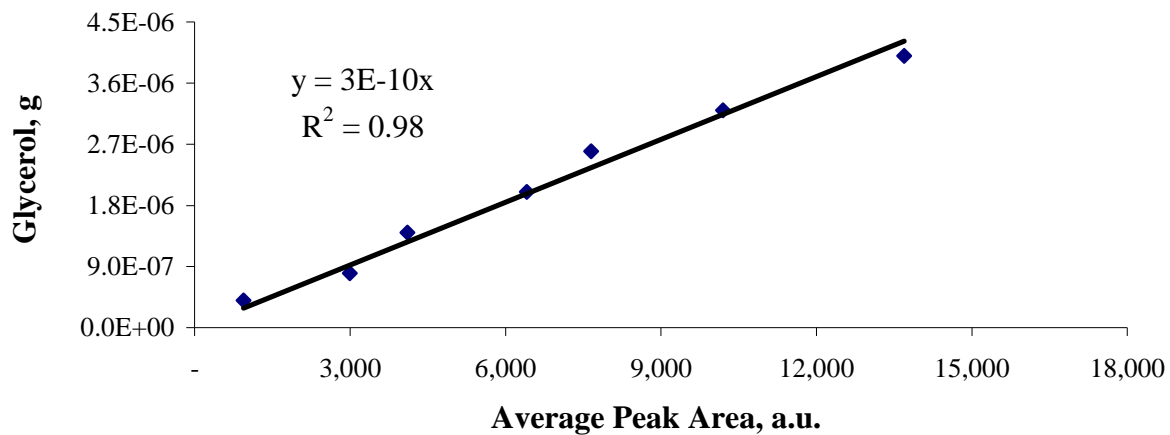
$y = 2E\text{-}10x$

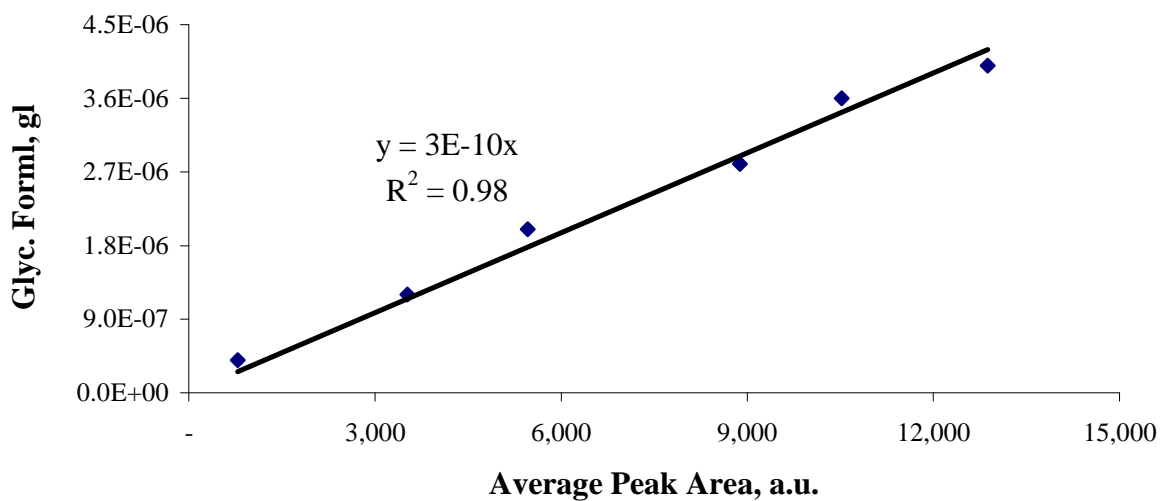$R^2 = 0.9829$

Figure: GC calibration curve for glycerol

Figure: GC calibration curve for glycerol formal (Glyc. Forml.)

Appendix H3: Sample calculations for mass balance

The calculations shown here are based on experiment 2 using HZSM-5

Feed glycerol (input) = 4.92 g

Mass balance calculations:

Total liquid product collected (including unconverted glycerol)   =   4.34 g

Weight of gas   =   3.68E-2 g

Weight of char and residue   =   0.20 g

Total product (output)   =   4.58 g

Mass balance =   100 - (input-output)/input*100

=   100 - (4.92-4.58)/4.92*100   =   93.02 wt%

Liquid product analysis:

Moisture content in the liquid product   =   11.98 wt%

Table Calculation of liquid product composition

Components	Peak areas from GC (a.u.)	Components (g)
Acetaldehyde	7883	0.103
Acetone	969	0.006
Acrolein	10478	0.068
Formaldehyde	3106	0.101
IPA	547	0.004
Allyl Alcohol	17286	0.113
Acetol	17462	0.227
Acetic Acid	1479	0.014
Propionic Acid	5909	0.038
Glycerol Formal	2524	0.025
Phenol	941	0.003
Glycerol	166219	1.623
Total area (known)	**234803**	

Total area of all peaks from GC   =   268425

Unknowns $=$ (1- total known area/ total area of all peaks)*100

$=$ (1- 234803/268425)*100 $=$ 12.5 wt%

Un-converted glycerol $=$ 1.62 g

Glycerol conversion $=$ (1- un-converted glycerol/glycerol fed)*100

$=$ (1 - 1.62/4.92)*100 $=$ 67.01 wt%

Gas product analysis:

Total volume of gas collected (excluding N_2) $=$ 0.02 L

Volume of injection $=$ 500 µL

Table: Calculations for product gas composition and weight

Component	Peak areas from GC	Moles in injected volume	Moles in total gas volume	Mole % excluding N_2	Weight (g)
CO	11591	1.16E-07	5.79E-04	5.33E+01	1.62E-
CO_2	8135	6.51E-08	3.25E-04	2.99E+01	1.43E-
CH_4	1135	5.69E-09	2.84E-05	2.61E+00	4.55E-
C_2H_4	2902	8.70E-09	4.35E-05	3.99E+00	1.22E-
C_2H_6	546	1.64E-09	8.20E-06	7.54E-01	2.46E-
C_3H_6	10303	2.01E-08	1.03E-04	9.47E+00	4.33E-
N_2	1742526	1.74E-05	8.71E-02		
					Total wt = 3.68E-2